Water-in-oil Microemulsions and Hydrogel Nanoparticles in Water-in-Oil Microemulsions for Local Intestinal Delivery of Peptides and Proteins

Dongyun Liu

A dissertation submitted to the faculty of the University of North Carolina at Chapel Hill in partial fulfillment of the requirements for the degree of Doctor of Philosophy in the Division of Molecular Pharmaceutics in the UNC Eshelman School of Pharmacy.

Chapel Hill
2013

Approved By

Russell J. Mumper, Ph.D.

Michael Jay, Ph.D.

Moo J. Cho, Ph.D.

William C. Zamboni, PharmD, Ph.D.

Scott E. Plevy, M.D.

ABSTRACT

DONGYUN LIU: Water-in-oil Microemulsions and Hydrogel Nanoparticles in Water-in-Oil Microemulsions for Local Intestinal Delivery of Peptides and Proteins
(Under the direction of Russell J. Mumper, Ph.D.)

The objectives of the present studies were to develop water-in-oil (W/O) microemulsions (MEs) and hydrogel nanoparticles in W/O MEs for effective local intestinal delivery of peptide and protein drugs.

Water-in-oil MEs consisting of Miglyol 812, Capmul MCM, Tween 80 and water were developed and characterized. Selected W/O MEs containing a model peptide, 5-(and-6)-carboxytetramethylrhodamine labeled HIV transactivator protein TAT (TAMRA-TAT), were evaluated both *in vitro* and *in vivo*. *In vitro* enzymatic stability studies showed the half-life ($t_{1/2}$) of TAMRA-TAT in ME was enhanced nearly three-fold compared to that in the water solution when challenged by modified simulated intestinal fluid. *In vivo* studies in mice showed TAMRA-TAT ME resulted in greater fluorescence intensity in all intestinal sections (duodenum, jejunum, ileum and colon) compared to controls after oral administration. The *in vitro* and *in vivo* studies together demonstrated that TAMRA-TAT was better protected in the W/O ME in an enzyme-containing environment, suggesting the W/O MEs developed in this study may serve as a delivery vehicle for local intestinal delivery of peptides or proteins.

To further improve the current W/O ME formulations, a thermoreversible gelling polymer Pluronic F127 (PF127) was explored to engineer hydrogel nanoparticles in the W/O MEs. Water-in-oil MEs with 14% PF127 were developed based on viscosity studies and construction of phase diagrams, and then physically characterized at different temperatures. After physical characterization, TAMRA-TAT loaded W/O MEs with 8% and 14% PF127,

were evaluated *in vitro* in enzymatic stability studies. The results showed the $t_{1/2}$ of TAMRA-TAT in the W/O ME with 14% PF127 was shorter than that in the W/O ME without PF127. In contrast, the $t_{1/2}$ of TAMRA-TAT in the W/O ME with 8% PF127 was almost the same as that in the W/O ME without PF127. This observation was explained by the large increase in droplet diameter, polydispersity index and turbidity of the ME with 14% PF127, which indicated a possible aggregation and precipitation of PF127 from the ME at 37˚C. Consequently, the aggregation and precipitation of PF127 might have exposed more TAMRA-TAT associated with it to enzymes, resulting in faster TAMRA-TAT degradation. The formation of hydrogel nanoparticles in the W/O MEs was not completely achieved; further research is necessary to better understand and improve the formulation.

In summary, the use of W/O ME systems proposed in this work is an attractive strategy to deliver peptides and proteins orally for the treatment of local intestinal pathologies such as inflammatory bowel diseases.

To my parents, Wengui Liu and Yuzhu Geng,
my husband, Ping Ma,
and my son, Ethan Liu Ma.

ACKNOWLEDGEMENTS

First and foremost, I would like to express my sincere appreciation and gratitude to Dr. Russell J. Mumper for his support, encouragement and guidance through my journey in graduate school at the University of North Carolina at Chapel Hill. Dr. Mumper is a devoted scientist, a great mentor and a role model in many aspects of my life. He is intelligent, efficient, organized and caring. He welcomed me to his lab, helped me during my hard times, and encouraged me when I was not so confident. I would like to thank him for providing me this great Ph.D. training opportunity, for helping me improve and mature as a scientist, and for openning my eyes to so many great things in science and life. On a personal note, I could not have found a more supportive and caring mentor as he is, and I am lucky to have become his student.

I would also like to thank my dissertation committee members, Dr. Michael Jay (chair), Dr. Scott E. Plevy, Dr. Moo J. Cho, and Dr. William C. Zamboni for serving as my committee, and for their time, support and guidance. I have known Dr. Jay for quite some years since I joined Dr. Mumper's lab. Dr. Jay is one of the professors I have seen most frequent on a daily basis. He often educates us on things about American culture, guides us on general things we should follow for being successful in the program, tests us with his newly learned Chinese phrases, shares with us his sweet home-made cakes and cookies. Dr. Jay is a great mentor both in science and life. Interactions with him have been a great pleasure for me during my graduate student life. I am also deeply grateful for the collaboration work and support from Dr. Plevy, Dr. Taku Kobayashi and Steven Russo. Without their help, I could not have published my work.

My sincere appreciation also goes to Dr. Johnny Carson and Todd Gambling for their help with my freeze fracture TEM studies, Dr. Karl Koshlap for his help with my exploration on NMR diffusion studies, animal facility core for their help with the mouse studies, Dr. Matthew Sadgrove in Dr. Jay's lab for his help with the rat studies, and Dr. Hong Yuan for her help with the IVIS imaging studies, Dr. Zhen Hu for his assistance with the statistical data analysis. I also thank MOPH faculty, Dr. Leaf Huang, Dr. Philip Smith and Dr. Xiao Xiao, MOPH staff and many MOPH students and posdocs for their support and friendship during my stay at UNC-Chapel Hill. I would also like to take this opportunity to thank many previous and current Mumper lab members, for their friendship, company and support.

Finally, I would like to express my gratitude to my family. I am grateful to my parents, Wengui Liu and Yuzhu Geng, for their unconditional love and support in my life, especially during my college time and my graduate studies at USA. I would also like to thank my brother, Guanglin Liu and my sister, Yunli Liu, for always standing behind me, and my parents in law, Jinzhang Ma and Yunyi Zheng for their generous support. My beloved son, Ethan Ma, has brought bundles of joy to my busy school life, and has helped me enjoy a more balanced and enriched life! Last but not least, I would like to thank my husband, Ping Ma, for his love, patience and support over these years!

TABLE OF CONTENTS

LIST OF TABLES

LIST OF FIGURES

LIST OF ABBREVIATIONS AND SYMBOLS

5-ASA	5-aminosalicylic acid
AA	acrylic acid
ANOVA	analysis of variance
ATP	adenosine triphosphate
AUC	area under the curve
BMA	butyl methacrylate
BODIPY® FL C_{12}	4,4-Difluoro-5,7-dimethyl-4-bora-3a,4a-diaza-*s*-indacene-3-dodecanoic acid
BSA	bovine serum albumin
CA	cubane-1,4-bis (methacryloyloxyethyl) carboxylate
CD	circular dichroism
CF	5(6)-carboxyfluorescein
CFU	colony forming units
cm	centimeter
CMC	critical micellization concentration
CMT	critical micellization temperature
cP	centipoises
DAPI	4',6-diamidino-2-phenylindole
DEAE	diethylaminoethyl
DHA	docosahexaenoic acid
'DiR'	1,1'-dioctadecyl-3,3,3',3'-tetramethylindotricarbocyanine Iodide
DMAAB	4,4'-di(methacryloylamino)azobenzene
DMEC	dimethylethylchitosan
DSS	dextran sodium sulfate

EC	ethylcellulose
ECH	epichlorohydrin
ECT	eel calcitonin
EPA	eicosapentaenoic acid
Ex/Em	excitation/emission
FDA	Food and Drug Administration
FEEM	freeze-etch electron microscopy
FFTEM	freeze fracture transmission electron microscopy
FI	fluorescence intensity
FITC	fluorescein isothiocyanate
FLs	fusogenic liposomes
g	gram
GI	gastrointestinal
h	hour
HCl	hydrochloric acid
HEC	hydroxyethylcellulose
HEMA	hydroxyethylmethacrylate
HIV	human immunodeficiency virus
HLB	hydrophilic-lipophilic balance
HPC	hydroxypropylcellulose
HPLC	high-performance liquid chromatography
HPMC	hydroxypropylmethylcellulose
HPMCAS	hydroxypropylmethylcellulose acetate succinate
HPMCP	hydroxypropyl methylcellulose phthalate
IBD	inflammatory bowel disease

IDE	insulin-degrading enzyme
IgG	immunoglobulin G
IM	intramuscular
IV	intravenous
i. p.	intraperitoneal
IPA	isopropyl alcohol
kg	kilogram
KPV	Lys-Pro-Val
kV	kilovolt
L	liter
LCST	lower critical solution temperature
LDH	lactate dehydrogenase
Luc	recombinant firefly luciferase
MAA	methacrylic acid
MA-IN	methacrylated inulin
MCT	medium-chain triglyceride
ME	microemulsion
Mg	milligram
mL	milliliter
mM	millimolar
min	minute
mN	millinewton
MS	mass spectrometry
MSIF	modified simulated intestinal fluid
mTorr	millitorr

Mw	molecular weight
N	Newton
NF	National Formulary
NF- κB	nuclear factor kappa-light-chain-enhancer of activated B
NIPAAm	N-isopropylacrylamide
NSAID	nonsteroidal anti-inflammatory drugs
o/w	oil-in-water
O.C.T.	Optimal Cutting Temperature
OVA	ovalbumin
PA	pharmacological availability
PCEFB	poly(p-(carboxyethylformamido) benzoic anhydride)
PCMB	p-chloromercuribenzoate
PCS	photon correlation spectroscopy
PEG	poly(ethylene glycol)
PEGMA	poly(ethylene glycol) monomethacrylate
PEI	polyethyleneimine
PEO-PPO-PEO	poly(ethylene oxide)-poly(propylene oxide)-poly(ethylene oxide)
PHB	prohibitin
PI	polydispersity index
PI	isoelectric point
PLA	poly(lactic acid)
PLGA	poly(lactide-*co*-glycolide)
PF127	Pluronic F127
P(MAA-g-EG)	poly(methacrylic-g-ethylene glycol)
PNIPAM	poly(N-isopropylacrylamide)

PVA	polyvinyl alcohol
q.s.	*quantum sufficit*
ROI	region of interest
RSA	resistant starch acetate
SAS	salicylazosulfapyridine
SCF	simulated colonic fluid
sCT	salmon calcitonin
SD	standard deviation
SeV	sendai virus
SIF	simulated intestinal fluid
SGF	simulated gastric fluid
Soln.	solution
SP	sulphapyridine
STZ	streptozotocin
TAMRA	5-(and-6)-carboxytetramethylrhodamine
TAT	trans-activator of transcription
TCP	tricalcium phosphate
TEC	triethylchitosan
TEM	transmission electron microscopy
$t_{1/2}$	half-life
TMC	trimethylchitosan
TNBS	2,4,6-trinitrobenzenesulfonic acid
TPP	tripolyphosphate
Tween 80	polyoxyethylene sorbitan monooleate
µg	microgram

µL	microliter
µm	micrometer
µS	microsiemens
USP	United States Pharmacopeia
W/O	water-in-oil
w/o/o	water-in-oil-in-oil
w/o/w	water-in-oil-in-water
wt.	weight

Chapter I

Local Intestinal Delivery of Peptides and Proteins: A Review

1.1 Introduction

With the advance of biotechnology, a wide variety of peptide and protein drugs have been produced on a commercial scale. Their incredible selectivity and potency have made them the drugs of choice for the treatment of numerous diseases. However, most of the peptide and protein drugs are administered by the parenteral route, which greatly limits their applications for the treatment of chronic diseases. In contrast to this inconvenient route of drug administration, the oral route offers the advantages of self-administration with good patient compliance and potentially lower manufacturing cost as well [1]. Various strategies have been pursued to develop safe and effective oral delivery systems for peptides and proteins [1-11]. In this chapter, we summarize some approaches investigated for local intestinal delivery of peptides or proteins via the oral route, with colon-specific peptide and protein delivery as our primary focus.

1.2 Brief Overview on the Anatomy and Physiology of the Colon

Anatomically, the large intestine includes the caecum, colon, rectum and anal canal. The colon starts from the caecum and ends with the rectum. The total length of the colon in adults is approximately 150 cm with a surface area of 0.3 m^2 which is relatively small as

compared to the surface area of the small intestine of 120 m^2). The average diameter of the colon is about 7 cm [12]. It is comprised of the ascending colon (right), transverse colon, descending colon (left), and sigmoid colon. The colon wall is composed of several overlapping layers, including the mucosa, submucosa, muscularis externa and the serona. The mucosa is the innermost layer of the colon wall, which opens to the lumen and directly contacts with luminal content. The mucosa layer is further divided into epithelium, lamina propria and muscularis mucosa. The epithelium consists of a single layer of columnar enterocytes and maintains the barrier function. The lamina propria is a layer of connective tissue with blood vessels and lymphatic vessels embedded, which lies outside the epithelium. The muscularis mucosa is a thin layer of smooth muscle and is the outer layer of the mucosa. The submucosa lies outside the mucosa, and contains lots of connective tissues with blood vessels, lymphatics and nerve vessels. The muscularis externa consists of an inner circular layer and an outer longitudinal layer of muscle. The circular layer of muscle provides squeezing action and the longitudinal layer of muscle provides propelling action. The serosa is the single cell layer on the outside of colon.

Compared to the small intestine which is the primary site of nutrient digestion and absorption, the colon is mainly responsible for the maintenance of fluid and electrolyte balance through absorption of water, sodium and chloride. In addition, the colon is also the site to form and store feces from undigested materials, residues of epithelial cell turnover and bacteria [13]. Similar to other part of the gastrointestinal (GI) tract, the colon functions as effective biophysical and biochemical barriers against the penetration of pathogens, toxins and other foreign substances into the body as well. Compared to the small intestine, the colon also possesses at least five distinct characteristics affecting its potential as a drug delivery site.

First, the colon has relatively a low volume of fluid and the luminal content in the colon is generally viscous. Studies by Schiller *et al*. [14] showed the free fluid volume in

human ranged from 1 to 44 mL (median 8 mL) in the fasted state and from 2 to 97 mL (median 18 mL) in the fed state in the colon. The limited free fluid volume may affect the drug distribution and dissolution in the colon, and likely resulting in higher local drug concentrations.

Second, the overall proteolytic activity in the colon is about 20-60 times lower and different compared to the proteolytic activity in the small intestine [15, 16], which makes colon a more favorable site for local peptide and protein delivery. Although, pancreatic peptidases are secreted in grams quantities every day, their residual levels in the colon is quite limited [17, 18]. It was reported that in the ileum, the trypsin and chymotrypsin activities were only one-half and one-third of that in the duodenum, respectively [19]. Moreover, the pH drops to weakly acidic in the cecum and ascending colon compared to ileum, which fails to provide the optimum pH range of 7 to 8 for the activity of pancreatic enzymes [12, 20]. Meanwhile, the brush-border membrane associated peptidases are quite limited in the colon compared to those in the small intestines [21].

Third, the microflora in the human colon is quite abundant and diverse, and the bacterial counts were reported as high as 10^{11}-10^{12} colony forming units (CFU)/mL in the colon, and there may be more than 3,000 different species colonizing in the colon [22, 23]. The microflora is able to ferment and metabolize a large range of polysaccharides, starch, dietary fiber and undigested proteins, and produce sugars, amino acids, short-chain fatty acids, branched chain fatty acids, hydrogen, methane and carbon dioxide etc. [12]. Consequently, the fermentation products are able to influence the colonic environment, such as the viscosity, pH and redox potential [24].

Fourth, the motility of the colon is relatively slow. It involves the combination of segmental and peristaltic contractions by smooth muscle layers. The segmental contractions are responsible for the mixing of luminal content, while the peristaltic contractions are associated with propulsive movements to propel the luminal content toward

the rectum [25]. Due to the special motility pattern and the infrequent propulsive movements, the overall motility is slow, which corresponds to a long colon transit time from several hours up to several days [26]. The slow and lengthy transit combined with a progressive decrease in colon fluid volume would make a healthy colon a reservoir system for both therapeutic drugs and unabsorbed nutrients.

Fifth, the luminal pH in normal GI tract progressively increases from the duodenum to the distal ileum, decreases in the cecum, and then increases slowly along the colon to the rectum. Compared to the luminal pH in the range of 6.5 to 7.5 in the distal ileum, the pH in the caecum and ascending colon drops to the range of 5.5 to 7.5, and then gradually rises in the descending colon and rectum to 6.1 to 7.5 [27]. Studies have also indicated the colonic mucosal pH in healthy subjects was consistently higher at all segments than the luminal pH, ranging from 7.1 to 7.5 [28]. Some data also reported the pH in the ascending colon was reduced in patients with active ulcerative colitis [27]. Since the disease state may affect the colonic pH, it should be considered when designing pH-dependent delivery systems.

Colon delivery has been used in clinic for the treatment of inflammatory bowel diseases (IBDs) [29, 30]. The benefits of local delivery of steroidal and non-steroidal anti-inflammatory drugs for long-term therapy of IBD have been well recognized. Local colonic delivery is also considered beneficial for the treatment of various colonic cancers and other local pathologies like some parasitic diseases affecting the colon. By targeting the drug to the local disease site, like the site of inflammation, colonic drug delivery can avoid extensive drug degradation and unneeded absorption in the upper GI tract, maximize local drug concentration thereby efficacy and minimize potential systemic side effects. Recently, colon delivery has been considered not only suitable for the treatment of local pathologies, but also as a promising strategy to improve systemic absorption of some drug molecules, especially those hydrophilic peptide and protein drugs that would undergo extensive enzymatic degradation in the upper GI tract. In summary, the colon's anatomical and

physiological properties has confirmed that the colon is an attractive site for local oral peptide and protein delivery.

1.3 Approaches to Achieve Colon Delivery

Various colon delivery systems for local oral peptide and protein delivery have been investigated and published [5, 8, 11, 31-33]. These systems are generally designed based on the typical variations in the physiological parameters along the GI tract, such as the abundance of microflora, luminal pH, intra-luminal pressure, and transit or residence time in each intestinal segment. Some systems utilized one of the above mentioned parameters [34-39], while others utilized a combination of two or more parameters to achieve a better targeting effect [40].

1.3.1 Microflora-dependent delivery systems

In humans, the GI tract is inhabited by a large variety of microflora species. In the stomach and small intestine, there are roughly 10^3-10^4 colony forming units (CFU)/mL [29]. However, the concentration of microflora increases significantly to 10^{11}-10^{12} CFU/mL passing from the distal ileum to the ascending colon [41]. The predominant species include *Bacteroides, Bifidobacterium*, and *Eubacterium* [42]. Anaerobic gram-positive *Cocci, Clostridia, Enterococci*, and various species of *Enterobacteriaceae* are also commonly found [43]. These bacteria survive by fermenting various substrates left undigested from the small intestines, such as oligosaccharides, di-, tri-polysaccharides, mucopolysaccharides [44]. The enzymes produced to ferment these substrates include azoreductase, β-glucuronidase, β-xylosidases, β-galactosidase, α-arabinosidase, nitroreductase, dextranase, deaminase, urea hydroxylase, etc. [43, 45, 46]. The unique ability of colonic bacteria species to catalyze degradations of substrates that do not undergo major dissolution, degradation or absorption in the small intestine is exploited for local colonic drug delivery.

Prodrugs

This microflora-dependent strategy was first pursued in a prodrug-based delivery system for local colonic delivery. In 1972, Peppercorn and Goldman [47] observed that salicylazosulfapyridine (SAS) was converted to sulphapyridine (SP) and 5-aminosalicylic acid (5-ASA) by the mammalian intestinal microflora via the reduction of the azo bond. In 1977, Khan *et al.* [48] found that the active moiety effective in IBD was 5-ASA and SP was only a carrier. After realizing the association of side effects with SP, several 5-ASA prodrugs, ipsalazide, balsalazide [49] and olsalazine [50] were designed accordingly. Ipsalazide and balsalazide are able to release one 5-ASA molecule and one nontoxic carrier, while olsalazine can generate two 5-ASA molecules after reduction of the azo bond by colon bacterial enzymes. Based on the same principle, Parkinson *et al.* [51] synthesized a polymeric prodrug to deliver 5-ASA. The 5-ASA precursor was attached to a polymeric compound through an azo-linkage. When the polymer passed through the mammalian GI tract, the azo-linkage was cleaved by colon bacteria and 5-ASA was released to the colon. Similar to the azo-linkage, several other linkages susceptible to bacterial hydrolysis in the colon (such as amide linkage, glycosidic linkage, glucuronide linkage and ester linkage) were utilized to design a variety of prodrugs for colon targeted delivery. The drug carrier moiety could be small molecules such as amino acid, glucose, galactose, glucuronic acid, or some synthetic or naturally occurring polymers. A large variety of prodrugs evaluated for local colon-specific drug delivery based on colonic bacterial enzymes were well summarized by Sinha *et al.* [43], and most of them showed great or promising colon targeting effects.

However, the prodrug approach for local colon delivery was mostly investigated for the delivery of small molecule drugs, and reports on prodrugs of peptides or proteins for either local or systemic colon delivery purposes were quite rare. A recent publication by Kennedy *et al.* [52] reported the synthesis of azo-prodrugs of nonsteroidal anti-inflammatory agents and antimicrobial peptides for local colonic delivery to treat infection and

inflammation by the bacterial pathogen *Clostridium difficile*. The structural design of the azo-prodrugs is shown in Figure 1.1. An antibacterial peptide temporin A analogue L512TA was linked to the anti-inflammatory agent 4-aminophenylacetic acid by an α-methylalanine linker via an azo bond. It was hypothesized that both components would stay inactive before reaching colon, thereby avoiding side effects from NSAID or disruption of commensal microflora in the upper GI tract. The authors reported the synthesis and purification of the prodrugs, but no further *in vitro* or *in vivo* evaluation data were available.

The prodrug approach is one of the options to solve many drug delivery related problems, such as poor chemical stability, or low aqueous solubility, but it is still very challenging when applied to peptide and protein delivery. The use of prodrugs to chemically or physically stabilize peptides or proteins has not been well evaluated yet, and for site-specific targeting of peptides or proteins to the colon, it becomes even more difficult for several reasons.

First, in general, the prodrug approach is not very versatile and it depends on the functional groups available on the drug for chemical conjugation. For peptides and proteins, which are polymers of amino acids, site-selective chemical conjugation is more difficult and complicated than that for small molecules. Meanwhile, to protect peptides or proteins from degradation in the upper GI tract, it involves many peptide bonds vulnerable to proteolytic enzymes. Proteolysis may happen at N-terminus, C-terminus, or at any distinct endo residues in a peptide or protein drug. Modification at one site may improve its stability to some enzymes but the peptide or protein may still be susceptible to other enzymes.

Second, for colon targeting, chemical conjugation to polymer carriers that are specifically degraded by colon bacteria has shown promising results for the colonic delivery of small molecule drugs [53]. However, when peptide or protein drugs are conjugated to these polymer carriers, the molecular weight, composition and 3D structure, hydrophobicity

and flexibility of both moieties have to be considered, and the conjugation chemistry, purification and characterization processes become more complicated.

Third, to successfully deliver the peptide or protein drugs to the target site *in vivo* with preserved biological activity is also very challenging for the design of peptide and protein prodrugs. Random conjugation may cause the loss of biological activity of the peptide or protein drug.

Fourth, prodrugs of peptides or proteins are new chemical entities and may become immunogenic or toxic, and will require a lot of additional evaluations before being used as drug carriers. The prodrug approach for local peptide and protein colon targeting is promising but not well studied yet, and publications on this topic are relatively limited.

Bacterial degradable polymer systems

Based on the abundance of colon microflora, many synthetic polymers like azo-polymers, and various naturally occurring polymers such as chitosan, pectin, dextran, guar gum, inulin, amylose, chondroitin sulphate, have been investigated for colon specific drug delivery [54-57]. Some attempts of using microbially-triggered polymer systems have been made for colonic peptide or protein delivery.

Azo-polymers were synthesized and evaluated as coating materials or hydrogel forming matrix according to their susceptibility to cleavage by azoreductase in the large intestine. Saffran *et al.* [39] did the early pioneering studies on the feasibility of oral colon delivery of insulin and other peptide drugs using the azo-polymer coating approach. Divinyl-azobenzene or substituted divinylazobenzene cross-linked copolymers of styrene and hydroxyethylmethacrylate (HEMA) were synthesized and used as water impervious film coating agents. The azoaromatic polymer coated capsules or pellets of vasopressin and insulin were tested in rats. The mean time to peak antidiuresis after oral administration of vasopressin protected by the azoaromatic polymers was about 2.5 h, while after

vasopressin in solution was only around 23 min. The difference was highly significant. However, the variation of the vasopressin response time was large, with a clustered of them around 2 h, and others ranging from 5 to 8 h. The azo-polymer coated pellets containing insulin were tested in streptozotocin-induced diabetic rats and resulted in a prolonged decrease in blood glucose levels compared to no decrease in blood glucose after given control pellets. However, the same formulation was shown to have reduced effects in non-diabetic rats. Saffran *et al.* [39] showed that the azo-aromatic polymer delivery system worked in principle, and could deliver its drug load to the colon, although more work was required for further characterization and optimization. Later, the same strategy based on azo-polymer coating was investigated using hard-gelatin capsules containing highly-dosed insulin [10]. The azo-polymer applied was a terpolymer of styrene, hydroxyethylmethacrylate and *N,N'*-bis (β-styrylsulphony)-4,4'-diaminoazobenzene. Bovine insulin was formulated into azo-polymer coated capsules along with a stoichiometric mixture of 5-methoxysalicylic acid and sodium bicarbonate. 5-methoxysalicylic acid functioned as an absorption enhancer to improve insulin bioavailability. Meanwhile, the mixture of bicarbonate and acid would produce carbon dioxide after water penetrated the hydrogel coating and the gelatin capsule, which would help rupture the gelatin capsule and release the insulin rapidly as a bolus. The capsules containing bovine insulin were orally administered to pancreatectomized dogs in a single dose or multiple doses, and then multiple responses were measured, such as the plasma glucose, plasma insulin, hepatic glucose production rate, hepatic plasma flow rate, and glucogon-like immunoactivity. Single oral doses of insulin produced plasma insulin peaks, and transient decreases in plasma glucose and other responses. Following intensive multiple dosing regimen, the data showed multiple peaks of plasma insulin and a continuous reduction in glucose as compared to pretreatment values. However, the total pancreatectomy eliminated the source of digestive enzymes in the small intestine and might have contributed to the preservation of insulin integrity in the GI luman. The authors [10]

performed another two trials with insulin in azo-polymer-coated capsules administered to normal dogs. They observed decreases in plasma glucose levels, which provided justification to the above experimental condition. Brondsted *et al.* [58] investigated novel azo-aromatic polymer-based hydrogels as enzymatic degradable protein carriers for site-specific systemic colon delivery. The hydrogels were prepared from newly synthesized azo-polymers of hydrophilic N-substituted (meth) acrylamides, N-tert-butylacrylamide and acrylic acid cross-linked with 4,4'-di(methacryloylamino)azobenzene (DMAAB). At low acidic pH, the hydrogels had a low degree of swelling and thus protected the drug against enzyme digestion in the stomach. As the hydrogels passed down the GI tract, the degree of swelling increased, and in the colon, the degree of swelling made the cross-links accessible to azoreductases and mediators. The hydrogel then was degraded and the drug was released from the gel. *In vitro* permeability experiments showed that the insulin permeability through the hydrogel membranes was lower at pH 2 than 7.4. Later, Cheng *et al.* [37] studied the feasibility of using azo-polymer-coated hard gelatin capsules for peptide and protein colonic delivery. DMAAB cross-linked copolymers of styrene and HEMA were used, and the resulting azo-polymer exhibited a pH-dependent swelling behavior. When the pH reached 6.8 and higher, it gradually gained weight due to water uptake. After *in vitro* formulation screening with different coating levels, capsules with around 10 mg/cm^2 of azo-polymer coating containing pork insulin were administered to dogs. Compared to plain uncoated capsules with the same level of insulin, the azo-polymer coated capsules provided slightly decreased glucose levels, and a higher average insulin level, but extreme large variation was observed in this study and the pharmacological response was inadequate. Therefore, more efforts were required for further improvement. Tozaki *et al.* [36] studied novel azo-polymer-coated pellets containing insulin and (Asu^{1,7})eel-calcitonin for colon specific delivery. Azo-containing polyurethanes were prepared and coated over the drug-containing pellets. Camostat mesilate was incorporated into the pellet as a protease inhibitor. *In vitro* release

experiments showed markedly increased release of a model drug from azo-polymer-coated pellets in the presence of rat cecal contents compared to that in phosphate buffered saline. After oral administration of azo-polymer-coated pellets containing insulin and ($Asu^{1,7}$)eel-calcitonin to rats, hypoglycemic and hypocalcemic effects were observed, respectively. The co-administration of camostat mesilate further increased the hypoglycemic effects dose-dependently. The hypocalcemic effects of ($Asu^{1,7}$)eel-calcitonin were improved by co-administration of camostat mesilate as well. These results suggested the feasibility of using azo-polymer-coated pellets as useful carriers for colon-specific peptide or protein delivery.

Due to some debate on azo-polymer potential toxicity, naturally occurring saccharide-based polymers have attracted a great deal of research interest. Polysaccharides such as chitosan, pectin, dextran, guar gum, inulin, amylose, chondroitin sulphate, are generally considered as safe and being actively investigated in the field for drug colon targeting.

Pectin is a group of non-starch linear polysaccharides found in the cell walls of many plants. It mainly consists of α-(1-4)-linked D-galacturonic acid residues interrupted by 1,2-linked L-rhamnose residues [43, 59]. Pectin is commercially available with an average molecular weight ranging from around 50,000 to 150,000 Dalton, and has been widely used as a stabilizer or thickening agents in the food industry. Pectin is stable in the physiological condition of stomach and small intestine, and degraded by the colon bacteria especially *Bacteroides* [60]. Its safety profile and microflora-dependent degradation have stimulated numerous studies using pectin as an excipient for small molecule and peptide/protein colon delivery. To avoid premature release in the upper GI tract, Rubinstein *et al.* [61] utilized calcium pectinate as a drug carrier, which is less water-soluble compared to pectin. Insulin and a low water soluble molecule indomethacin were formulated into plain matrix and compression coated calcium pectinate tablets. *In vitro* indomethacin release studies showed that in the absence of pectinolytic enzymes, indomethacin was retained in both

plain matrix and compression coated tablets in simulated gastric and intestinal fluids, although a small percentage of drug leakage was observed from plain matrix tablets without compression coating. Calcium pectinate compression coated tablets containing insulin in an inner core with an outer layer of calcium pectinate coating, and insulin plain matrix tablets were given orally to pancreatectomized dogs. Soybean trypsin inhibitor and an absorption enhancer sodium cholate were mixed in both types of formulations. Compression coated tablets delayed the insulin absorption after a lag time of around 5-8 h, which was consistent with their colon arrival time. In contrast, plain matrix tablets were not able to delay the drug release and provided a sustained insulin absorption followed by a slow decline of the blood glucose level. The colonic bacterial surface adhesion onto solid dosage forms and their potential implications on the colon delivery system were investigated by Rubinstein *et al*. [62]. Paper strips loaded with recombinant human insulin, sodium deoxycholate and aprotinine were completely covered with pre-cast pectin films and implanted to the cecal region of rats. The blood glucose level dropped when antibiotics was co-administered, indicating the adhesion of colon bacteria onto the pectin film surface interfered with the insulin release. *In vitro* studies showed the number of bacteria cells adhering to pectin surfaces decreased with increasing agitation rate. It was concluded that biodegradable polymers such as pectin will function as colon delivery system only if the enzymatic degradation was accompanied with physical erosion. The bacterial adherence to the surface of the dosage form would interfere with the polymer erosion and drug release. Another study by Musabayane *et al.* [11] investigated using amidated pectin hydrogel beads to deliver human insulin orally in streptozotocin (STZ)-diabetic rats. Oral administration of human insulin once (30 or 46 μg) or twice (60 μg) daily for 2 weeks significantly decreased blood glucose levels compared to untreated rats. In contrast, significant increase in blood insulin level was only observed following the high doses of 46 μg once a day and twice (60 μg) daily regimens. Pharmacokinetic parameters in STZ-diabetic rats showed that orally

administered pectin-insulin beads (30 μg) were more effective to maintain blood insulin levels than a subcutaneous insulin injection. It was inferred that the insulin release from the pectin beads and absorption were not limited to the colon, and mostly started from the upper intestine already. Overall, the results suggested the amidated pectin hydrogel beads could produce sustained release of insulin, but not enough to limit the drug delivery to the colon specifically, and the combination with polymeric coatings and other strategies was suggested. To develop colonic delivery system, Cheng *et al*. [38] engineered calcium pectinated nanoparticles containing porcine insulin, which were expected to undergo bacteria-triggered degradation in the colon very quickly based on their nano-scale dimension. Two types of pectin and the formulation pH were evaluated on the characteristics of the nanoparticles. Particles with a narrow size distribution were obtained by ionotropic gelation and purified by cross-flow filtration method. The pH of the formulation significantly influenced the insulin association efficiency and the stability of the particles. Increasing the pH from 2 to 3 enhanced the insulin association efficiency by 3-fold, which was correlated to the charge density on the pectin molecules as a function of pH. The insulin release from the particles was dependent on the extent of the dilution and the pH of the dissolution medium. However, the *in vitro* release of insulin in simulated gastric fluid was high, which indicated that these calcium peptinate particles were probably not able to protect insulin release from the upper GI tract. In addition, there were no enzymes in the tested dissolution medium. Therefore, the potential of calcium pectinate nanoparticles for colon-specific delivery required further thorough evaluation. Calcium peptinate beads for colonic peptide delivery were also evaluated using bovine serum albumin (BSA) as a model peptide by Atyabi *et al.* [63]. Calcium pectinate beads containing BSA were prepared by extruding BSA-loaded solution into calcium chloride solution during agitation, and pectinate beads were instantly formed by ionotropic gelation. The entrapment efficiency of BSA was high. The presence of pectinolytic enzymes in the *in vitro* release medium facilitated the

drug release. However, additional experiments would be necessary to confirm the feasibility of the proposed formulation.

Chitosan is a high molecular weight cationic polysaccharide, poly(*N*-glucosamine), derived from naturally occurring chitin in crab and shrimp shells by deacetylation. Chitosan has been shown to be biocompatible and biodegradable with extremely low toxicity [64]. Chitosan is degraded by colon-rich microflora, and has been evaluated as an excipient for colonic specific drug delivery. Enteric-coated chitosan capsules were evaluated by Tozaki and Yamamoto *et al.* [35, 65] for colonic delivery of peptides including insulin. *In vitro* release studies using a marker molecule 5(6)-carboxyfluorescein (CF) showed little release of CF from the capsules in either artificial gastric juice (pH 1) or artificial intestinal juice (pH 7), but a marked release in the presence of rat cecal contents. Chitosan capsules containing insulin with or without differing protease inhibitors (bacitracin, aprotinin, and soybean trypsin inhibitor) and absorption enhancers (sodium glycocholate, sodium oleate and n-dodecyl-β-D-maltopyranoside) were enterically coated with hydroxypropyl methylcellulose phthalate (HPMCP) and intragastrically administered to rats. The chitosan capsules were able to function as an effective carrier to deliver insulin to the colon and increase insulin blood concentration in the presence of sodium glycocholate, as compared to gelatin capsules containing insulin or insulin solution. Hypoglycemic effects accompanied the increase in plasma insulin levels. The hypoglycemic effects were further increased by the co-administration of various protease inhibitors and absorption enhancers, especially in the presence of sodium glycocholate and aprotinin. The times to peak plasma insulin levels and hypoglycemic effects were in agreement with the GI transit time of chitosan capsules as measured in the same animal model, which supported the hypothesis that enteric-coated chitosan capsules were site-specifically delivered insulin to the colon. Similarly, Fetih *et al*. [66] evaluated using chitosan capsules for colonic delivery of ($Asu^{1,7}$)eel calcitonin (ECT). Chitosan capsules containing ECT and different absorption enhancers (S-nitroso-N-acetyl-

D,L-penicillamine, sodium glycocholate) and protease inhibitors (bacitracin, aprotinin) were enteric-coated with hydroxypropyl methylcellulose phthalate (HPMCP) and administered to rats. The hypoglycemic effects appeared 6-8 h after oral administration and sustained for 24 h. The greatest hypoglycemic effects were observed with chitosan capsules containing ECT with all four additives in combination. These results confirmed the feasibility of using enteric-coated chitosan capsules for colonic peptide or protein delivery. Bayat *et al.* [67] explored nanoparticles engineered from chitosan, triethylchitosan (TEC) and dimethylethylchitosan (DMEC) by polyelectrolyte complexation for colon delivery of insulin. TEC and DMEC were synthesized by partial quaternization of chitosan. Chitosan is positively charged at pH <6.5, and quaternized chitosan derivatives are permanently positively charged. In contrast, insulin is negatively charged at pH above its isoelectric point (apparent PI: 6.4). Therefore, insulin nanoparticles could be easily prepared by electrostatic interaction between positively charged chitosan or its derivatives and negatively charged insulin. Due to the harsh synthetic conditions, the molecular weight of quaternized derivatives was reduced, which resulted in smaller particle size. The insulin loading was more than 80% for all three types of nanoparticles (chitosan-insulin, TEC-insulin, and DMEC-insulin nanoparticles). The *in vitro* release showed a small burst release and then sustained release for 5 h. The release from TEC-insulin and DMEC-insulin nanoparticles was higher than chitosan-insulin nanoparticles due to higher solubility of TEC and DMEC polymers at neutral and alkaline pH. *In vivo* studies in streptozotocine-induced diabetic rats showed enhanced colon absorption of insulin via these nanoparticle carriers compared to free insulin. However, the slow *in vitro* release pattern of insulin might suggest that these nanoparticles of chitosan and its derivatives alone were not able to site-specifically release insulin in the colon and a combination with other targeting strategies would probably provide better targeting effects. Zhang *et al.* [68] performed *in vitro* evaluation of chitosan hydrogel beads containing bovine serum albumin (BSA) as a model protein for colon-specific delivery

of macromolecules. The hydrogel beads were prepared by polyelectrolyte complexation of chitosan with its counterion, tripolyphosphate (TPP). The protein release was markedly accelerated by the rat cecal and colonic medium independent of the pre-treatment conditions. A commercial almond beta-glucosidase preparation was less effective to degrade the chitosan containing beads, and therefore could not substitute for rat cecal and colonic enzymes for the *in vitro* assessment. The large amount of protein release in simulated intestinal fluid containing porcine pancreatin suggested a potential premature protein release in the upper GI tract, which was later confirmed to be attributed to the enzyme function of porcine pancreas lipase. Whether human lipase shares the same property to degrade chitosan needs further investigation. Degradation of chitosan-TPP beads in the rat cecal and colonic medium indicated the potential of the chitosan-containing beads to deliver macromolecules specifically to the colon. Smoum *et al.* [69] completed a proof-of-concept study of using a new chitosan-pentaglycine-phenylboronic acid conjugate as a multifunctional colonic-specific vehicle for oral delivery of salmon calcitonin. It was hypothesized that chitosan conjugates linked to a boronic acid protease inhibitor could protect peptide or protein drugs against proteolysis by serine protease. 4-formylphenylboronic acid was conjugated to chitosan with or without two spacers of glycylglycine and pentaglycine. Enzyme-inhibitory assays showed all the chitosan conjugates containing phenylboronic acid with or without spacers did not inhibit serine proteases, which was probably because the conjugates were too bulky to access the active sites of the enzymes. After incubation with chitosanase, the chitosan-pentaglycine-phenylboronic acid conjugates demonstrated inhibitory effects toward trypsin and elastase, and the inhibitory activity increased with the increase of substitution. Chitosan-pentaglycine-phenylboronic acid conjugates with the highest degree of substitution (43%) were able to decrease the salmon calcitonin degradation rate by trypsin in the presence of chitosanase, but still 60% of salmon calcitonin was lost in 10 min. The overall protection effect from the

proposed inhibitor conjugates was far enough to guarantee a colon-specific delivery, but it provided a proof-of-concept for further research to identify boron-based protease inhibitors.

Inulin is another naturally occurring polysaccharide found in plants. It consists of β-2-1 linked D-fructose molecules, and most fructose chains have a glucose unit at the reducing end [70]. It is not significantly hydrolyzed by the enzymes from endogenous secretions of human digestive tract [71]. However, colon bacteria, especially *Bifidobacteria,* which constitute up to 25% of normal human gut microflora, are known to ferment inulin [72, 73]. Inulin hydrogels have been investigated for colon drug delivery. *In vitro* degradation of inulinHP (inulin with an average degree of polymerization of 23) suspended in Eudragit RS films by human fecal bacteria was observed by Vervoot *et al*. [74]. To develop inulin hydrogels, Vervoot *et al*. [75] synthesized a methacrylated inulin (MA-IN) derivative. Cross-linked inulin hydrogels were prepared by free radical polymerization. The resulting hydrogels were shown to be degraded by the presence of inulinase concentration-dependently. To characterize MA-IN hydrogels with respect to their release properties, BSA or lysozyme was used as model proteins [34]. The results showed the *in vitro* release of incorporated protein from the MA-IN hydrogels was influenced by many factors such as drug loading procedure, loading concentration, protein molecular weight, the feed composition and degree of substitution of inulin. Protein release was greatly enhanced by the presence of inulinase. These hydrogels showed interesting properties related to colon-specific drug delivery systems, but more work like selection and optimization of the hydrogels and further in *vitro* and *in vivo* evaluations would be investigated for colonic drug delivery. More recently, Tripodo *et al*. [76] developed novel UV induced polysaccharide/poly(amino acid) hydrogels using human IgG as a model protein for colon delivery of peptide and protein drugs. A poly(amino acid), α,β-poly[*N*-(2-hydroxyethyl)-D,L-aspartamide], was functionalized with methacrylic anhydride, and the polysaccharide, inulin, was functionalized with methacrylic anhydrideand succinic anhydride. The hydrogels were engineered by UV

irradiation at low temperature without the use of radical initiators and in the presence or absence of a co-crosslinker, $PEGDM_{550}$. The obtained hydrogels were degradable by inulinase, did not cause significant variation in Caco-2 cell viability and the human IgG released from the hydrogels retained their biological activity. However, these hydrogels were not able to delay the protein release even in the release buffer without any enzymes. The hydrogels with the co-crosslinker showed pronounced burst release with about 70% of the entrapped protein released in 15 min, while hydrogels without the co-crosslinker showed a slower but steady protein release rate since time zero. These results indicated these hydrogels alone were not able to prevent the protein release into the upper GI tract.

Dextrans are polysaccharides composed of a linear backbone with mainly 1,6-α-β-glucopyraonosidic linkage. Dextrans are degraded by dextranases, enzymes secreted by gram negative bacteria in the colon especially *Bacteroides* [77]. Dextrans have been used as drug carriers for the formation of conjugates/prodrugs [43], and other type of dosage forms have been investigated as well. Basan *et al*. [78] studied dextran hydrogels for colon-specific delivery of salmon calcitonin (sCT). Biodegradable dextran hydrogels were synthesized by crosslinking dextran (T-70) with epichlorohydrin (ECH) in the presence or absence of ethanol at 10 and 23°C. *In vitro* biodegradation studies showed that dextran-ECH hydrogels were slowly degraded in buffer with dextranase at pH 5 and 7. *In vitro* release studies showed rapid sCT release from hydrogels prepared in the presence of ethanol in simulated colonic medium containing dextranase. However, without dextranase in the release medium, the sCT release was also substantial, although lower than that in the medium with dextranase, which indicated this dextran hydrogel system could provide sustained release of peptides or proteins, but probably not able to sufficiently protect them from premature release in the upper GI tract.

Starch is a naturally occurring polysaccharide most common in human diet. It is highly stable, safe, nontoxic, biodegradable, and has been used as an excipient in many

drug products. However, it is easily digestable by enzymes and acid in the upper digestive tract. For colon delivery purposes, starch was modified by cross-linking and pre-gelatinization to make it more resistant to digestion and acidolysis in upper GI tracts [79]. The modified starch was called resistant starch. Dry-coated matrix tablets consisting of a core with BSA and cross-linked pre-gelatinized starch shell were evaluated in simulated gastric fluid (SGF) for 2 h, and then in simulated intestinal fluid (SIF) for 6 h, and then in simulated colonic fluid (SCF) for additional 28 h. The BSA release in the SGF and SIF for the first 8 h was around 10%, and then dramatically increased in SCF, and reached 90% after 36 h. Overall, the cross-linked pre-gelatinized starch tablets showed a potential for targeting peptide and protein drugs to the colon. The same research group also investigated using acetylated maize starch as a tablet coating agent for colon targeting of biomacromolecule drugs [80]. Tablets based on microcrystalline cellulose containing BSA were coated with starch acetate with different degrees of substitution using a pan-coating apparatus. Similar *in vitro* release studies were performed in SGF, SIF and SCF. A higher degree of substitution by acetylation resulted in slower degradation of starch acetate. The release of BSA from uncoated tablets quick and 100% released within 4 h, while from starch acetate coated tablets in SGF and SIF after 6 h was less than 10%. The BSA release was greatly increased when incubated in SCF made of rat colonic content compared to buffer without colonic content. The results showed starch acetate coated tablets could potentially help the protein drug pass though the upper GI tract. Their further study on resistant starch acetate (RSA) coated pellets also showed promising results [81]. The effects of plasticizer content, film coating thickness, drug loading and drug molecular weight on drug release were investigated. An RSA film coating thickness of 7% (w/w) with 15% of plasticizer resulted in 12.8% drug release after the initial 8 h, and 68.2% drug release after 48 h. The drug release from RSA film coated pellets containing HGF, insulin and BSA, respectively, showed the diffusion of higher molecular weight through the RSA film was slower. SEM

examination showed the RSA film stayed intact in SGF and SIF, but showing cracks and holes in SCF after incubation. Collectively, the results indicated the potential of RSA film coated pellets as a colon-specific drug delivery system.

A novel targeted delivery system (CODES^{TM}) containing lactulose was investigated by Katsuma *et al*. [40, 82, 83]. Lactulose is a synthetic disaccharide, which is not absorbed in the upper GI tract, but degraded by enterobacteria to organic acids in the lower GI tract [84]. The concept of the CODES is shown in Figure 1.2 [40]. This system mainly included three components: a tablet core containing lactulose and drug, an inner acid-soluble coating layer, and an outer enteric coating layer. In the stomach, the drug was protected by the enteric coating layer and was not released. After reaching the small intestine, the enteric coating layer dissolved, but the drug was still not released from the core due to the presence of its inner acid soluble coating layer. However, the gastrointestinal fluid started to penetrate into the tablet core causing lactulose to dissolve during the small intestinal transit. When it arrived in the colon, lactulose leached out through the acid-soluble coating and was degraded by the colon bacteria producing organic acids. The organic acids would then dissolve the acid-soluble coating layer and release the drug. The onset of drug release *in vivo* from the CODES tablets using a model drug was proven to be dependent on the colonic availability rate of lactulose [83]. The CODES system was also explored for oral delivery of insulin to the colon [82]. Tablet cores containing insulin, lactulose and sodium glycocholate with or without other adjuvants were first coated with a mixture of Eudragit® E100 and RL100, and then coated with a layer of hydroxypropylmethylcellulose (HPMC) 2910 as an undercoating, and finally coated with enterosoluble Eudragit L100 as the outer layer. The colon-specific delivery of insulin from the CODES system was evaluated in beagle dogs. Results showed a sharp and sustained decrease in plasma glucose as well as an increase in insulin plasma levels after 6 h following oral administration of insulin-CODES tablets containing sodium glycocholate. The further addition of other adjuvants did not bring

significant changes in these data. The CODES system was shown to be a promising colon-targeting delivery system.

Limitations of microflora-dependent delivery systems

Criticisms have been raised on the microflora-dependent approach, especially because of the variability in the intestinal microflora. It is believed that the change of diet, stress, disease state or ongoing therapies may strongly affect the intestinal microflora composition, resulting in more intra- and inter-subject variation in delivery efficacy. Moreover, the application of synthetic polymers will likely add extra work load to the drug regulatory approval process because they are new chemical entities and require comprehensive safety evaluations before being used as drug delivery systems. Some criticism also questions the robustness of the microbiota-triggered degradation process of some polymers, like azo-polymers. It was pointed out that the azo function in azo-polymers was not always reduced in the same way as in small azo-aromatic molecules and the resulting degradation products were not always as thought to be aromatic amines [85]. Kimura *et al.* [86, 87] showed the azo bonds in polyurethanes were reduced to hydrazo intermediates after incubation with a culture of intestinal flora, because they did not observe any molecular weight reduction. Therefore, the drug release from pellets with these azo-polymer coatings was thought to be a result of a conformational change and breakdown of coating film. Schacht *et al.* [88] also observed that azo-containing polyamides were reduced to hydrazo intermediates or amines. It is also indicated that the microflora-triggered polymer degradation is strongly influenced by polymer hydrophilicity. If the polymer is too hydrophobic, enzymes cannot penetrate into the polymer network, leading to very slow polymer degradation. Only polymers with enough hydrophilicity can be degraded within an acceptable time frame, but too high hydrophilicity will lead to premature drug release before the colon is reached. In addition, the toxicity of azo-polymers is still under debate, and the

possible toxicity of the degradation products must also be considered [89]. The application of naturally occurring polymers is more preferred in the safety aspect, but more concerns are raised on their hydrophilicity and in some cases, they failed to effectively prevent the drug release from the upper GI tract. Some chemical modifications have been considered based on polymers of natural origin, but sometimes these derivitization products are less prone to degradation because they are no longer recognizable by the enzyme system responsible for biodegradation.

1.3.2 pH-dependent delivery systems

The pH-dependent delivery systems utilize the progressive increase in pH values along the GI tract. In this approach, enteric-soluble polymers are most often used as coating materials to prevent the drug dissolution and release from the upper GI tract. Some pH-dependent colonic delivery systems for peptide and protein drugs mostly using insulin as a model protein were reviewed as follows.

Enteric-coated capsules

Touitou *et al*. [90] investigated the effectiveness of colon-targeted delivery using small soft gelatin capsules filled with porcine insulin and a surfactant mixture (sodium laurate and cetyl alcohol) in arachis oil, and coated with mixtures of acrylic polymers (Eudragit® RS, L and S) at differing ratios. Two formulations without much premature release at pH < 7.0 were selected for an *in vivo* rat study, and showed promising hypoglycemic effects after approximately 2 h following oral administration. Interestingly, they also observed that the pre-administration of capsules only containing surfactants did not affect the glycemic profile, while the post-administration extended the hypoglycemic effect by one hour. This was explained as the results of differing absorption rates of the insulin and the enhancers employed. Ritschel *et al*. [91-93] explored colonic delivery of insulin in gel microemulsions

(MEs) encapsulated in formaldehyde-treated hard-gelatin capsules, which were further coated with a combination of acrylic polymers (Eudragit S100 and Eudragit NE 30D at a 3:7 ratio), followed by another coating layer of cellulose acetate phthalate. Five MEs containing insulin gelled by adding silicon dioxide were encapsulated, coated and orally administered to beagle dogs. One of them with ME consisting of polyoxylated caprylcaprinic acid glycerides (Labrasol®), polyglycerol isostearate (Plurol Isostearique), oleic acid decylester (Cetiol V) and triethanolamine/HCl buffer pH 7.4 showed greater pharmacological availability (PA) compared to its non-encapsulated liquid insulin ME and an insulin-free colon-targeted capsules, as well as the other four encapsulated gel MEs containing insulin. PA was calculated as the ratio of area under the curve (AUC) of glucose reduction vs. time profile after oral dosing to that after intravenous injection (i.v.), then corrected for dose strength. However, after *in situ* injected into isolated GI segments of rats, the liquid ME was able to lower blood glucose level only when insulin was delivered to the small intestine [91, 92]. It was suggested that bile salts and lipase in the small intestine played an important role for drug absorption when delivered by microemulsions. Gwinup, Elias and Domurat [94] reported a preliminary investigation of using methacrylic acid copolymer (soluble at pH >7) coated hard gelatin capsules for oral colonic delivery of bovine insulin. These copolymer coated capsules had shown to remain intact until they reached cecal area and then rapidly disintegrated via X-ray studies. Four to five hours after intake by three healthy volunteers, the plasma insulin concentrations increased significantly with a concomitant fall in the C-peptide concentration, which reflected the exogenous origin of the administered bovine insulin. This study demonstrated methacrylic copolymer coated capsules were able to deliver insulin to the proximal colon in a safe and simple manner. To measure both the portal and systemic insulin concentrations and glucose concentrations, recombinant human insulin encapsulated in methacrylic acid polymer (Eudragit S) coated capsules was introduced into the cecum of pancreatectomized pigs directly [95]. Following administration

of the insulin-containing coated capsules, both plasma insulin concentrations in the portal vein and systemic circulation increased greatly and peaked at 75 min. The increase in plasma insulin levels was accompanied by a corresponding decrease in glucose levels. The co-administration of a protease inhibitor aprotinin further enhanced insulin concentrations. Later, they also investigated orally administered insulin in enteric-coated capsules to streptozotocin-induced chronic diabetic pig model [96]. Similarly, recombinant human insulin-containing capsules were coated with pH-sensitive methacrylic acid copolymer and administered directly into the cecal lumen of the diabetic pigs. Results showed an increase in serum insulin with peak insulin concentrations observed between 2.5 to 4 h after insulin administration, and a decrease in serum glucose levels with nadir values seen between 3.5 to 5 h after insulin administration. After diabetic pigs received encapsulated insulin intracecally for 8 days, the serum glucose concentrations were comparable to those achieved with once-daily injections of subcutaneously administered insulin, and no injectable insulin supplementation was needed. However, the effects observed in the streptozotocin-induced chronic diabetic pig model appeared later and were not as good as reported in the acutely pancreatectomized pigs [95]. The difference was explained as due to the ablation of the glucogan-secreting cells in pancreatectomized pigs. Enteric-coated hard gelatin capsules containing microspheres were also investigated for oral colonic peptide delivery by Geary *et al.* [97]. Porcine insulin microspheres were prepared by a rotating disk method using Paramont X and Grocol 600E (triglycerides) as the matrix. *In situ* experiments in rats showed sodium glycocholate and Na_2EDTA could enhance the colonic absorption of insulin. Different formulations were tested using another marker molecule in rats and dogs. Insulin lipid microspheres were dry-mixed with Carbopol® 934 (1:1 by weight), sodium glycocholate and Na_2EDTA, and then encapsulated into Eudragit S100 coated hard gelatin capsules, and administered to two nondiabetic dogs. A modest but prolonged reduction in plasma glucose levels was observed. However, the limited animal

number (n = 2) impaired the statistical analysis of the data. More recently, Hong *et al*. [98] investigated the colon-targeted local delivery of a cell-permeable NFκB inhibitory peptide using colon-specific polymer coated capsules. To prepare colon-targeted capsules, rodent capsules containing a selected potent NFκB inhibitory peptide, CTP-NBD, were dip-coated with a layer of azo-containing polyurethane [87], which was further overlaid with Eudragit S100 for mechanical strength. Capsules coated only with Eudragit S100 were termed as enteric capsules. The colon targetability of the azo-polymer and Eudragit S100 coated capsules (colon-targeted capsules) were confirmed by X-ray studies with barium sulfate and FITC. The *in vivo* efficacy studies in 2,4,6-trinitrobenzenesulfonic acid (TNBS) induced rat colitis model showed that CTP-NBD in colon-targeted capsules ameliorated the rat colitis in a dose dependent manner with a parallel decrease in myeloperoxidase activity and levels of inflammatory mediators, while the colon-target NBD capsules and enteric CTP-NBD capsules did not improve the inflammatory events in the inflamed colonic tissue. It was suggested that the anti-inflammatory activity of the CTP-NBD observed via the colon-targeted capsules was mainly through local action, which was supported by a further study showing ameliated rat colitis after intracolonic treatment with CTP-NBD via the rectal route. A sharp concentration decrease of CTP-NBD-FITC in the submucosal layer compared to mucosal layer provided further supporting evidence for this argument. The overall results suggested that colon-specific targeted capsules were a viable approach to deliver cell-penetrating peptide conjugated therapeutic peptides locally to the colon for the treatment of colonic diseases, such as IBDs.

Enteric polymer-based microspheres

Enteric soluble polymers, such as Eudragit S100, were also investigated as coating or matrix-forming excipients to engineer microspheres for colon-targeted peptide and protein delivery. Paul *et al.* [99] explored the feasibility of using calcium phosphate ceramic

microspheres coated with a pH-sensitive methacrylate polymer for insulin colonic delivery. Tricalcium phosphate (TCP) is a safe and biocompatible material that has been used in human as bone substitutes by FDA and as a matrix for protein purification. Ceramic porous TCP microspheres in the size range of 106-200 μm were prepared by a standard procedure, loaded with porcine or human insulin by diffusion filling, and then coated with Eudragit S100. Insulin released in simulated intestinal fluid (SIF, pH 6.8) preserved the native conformation without showing any aggregation as assessed by Photon Correlation Spectroscopy (PCS) and Circular Dichroism (CD). *In vitro* release studies showed minimal insulin release in simulated gastric fluid (SGF, pH 1.2), a slow release in SIF and rapid release when the medium was switched to simulated intestinal fluid (SIF, pH 7.4). After oral delivery to streptozotocin-induced diabetic rats, enteric coated TCP microspheres containing either porcine or human insulin resulted in a decrease in elevated glucose level up to 50% of the initial value. The delivery of porcine insulin induced a dose-dependent response, while for human insulin the decrease in blood glucose level was much delayed, indicating the variation in action with different species of insulin. Jain *et al*. [100] studied microspheres using Eudragit S100 as the matrix-forming agent for oral colonic delivery of peptide drugs like insulin. Insulin-loaded microspheres were prepared by water-in-oil-in-water (w/o/w) double-emulsion solvent evaporation method with polysorbate 20 as a dispersing agent in the interal aqueous phase and polyvinyl alcohol (PVA)/polyvinyl pyrrolidone as a stabilizer in the external aqueous phase. The PVA stabilized microspheres showed a mean particle size of 32.51 ± 20 μm by laser diffractometry. Permeation enhancers were not used to avoid potential damage to the intestinal mucosa. *In vitro* release studies showed a 2.5% of insulin release at pH 1.0 in 2 h, while an initial burst release of 22% in 1 h followed by an additional 28% release over the next 5 h in phosphate buffer of pH 7.4. Oral administration of PVA-stabilized microspheres containing insulin in normal albino rabbits showed a remarkable decrease in blood glucose levels, with maximum glucose reduction in 2 h and lasted for up

to 6 h. Results indicated Eudragit S100 microspheres were promising delivery vehicles for protein and peptide oral intestinal delivery. Similarly, Jelvehgari *et al*. [101] formulated insulin microspheres using Eudragit S100 as the matrix by a water-in-oil-in-oil (w/o/o) double emulsion solvent evaporation method. Formulations with different drug/polymer ratios were prepared and characterized. The selected formulation showed a drug loading efficiency of 77% with a mean particle size of 222 μm. *In vitro* enzymatic degradation studies indicated insulin could be protected in the microspheres without much degradation after trypsinic incubation. After orally gavaged to streptozotocin-treated diabetic rats, insulin microspheres with or without protease inhibitor aprotinin yielded similar hypoglycemic effect. Torres *et al*. [102] explored using enteric soluble hydroxypropylmethylcellulose acetate succinate (HPMCAS) to encapsulate bovine insulin containing lipid microspheres for colon targeted delivery. The insulin microspheres were prepared by a modified solvent evaporation technique with the drug incorporated as a solid (s/o/w) or as a solution (w/o/w). Chitosan was added to the lipid (tetraglycerol pentastearate) matrix of insulin-loaded cores to provide potential mucoadhesive and absorption enhancing properties to the system. To encapsulate the lipid cores, a solvent extraction technique was employed, in which the microspheres were first suspended in an HPMCAS methylene chloride solution and then emulsified into PVA solution under mechanical stirring. The resulting pH-sensitive polymer coated microspheres showed a mean particle size around 170 μm. *In vitro* release studies in phosphate buffer of pH 7.4 showed a controlled and progressive release of insulin from lipid-chitosan cores made through both s/o/w and w/o/w methods. The HPMCAS lipid-chitosan cores represented a promising approach for the specific delivery of peptide to the colon region, but further work would be necessary to tailor the controlled release profile.

pH-sensitive hydrogels

pH-sensitive hydrogels using various polymers were also investigated as potential colon delivery systems for peptide and protein drugs. Mahkam [103] designed a hydrogel delivery system based on copolymers of 2-hydroxyethyl methacrylate (HEMA) and methacrylic acid (MAA) cross-linked with cubane-1,4-bis (methacryloyloxyethyl) carboxylate (CA) by free radical copolymerization. In the pH range of the stomach, the gels had a low degree of swelling and the drug would be protected against digestion by enzymes. The swelling of the hydrogels increased with increased pH as it passed down the GI tract. In the colon, the hydrogels swelled to a high degree and the drug was released. Insulin hydrogels were prepared by adding hydrogels in the insulin buffer, which was then dried under vacuum at room temperature. Insulin was physically adsorbed to the copolymers and stayed stable during *in vitro* release studies. The drug release of insulin showed to be depended on the swelling and hydrolysis of the network polymers, which were significantly affected by polymer composition. According to the different hydrolysis rate at pH 1 and pH 7.4, these hydrogels would be potential candidates for colon-specific drug delivery. Ramkissoon-Ganorkar *et al*. [104] investigated using pH/thermosensitive polymeric beads prepared from terpolymers of N-isopropylacrylamide (NIPAAm) (temperature-sensitive), butyl methacrylate (BMA) and acrylic acid (AA) (pH-sensitive) of various molecular weight at feed molar ratio of 85/5/10 for peptide/protein oral delivery. Insulin, as a model protein drug, was loaded into the beads by dropping a polymer solution with insulin prepared at low pH (pH 2.0) and below the lower critical solution temperature (LCST) into an oil bath above the LCST (35°C). *In vitro* release studies were performed at pH 2.0 and 7.4 at 37°C. Negligible insulin release was observed at pH 2.0, while at pH 7.4, substantial insulin release at varying release rate as a function of polymer molecular weight was observed. The high molecular weight polymeric beads swelled slowly and gradually released the loaded insulin over 8 h due to increased cross-linking. The loaded and released insulin were confirmed to be fully

bioactive. The high molecular weight polymeric beads could be potentially used to target protein drugs to the colon.

pH-sensitive dextran hydrogels as a potential colon-specific drug delivery system was reported by Chiu *et al*. [105]. This pH-sensitive dextran hydrogel system was designed for colon drug delivery based on two reasons: (1) the hydrogels exhibited a low degree of swelling at low pH, and increased swelling with pH increase along the GI tract, which would protect bioactives from enzymatic degradation; and (2) the hydrogel swelling and enzymatic degradation in the colon would facilitate site-specific drug release. To prepare pH-sensitive dextran hydrogels, dextran was activated by 4-nitrophenyl chloroformate, and then conjugated with 4-aminobutyric acid and cross-linked with 1,10-diaminodecane. Incorporation of carboxylpropyl groups in dextran hydrogels led to a faster swelling at high pH. BSA was used as a model protein in release studies. The BSA release from one of the hydrogels showed relatively slow release at pH 2.0, highly enhanced release in a pH 7.4 buffer and further increased and complete release by adding dextranase in the buffer of pH 7.4. The polymer swelling extent was a primary factor to determine the drug release rate. Lowman and Peppas *et al*. [5] investigated the use of pH-responsive, poly(methacrylic-g-ethylene glycol) (abbreviated as P(MAA-g-EG)) hydrogels for insulin oral intestinal delivery. Microparticles of P(MAA-g-EG) were prepared by a free-radical polymerization of methacrylic acid and poly(ethylene glycol) monomethacrylate (PEGMA). The resulting polymer exhibited pH sensitive swelling behavior because of the reversible formation of interpolymer complexes, which were stabilized by hydrogen bonding between the carboxylic acid protons and the etheric groups on the grafted chains. In the stomach, these gels were unswollen due to the polymer complexation, and at the basic and neutral pH in the lower GI tract, the complexes dissociated and resulted in rapid gel swelling and drug release. Porcine insulin was loaded to P(MAA-g-EG) microparticles by equilibrium partition. The insulin loaded microparticles were then dried under vacuum, encapsulated into gelatin

capsules and orally administered to healthy and streptozotocin-induced diabetic rats. Within 2 h following oral administration of insulin-containing complex gels, strong dose-dependent hypoglycemic effects were observed in healthy rats, and even much stronger hypoglycermic effects were obtained in the diabetic rats. These hypoglycermic effects lasted for up to 8 h and were observed without the addition of protease inhibitors or absorption enhancers. A comparison study to Eudragit L100 microspheres in healthy rats showed insulin in these complex gels induced much greater hypoglycemic effects than the Eudragit L100 microspheres because of the presence of PEG grafts in the complex gels, which stabilized insulin. Due to the neutral to weakly alkaline pH encountered in the lower small intestine, insulin in these complex gels was probably delivered and released into the distal small intestine. The neutral to weakly alkaline pH values in the distal small intestine proposed a potential hurdle for all the pH-dependent formulations for colonic drug delivery. A combination with other colon-targeting strategies would make pH-dependent formulations more applicable to deliver drugs specifically to the colon.

1.3.3 Time-dependent delivery systems

The time-controlled oral delivery system for colon-targeting relied on the reasonably predictable small intestine transit time, which was remarkably constant in the range of 3 ± 1 h (mean ± SD) independent of the dosage forms and fasting or fed states of the subjects [106, 107]. Contrary to the constant small intestinal transit, the gastric emptying time was highly variable and affected by many factors, such as the quantity and nature of the food, or the nature of the dosage forms. To design time-dependent systems for colon delivery, the dosage forms had to stay intact in the stomach during the unpredictable gastric resident time, and after entering the duodenum, they would be triggered to start a lag time of at least 3 h, during which the drug should still be protected without significant release before the colon was reached. The trigger to initiate the lag time in the small intestine was generally

based on the sharp change in the pH between the stomach and the intestine, and thus, a layer of enteric coating is often used. Based on different design characteristics and release mechanisms, the most often encountered time-dependent delivery systems could be categorized into reservoir, capsular and osmotic platforms [108]. Reservoir systems were the largest and most versatile among these three categories. They mostly comprised an inner drug-containing core and an outer release-controlling layer, and could be further differentiated into erodible, rupturable, and diffusive reservoir systems. Erodible systems were mainly obtained by the application of hydrophilic swellable polymers. Hydrophilic cellulose derivatives, such as hydroxypropylmethylcellulose (HPMC), hydroxyethylcellulose (HEC) and hydroxypropylcellulose (HPC), were widely used mainly because of their safety profile, versatility and cost-effectiveness. The application of these polymers was generally done by press-coating, spray-coating and powder-layering techniques. When contacting aqueous media, these polymers underwent swelling, dissolution and erosion, so to delay the onset of drug release for a certain lag time depending on the polymer type and coating thickness. Additionally, a mixture of wax and surfactant was also explored as an erodible coating material [109]. With the polymeric or wax coating layer, plus another enteric coating as the outer layer, the erodible systems using the combination of both pH- and time-dependent principles had exhibited very promising colon targeting results. The rupturable reservoir systems for time-dependent drug release to the colon were often composed of inner drug cores coated with a water insoluble and modestly permeable polymeric film. Ethylcellulose (EC) in combination with a plasticizer and/or a pore-forming agent was frequently used. In general, the polymeric film was ruptured mechanically by the expansion of the core formulation. For diffusive reservoir systems, the drug release was delayed by the time lapse required for full water penetration through the diffusive layer, which should prevent drug release from the upper GI tract during transit. For example, drug-containing cores coated with a layer of Eudragit RS mixed with pore-forming agents delayed drug

release until the pore-forming agents were entirely dissolved and a pore network was formed in the outer coating layer, which allowed water influx and drug release to be accomplished [110]. With a layer of diffusive coating, a fast drug release following the lag time could be hard to achieve. Capsular systems for potential colon targeting were designed in the form of capsules with a release-controlling polymeric plug inserted in their body opening. The physical-chemical properties, size and position of the plug all would influence the duration of the lag time. An example is the device of Pulsincap® (Scherer DDS Ltd), which consisted of a water-soluble cap and a rigid, insoluble and impermeable body filled with the drug and sealed with a hydrogel plug of crosslinked PEG_{8000} [111]. When contacting with the aqueous media, the cap quickly dissolved and the plug started swelling until ejection from the body, thus releasing the drug. Osmotic time-dependent systems were also explored for colonic drug delivery. A recent example is a tablet system containing a bronchodilator for the treatment of nocturnal asthma using sodium chloride as an osmotic agent [112]. This osmostic system contained a low swellable HPMC layer and an outer insoluble and moderately permeable film composed of Eudragit RS/Eudragit RL mixtures. *In vitro* studies showed pulsatile delivery after delayed times depending on the external coating thickness, and the delivery was unaffected by pH. Through these varieties of mechanisms, *i.e.*, programmable disruption, swelling/erosion, dispersion, pH-induced dissolution, water-permeation of the polymeric coatings, or a timed ejection or a progressive erosion of matrix plugs sealing capsular devices etc., time-based colon delivery approaches have accomplished promising results. Some examples using time-based systems for peptide and protein colon delivery are described as follows.

A time-dependent delivery platform (Chronotopic™) was investigated for oral colonic delivery of insulin by Marino *et al*. [113]. The influence of manufacturing process and storage conditions on bovine insulin was evaluated. Insulin and its degradation products were assayed after each processing steps by HPLC. The powder mixing, direct

compression of the insulin-loaded cores, and aqueous spray-coating of HPMC at elevated temperature showed no major impact on insulin content and its corresponding degradation products. After long-term storage at 4°C for one year, approximately 5% of insulin was degraded with a slightly increase in degradation products, which were still within their compendia limits. The insulin *in vitro* release behavior from the Chronotopic™ formulation in terms of the lag time and release kinetics was unchanged after the one year storage (4°C) as well. In addition, the compatibility of insulin with a selected protease inhibitor (camostat mesilate) and absorption enhancer (sodium glycocholate) in solid state (physical and compacted power mixtures) was assessed [114]. After storage at 4°C for 12 months, the decrease in insulin content and increase in degradation products were not significant and all within the compendia limits. The HPMC coated unit containing insulin and the adjuvants (camostat mesilate and sodium glycocholate) showed a fast and quantitative release of insulin and the adjuvants after a reproducible lag time. Based on a hypothesis that the adjuvant release prior to that of the protein could potentially further improve the protein absorption, Del Curton *et al*. [114] investigated using a two-pulse time-based system for colonic delivery of protein drugs and protease inhibitors/absorption enhancers. This system consisted a drug-containing immediate-release tablet cores, an inner swellable/erodible low-viscosity HPMC coating, an intermediate adjuvant layer and an additional outer layer of HPMC coating. For gastro-resistant systems, another enteric coating of Eudragit L 30D-55 layer was applied. Different thickness of the HPMC coating layers and the camostat mesilate/sodium glycocholate coating layers were applied to the immediate-release cores containing bovine insulin. The outer HPMC layer was applied to delay the adjuvant release in the small intestine, while the inner HPMC layer was designed to delay the insulin release. *In vitro* release studies in hydrochloric acid medium (pH 1.2) for 2 h and then phosphate buffer (pH 6.8) showed that all the systems exhibited satisfactory pulsatile release behavior, with a programmable lag phase before the protease inhibitor/absorption enhancer release,

and another lag phase before insulin release. This two-pulse time-based system could be easily modulated in terms of the lag times by HPMC coating thickness and could be an interesting candidate for colon-specific delivery of peptide and protein drugs.

Although showing promising results *in vitro* and some even in animals, criticisms have arisen on time-based colon delivery systems. One of the criticisms related to the highly variable and unpredictable gastric emptying time, which varied with the feeding conditions (such as fasted or fed, light meal or heavy meal) and the physical forms of the drug formulations, etc. [107]. To develop effective time-based delivery systems, the drug to be delivered has to be completely protected while in the stomach before exploring the subsequent relatively constant small intestinal transit time (3 ± 1 h, Mean ± SD) [106, 107]. Another criticism is related to the formulation evaluation methods. It is generally hard to set up *in vitro* performance evaluation experiments that would correlate very well to the *in vivo* situations because of many factors involved, such as pH, ionic strength, surfactants, enzymes, microorganisms, viscosity, gas, intraluminal pressure, intestinal motion and water content in different GI segments [115]. *In vivo* evaluations have been investigated using animal models, but this approach has been criticized for being poorly representative of the human GI transit. Therefore, *in vivo* scintigraphic imaging studies have been performed on human subjects. For example, Hodges *et al*. [116] utilized scintigraphy imaging to evaluate colon-targeting pectin-HPMC tablets in six healthy volunteers. The pectin-HPMC coating was applied by press-coating method. Scintigraphy studies provided solid proof that the pectin-HPMC coating was robust enough to protect the tablets during transit until they reached colon intact in all the subjects without any premature release in the upper GI tract. Human scintigraphic imaging studies are effective *in vivo* evaluations tools, but they are costly and not always easy to access.

1.3.4 Other formulations

In addition to the aforementioned three major types of colon-specific delivery systems, several other types of formulations have been explored for targeting peptide and protein drugs to the colon as well.

Microspheres/Spheres

Kimura *et al*. [117] explored using poly(vinyl alcohol)-gel spheres to delivery insulin to the lower intestine of diabetic rats. The insulin-containing PVA spheres were prepared by ultrasonic agitation. After intragastric administration of PVA spheres containing insulin with or without aprotinin or bacitracin to streptozotocin-induced diabetic rats, significant and prolonged reduction of blood glucose levels were observed. The prolonged residence time of PVA spheres in the lower intestine and synchronous release of insulin and the protease inhibitor were accounted for the improved hypoglycemic effects. Jiang *et al*. [118] investigated bioadhesive fluorescent microspheres as visible carriers for local delivery of proteins, and insulin was used as a model protein in the study. Intrinsic fluorescent microspheres were prepared using a combination of a fluorescent polyanhydride, poly(p-(carboxyethylformamido) benzoic anhydride) (PCEFB), and poly(lactide-*co*-glycolide) (PLGA) by the water-in-oil-in-water (w/o/w) double emulsion solvent evaporation method. The application of intrinsic fluorescent microspheres as drug carriers could circumvent the complex fluorescent dye labeling process and avoid the interference from free dye leached into the tissue. *In vitro* release studies in PBS at pH 7.4 showed sustained release of insulin over a period of around 4 days. The insulin-loaded PCEFB/PLGA microspheres with the diameter of less than 5 μm (70 % of spheres < 2 μm) were further evaluated in streptozotocin-induced diabetic rats [119]. After oral feeding of a single dose of microspheres, plasma glucose levels were reduced to subcritical levels within 4 h and the hypoglycemic effects lasted up to 6 h. Fluorescence microscopy studies showed these

microspheres could adhere to the intestinal epithelium and traverse the absorptive cells. The intrinsic fluorescence highlighted these microspheres for convenient *in vitro* and *in vivo* evaluations. With combination of other colon-targeting strategies, these microspheres could be potentially applied for local intestinal peptide/protein delivery, such as colon-specific delivery. Lamprecht *et al*. had developed microparticles [120] and nanoparticles [121] for colonic drug delivery. They studied the size-dependent deposition of microparticles and nanoparticles to the inflamed colonic mucosa in trinitrobenzenesulfonic acid (TNBS) induced colitis rat models after oral administration [122]. Their results showed significantly increased deposition of particles at the thicker mucus layer and in the ulcerated regions compared to that in the healthy control group. The accumulation of particles also size-dependently increased with the decrease of particle size from 10 μm to 0.1 μm. These results shed some light on considerations of designing particulate carriers for local delivery of drugs for the treatment of inflammatory bowel disease (IBD).

Nanoparticles

Nanoparticle-based delivery systems have also been explored to target drugs to the colon, especially for the treatment of IBDs. Theiss *et al*. [33] reported oral delivery of a biologically active protein, prohibitin (PHB), by nanoparticles encapsulated in hydrogel to the colon. Prohibitin1 (PHB) is an evolutionarily conserved, multifunctional 30 kDa protein, which is decreased in mucosal biopsies from IBD patients and in animal models of colitis. Restoration of PHB has shown to reduce the severity of colitis. The nanoparticles were prepared by double emulsion solvent evaporation method. Recombinant human PHB was complexed to polyethyleneimine (PEI) and then to bovine serum albumin (BSA). The PHB complex was surrounded by poly(lactic acid) (PLA) in a water-in-oil emulsion to form the core, which was then further coated with polyvinyl alcohol (PVA) in a second water-in-oil-in-water emulsion. The resulting nanoparticles had a diameter of around 440 nm. The PHB-

loaded nanoparticles were then encapsulated into a polysaccharide solution of alginate (7 g/L) and chitosan (3 g/L). This PHB-loaded nanoparticles in polysaccharide solution was orally gavaged to dextran sodium sulfate (DSS) treated mice, followed by oral administration of the chelation solution of calcium chloride and sodium sulfate. A hydrogel containing nanoparticles was then formed inside the mouse stomach. The PLA/PVA based nanoparticles had shown previously to release content at pH 6.0, so as to protect drugs from degradation at acidic pH and by digestive enzymes [123]. Mice treated with PHB-loaded nanoparticles showed increased levels of PHB in the colon surface epithelium and ameliorated DSS-induced colitis as indicated by body weight loss, clinical score, myeloperoxidase activity, proinflammatory cytokine expression, histological score and protein carbonyl content. This approach was also investigated to deliver an anti-inflammatory tripeptide Lys-Pro-Val (KPV) to the colon [123]. These nanoparticles were shown to be safe and did not affect cell viability or barrier functions. After oral administration of dextran-FITC-loaded nanoparticles in the polysaccharide solution/chelation solution to mice, a much higher level of dextran-FITC was observed in the colon than in other GI tissue sections, indicating that nanoparticle release from the polysaccharide hydrogel happened mostly in the colonic lumen compared to other parts of the GI tract. Oral gavage of KPV-loaded nanoparticles in alginate and chitosan solution with a following oral administration of chelation solution resulted in significantly reduced DSS-induced colonic inflammation. Using these nanoparticles with polysaccharide hydrogel, KPV could be delivered at a much lower (12,000-fold lower) concentration than using KPV free solution, while still eliciting similar therapeutic efficacy. The system of PLA/PVA-based nanoparticles in a polysaccharide solution/chelation solution with a double gavage method seemed to be a feasible platform for colon-specific peptide and protein delivery. More recently, Coco *et al.* [32] compared using three different polymeric nanoparticles to deliver peptide or protein drugs to the inflamed colon. Ovalbumin (OVA) was used as a model drug. pH sensitive nanoparticles

were prepared from Eudragit S100 by a water-in-oil-in-water (w/o/w) method. Mucoadhesive nanoparticles were engineered with trimethylchitosan (TMC) by ionic complexation/gelation method. PLGA-based nanoparticles were prepared from the mixture of PLGA, PEG-PLGA and PEG-PCL by a w/o/w double emulsion solvent evaporation method. Immune cell targeting ligands (GSQSHPRH and mannose) were grafted onto the PEG chain of PCL and incorporated into the PLGA-based nanoparticles. *Ex vivo* studies in horizontal diffusion chambers were set up using healthy mouse colon or inflamed colon from DSS-treated mice. Mannose-grafted PLGA nanoparticles resulted in the highest accumulation of OVA in the inflamed colon compared to the other formulations. Results suggested nanoparticles targeting immune cells in the inflamed colon might be a promising approach for the treatment of IBD.

Multiple emulsions

Matsuzawa *et al*. [124] investigated using w/o/w emulsions as carriers for insulin intestinal delivery. The emulsions were prepared by a two-step emulsification procedure. Gelatin was added to the inner phase containing insulin, which was then emulsified into the oil phase of 5% lecithin, 20% Span 80 and 75% soybean oil. Water containing 3% Tween 80 was used as the outer aqueous phase. A significant hypoglycemic effect was observed after administration of the emulsion into the cecum and colon using an in situ loop method. Later, two highly purified polyunsaturated fatty acids, eicosapentaenoic acid (EPA) and docosahexaenoic acid (DHA), were incorporated into the insulin w/o/w emulsions and evaluated in *in situ* and *in vivo* experiments [125]. Water-in-oil-in-water emulsions containing insulin and 2% DHA or EPA resulted in potent increase of serum insulin levels and decrease of serum glucose levels after administered into the colonic and rectal loops *in situ.* Insulin dose-related responses were observed, especially with the presence of DHA. In the *in vivo* absorption experiments, rectal administration of insulin emulsion with 2% DHA produced

rapid but short increase of serum insulin levels along with a strong decrease of serum glucose levels lasted for 4 h. Lactate dehydrogenase (LDH) release studies showed emulsions with 2% DHA or EPA did not induce significant LDH release. These findings indicated that the w/o/w emulsions with highly purified long-chain polyunsaturated fatty acid could be potential carriers for intestinal delivery of insulin, and other protein and peptide drugs.

Liposomes

Manosroi *et al*. [126] studied the gastrointestinal delivery of human insulin and an human insulin complex using different liposomes. The insulin-DEAE (diethylaminoethyl) dextran complex was designed to avoid leakage of insulin from liposomes by increased molecular size and potentially improve its intestinal uptake. When administered intravenously in normal rats, the human insulin and human insulin-DEAE dextran complex exhibited same blood glucose lowering effects. Positive, neutral and negative liposomes were prepared by high pressure homogenization using a hydrogenated soy lecithin. The human insulin-DEAE complex in reconstituted positive liposomes resulted in more effective blood glucose lowering effects when injected into the colon compared to the duodenum of normal rats. The complexed insulin in positive liposomes seemed to be more stable and better absorbed in the colon than in the duodenum. Goto *et al*. [31] investigated intestinal mucosal delivery of insulin using novel fusogenic liposomes (FLs), which can directly deliver encapsulated contents to the cytoplasma through membrane fusion with the help of envelope proteins of Sendai virus (SeV). Unilamellar liposomes containing insulin were prepared by the freeze-thawing method with or without insulin-degrading enzyme (IDE) inhibitor PCMB. Then, the unilamellar liposomes were mixed with SeV and incubated at 37°C for 2 h, which were further purified by sucrose density-gradient centrifugation. Following *in situ* administration of into the colonic and rectal segments, insulin-loaded FLs

resulted in a significant increase in plasma insulin levels with a decrease in blood glucose levels compared to insulin solution or insulin liposomes. These effects were further improved by the addition of IDE inhibitor into insulin FLs. In contrast, after the insulin-loaded FLs were administered into the ileal segment *in situ,* no apparent increase in plasma insulin levels or decrease in blood glucose levels were observed, which was because the mucous/glycocalyx layers over the ileal epithelium functioned as a barrier to hinder the fusion of liposomes to the ileal membrane. This was confirmed by enhanced SeV viral gene expression in the ileum not the colon or the rectum with hyaluronidase pretreatments. LDH leakage experiment showed that insulin-loaded FLs did not cause intestinal mucosal damage. These results suggested fusogenic liposomes might be a novel mucosal delivery method to improve the targeting of macromolecules, such as peptides, proteins or gene, to the colon region. Liposomes have been widely studied as drug delivery carriers for many bioactive molecules. They can be easily modified with a variety of targeting moieties to improve their site-specific delivery. However, liposomes as drug delivery systems are also limited by some potential problems, such as the leakage of water-soluble drugs during GI transit, the low drug entrapment efficiency, the heterogeneity of particle size, the poor batch to batch reproducibility, the instability of liposome formulations and the short circulation half-life [127]. Some of the issues have been resolved, such as increasing stability by lyophilization, but there are still more to be improved to develop effective clinically applicable formulations.

1.4 Concluding Remarks

Intestinal delivery, and especially colonic delivery of peptide and protein drugs, has gained a great deal of attention in the past two decades. The colon as a multi-functional organ possesses unique anatomical and physiological properties that distinguish itself from other part of the GI tract. Local colonic delivery has been considered beneficial not only for the treatment of local diseases, such as IBDs, but also for its potential to improve systemic

delivery of peptide and protein drugs. For either local or systemic delivery, peptide and protein drugs need to be successfully protected from the harsh acidic environment in the stomach and the extensive enzymatic digestion in the small intestine, and safely arrive at the colon to exert their local therapeutic effects or to be absorbed into systemic circulation. A wide variety of colonic delivery strategies have been explored based on the unique features of the colonic environment, such as pH values, enzymes produced by colonic bacteria, and GI transit time. Accordingly, these approaches are classified into three major categories: microflora-dependent systems, pH-dependent systems and time-dependent systems. The chemical modification of drugs or carriers based on enzymes in the colon has been successful for colonic delivery of small molecules, such as sulphasalazine, but has not extensively been explored for peptide and protein drugs, most likely due to the constraints of preserving their biological activities and the requirement for safety and efficacy profiles for the resulting derivatives and degradation products. Other microflora-dependent systems are mostly developed based on azo-polymers and polysaccharide-based polymers. These polymers are specifically degraded by colonic bacteria, and have been used as coatings and/or matrix forming agents. Due to the debate on the potential toxicities related to azo-polymers, natural-occurring polysaccharides become more popular. However, some of them are too hydrophilic leading to premature release in the upper GI tract. To resolve this problem, chemical modifications were done to make polysaccharide derivatives with increased hydrophobicity. Microflora-based systems have showed promising results based on its design principle. pH-dependent systems have been used as a colon delivery platform in clinic for the treatment of IBD patients. Based on the progressive increase in pH values along the GI tract, various pH-responsive materials, such as Eudragit S100, were applied as coatings, matrices or hydrogels for colon-targeted delivery. Time-dependent systems were designed based on the relative constant small intestinal transit time (3 ± 1 h). The pH difference between the stomach and small intestine was often used as a trigger signal to

initiate the lag time before the drug was released in the colon. Time-based devices for colonic delivery can be classified into reservoir, capsular and osmotic delivery systems. Scintigraphy studies have proved the feasibility for colon-specific delivery using some of the time-based systems. The above mentioned GI physiology-based systems for peptide and protein colonic delivery have shown promising results with success to different extent. However, these systems are susceptible to the GI physiological changes, which are often affected by diet, stress and medications etc. Meanwhile, the GI physiology is known to be affected by the patient disease state. For example, patients with active ulcerative colitis showed a wide range of pH values in the cecum and ascending colon and lots of them showed much lower pH values compared to that in healthy subjects [27]. Therefore, a combination of different colon targeting strategies is recommended to achieve effective local peptide and protein colon-targeting. Furthermore, the patient disease state should be considered during formulation design and the delivery efficacy of the colon-targeting formulations should be evaluated in patients as well. In addition to these GI physiology-based formulations, a variety of other formulations were also explored for intestinal or colonic delivery of peptide and protein drugs, such as microspheres, nanoparticles, liposomes, multiple emulsions. Most of these formulations showed better delivery efficacy compared to the controls. Finally, numerous studies have observed enhanced colonic peptide or protein delivery when protease inhibitors were co-administered or co-formulated. Therefore, after qualitative and quantitative selection, protease inhibitors might be able to further enhance the colonic peptide/protein delivery. Since the co-formulated protease inhibitor(s) would be selectively released into the colon, it would raise less concerns about their potential influence on the digestive enzymes in the upper GI tract.

Table 1.1 Properties of human GI-tract related to local oral peptide and protein delivery[a].

GI region		pH	Transit time (h)	Bacterial concentration (CFU/mL)
Stomach		1-3.5	0.5-4.5	$< 10^3$
Small intestine	Proximal	5.5-7.0	3-4	10^3-10^4
	Distal	6.5-7.5		
Large intestine	Cecum/Ascending colon	5.5-7.5	18-144	10^{11}-10^{12}
	Descending colon/ Rectum	6.5-7.5		

[a] Adapted from References [18, 27, 41, 128].

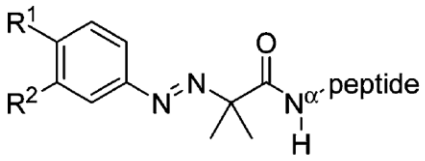

a. $R^1 = CH_2COOH$, $R^2 = H$; **b**. $R^1 = OH$, $R^2 = COOH$.

Figure 1.1 The structural design of the azo-prodrugs (Reprinted with permission from reference [52]. Copyright © 2011, American Chemical Society).

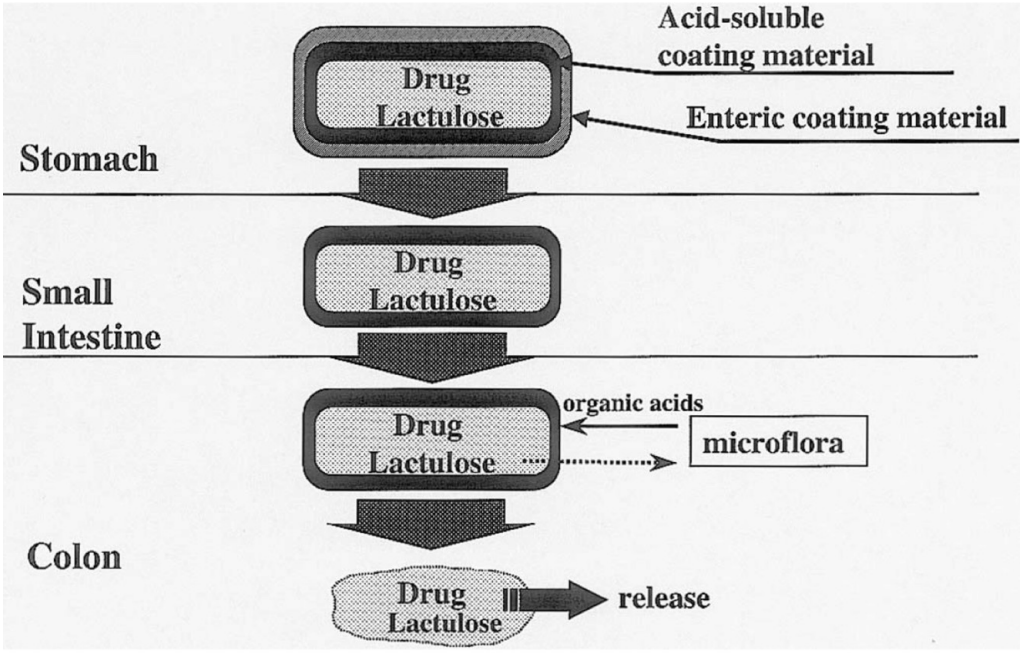

Figure 1.2 The concept of CODES for colon-targeted drug delivery (Reprinted with permission from reference [40]. Copyright © 2002, Elsevier).

Chapter II

In Vitro and *In Vivo* Evaluation of a Water-in-Oil Microemulsion System for Enhanced Peptide Intestinal Delivery

2.1 Summary

Peptide and protein drugs have become the new generation of therapeutics, yet most of them are only available as injections, and reports on oral local intestinal delivery of peptides and proteins are quite limited. The aim of this work was to develop and evaluate a water-in-oil (W/O) microemulsion system *in vitro* and *in vivo* for local intestinal delivery of water-soluble peptides after oral administration. A fluorescent labeled peptide, 5-(and-6)-carboxytetramethylrhodamine labeled HIV transactivator protein TAT (TAMRA-TAT), was used as a model peptide. Water-in-oil microemulsions consisting of Miglyol 812, Capmul MCM, Tween 80 and water were developed and characterized in terms of appearance, viscosity, conductivity, morphology and particle size analysis. TAMRA-TAT was loaded and its enzymatic stability was assessed in modified simulated intestinal fluid (MSIF) *in vitro*. In *in vivo* studies, TAMRA-TAT intestinal distribution was evaluated using fluorescence microscopy after TAMRA-TAT microemulsion, TAMRA-TAT solution and placebo microemulsion were orally gavaged to mice. The half-life of TAMRA-TAT in microemulsion was enhanced nearly three-fold compared to that in the water solution when challenged by

---

Liu D, Kobayashi T, Russo S, Li F, Plevy SE, Gambling TM, Carson JL,and Mumper RJ, "*In Vitro* and *In Vivo* Evaluation of a Water-in-Oil Microemulsion System for Enhanced Peptide Intestinal Delivery." *The AAPS Journal,* 2013, Jan; 15(1):288-98. Epub 2012 Nov 30.

MSIF. The treatment with TAMRA-TAT microemulsion after oral administration resulted in greater fluorescence intensity in all intestine sections (duodenum, jejunum, ileum and colon) compared to TAMRA-TAT solution or placebo microemulsion. The *in vitro* and *in vivo* studies together suggested TAMRA-TAT was better protected in the W/O microemulsion in an enzyme-containing environment, suggesting that the W/O microemulsions developed in this study may serve as a potential delivery vehicle for local intestinal delivery of peptides or proteins after oral administration.

2.2 Introduction

With biotechnological advances, peptide- and protein-based drugs have gained an increasing and irreplaceable share of the pharmaceutical market. However, the majority of peptide and protein pharmaceuticals such as insulin, monoclonal antibody-based drugs, human growth hormone and interferon-α require administration as injections [129]. As a consequence, more widespread applications to treat chronic conditions where the patient can self-medicate are limited. The past decades have seen a great deal of efforts to develop nonparenteral routes of delivery for peptides and proteins. Oral delivery may be the most attractive route yet arguably the most challenging due to poor chemical and physical stability of these molecules. Being polymers of amino acids linked together by peptide bonds with specific three-dimensional conformations [130], most peptides and proteins are hydrophilic with poor membrane permeability, susceptible to proteolytic degradation and low gastric pH. To overcome these obstacles, many strategies have been applied, such as macromolecular chemical modifications [131-133] and simple and complex formulation approaches [5, 134, 135]. Among various formulation approaches, microemulsions [130, 136] have received considerable attention for the oral delivery of peptides and proteins, especially for enhanced oral absorption [137, 138].

Microemulsions are thermodynamically stable dispersions of two immiscible liquids stabilized by surfactants [138], and mainly classified into three categories: (a) oil-in-water (o/w); (b) water-in-oil (W/O); and (c) bicontinuous microemulsions. Oil-in-water microemulsions are promising in improving the bioavailability of hydrophobic molecules, including hydrophobic peptides, such as cyclosporine A [139]. Water-in-oil microemulsions, on the other hand, have shown potential to improve the oral delivery of hydrophilic peptides or proteins [137, 138, 140, 141]. The mechanisms proposed for improved bioavailability using W/O microemulsions were based on increased protection from luminal enzymatic degradation and/or enhancer-induced structural and fluidity changes in the mucosal

membrane [140, 142, 143]. The safety evaluation of several orally delivered W/O microemulsions has been investigated [137, 138, 141], and histological examination showed no intestinal tissue damage or irritation upon acute dosing of the specific vehicles.

However, so far, most investigations of W/O microemulsions for peptide or protein oral delivery have been focused on systemic absorption, while the local intestinal delivery of peptides or proteins for the treatment of local pathologies has been less studied. In this work, the potential of W/O microemulsions for local intestinal delivery of water-soluble peptides after oral administration was explored. The ultimate goal of this work was to develop an oral dosage form to deliver therapeutic peptides locally to the gastrointestinal tract for the treatment of gastrointestinal inflammatory disorders. In gastrointestinal inflammatory disorders, like inflammatory bowel disease (IBD), there is a significant unmet need to deliver immunomodulatory compounds directly to the intestinal mucosa to maximize local concentrations (thereby efficacy) and to minimize systemic toxicity. A novel nuclear factor kappa-light-chain-enhancer of activated B cells (NF- κB) inhibitor peptide, 8K-NBD (KKKKKKKKGG-TALDWSWLQTE), has shown efficacies *in vitro* and *in vivo* to inhibit activated NF-κB, a hallmark of chronic inflammation, but not basal NF-κB activity, and ameliorated intestinal inflammation in experimental IBD models [144]. The selective targeting of 8K-NBD to activated NF-κB makes it an excellent therapeutic candidate and our research interest. However, a significant challenge for oral delivery of 8K-NBD is the chemical and biological degradation in the gastrointestinal tract. To address this issue and deliver 8K-NBD or other water-soluble peptides locally to the inflamed intestine, the peptide will be incorporated into W/O microemulsions, which will be followed by encapsulation of the optimal W/O microemulsion into enteric-coated capsules to further enhance local peptide delivery in the GI where needed. The current work is to test the first part of the hypothesis that W/O microemulsions may provide protection to the peptide incorporated when

challenged *in vitro* and *in vivo*, and serve as a viable oral delivery system to enhance intestinal delivery of intact and biologically active water-soluble peptides.

Based on some prior research results [137, 138, 140, 141], W/O microemulsions were developed using several commercially available and pharmaceutically acceptable lipid-based excipients. Miglyol 812 and Capmul MCM are medium-chain (C_8/C_{10}) glycerides, generally recognized as safe, and meet the requirements of the United States Pharmacopeia (USP) and the National Formulary as medium-chain triglycerides (MCTs) and mono- and di-glycerides [145, 146], respectively. Tween 80 is a nonionic surfactant included in the FDA Inactive Ingredients Database for oral, IV, IM, topical, and many other preparations [147]. Phase diagrams were constructed and microemulsion windows were defined. Representative microemulsions across the microemulsion window of interest were characterized for formulation screening. To test the protective effect of the W/O microemulsions, a fluorescent labeled peptide, 5-(and-6)-carboxytetramethylrhodamine labeled HIV transactivator protein TAT (TAMRA-TAT), which has similar cationic content and cell penetrating properties to 8K-NBD [148], was used as a model peptide. TAMRA-TAT was loaded into a selected W/O microemulsion and evaluated *in vitro* and *in vivo*.

2.3 Materials and Methods

2.3.1 Materials

Miglyol 812 (Caprylic/Capric triglycerides, neutral) was provided by Sasol Germany GmbH (Eatontown, NJ, USA). The fatty acid distribution of Miglyol 812 according to the manufacturer is 57.7% caprylic acid (C_8), 41.6% capric acid (C_{10}), 0.2% caproic acid (C_6), and 0.3% lauric acid (C_{12}). Capmul MCM NF (C_8/C_{10} mono- and diglycerides) was supplied by Abitec Corporation (Janesville, WI, USA). Capmul MCM contains 53.6% of monoglycerides with 6.3% free glycerol and its fatty acid distribution is 82.6% caprylic acid and 17.4% capric acid. Tween 80 (polyoxyethylene sorbitan monooleate, NF grade) was purchased from Spectrum Chemical MFG. Corporation (Gardena, CA, USA). 5-(and-6)-Carboxytetramethylrhodamine-labeled TAT (47-57) peptide (sequence: TAMRA-YGRKKRRQRRR) was purchased from ANASPEC Inc. (Fremont, CA, USA). 4,4-Difluoro-5,7-dimethyl-4-bora-3a,4a-diaza-*s*-indacene-3-dodecanoic acid (BODIPY® FL C_{12}) was purchased from Invitrogen (Eugene, OR, USA). Pancreatin from porcine pancreas (8 × USP specifications) was purchased from Sigma-Aldrich Corporation (St. Louis, MO, USA). Tissue-Tek O.C.T. Compound (O.C.T. stands for Optimal Cutting Temperature) was supplied by Sakura Finetek USA (Torrance, CA, USA). Fluoro-Gel II, with 4',6-diamidino-2-phenylindole (DAPI), was purchased from Electron Microscopy Sciences (Hatfield, PA, USA). Purified deionized water from a Milli-Q Advantage System was used for all of the sample preparation. All other chemicals were of analytical grade.

2.3.2 Microemulsion preparation and phase diagrams

Three pseudoternary phase diagrams were constructed to define the microemulsion windows using the following four components: (a) Miglyol 812, a neutral oil of medium-chain (C_8/C_{10} triglyceride) fatty acid triglyceride; (b) Capmul MCM, a low hydrophilic-lipophilic balance (HLB) surfactant (HLB = 5.5-6.0); (c) Tween 80, a high HLB non-ionic surfactant

(HLB = 15.0); and (d) deionized water. Miglyol 812 and Capmul MCM were combined together at three weight ratios (4:1, 65:22, and 2:1, w/w). The mixture of Miglyol 812 and Capmul MCM at each weight ratio occupied one apex of the ternary phase diagram, and Tween 80 and water occupied the other two apices, respectively. Samples were prepared by mixing appropriate amounts of Miglyol 812, Capmul MCM, Tween 80, and water in screw-capped scintillation vials at room temperature by shaking. Hundreds of samples were prepared to define the phase boundaries in each phase diagram. Each sample was further allowed to equilibrate at room temperature for at least 24 h before evaluation, and re-examined after 1 week. The existence of the microemulsion window was identified as the region where clear and transparent formulations were obtained upon visual inspection. All samples were stored at room temperature and the stability of each sample was accessed by visual inspection in terms of clarity over time.

2.3.3 Microemulsion characterization

Rheological properties

The shear viscosity of the W/O microemulsions was measured using a Brookfield LVDV-III + Cone and Plate Rheometer (Brookfield Engineering Laboratories, Inc., Middleboro, MA, USA). The temperature was controlled by coupling to a Brookfield TC-500 Refrigerated Bath. Instrument calibration was performed using Brookfield silicone viscosity standards. A CPE 40 spindle was utilized for sample measurements. The shear stress, shear rate, and viscosity of a series of representative microemulsion samples in the microemulsion window of interest were measured. The relationship of shear stress (dynes per square centimeter) versus shear rate (per second) was utilized to assess the microemulsion flow behavior.

Photon correlation spectroscopy

The droplet diameter of the microemulsion was measured by photon correlation spectroscopy (PCS) using a Zetasizer Nano ZS (Malvern Instruments Inc., Worcestershire, UK) by backscattering at a fixed angle of 173˚ at 25°C. All the samples were measured in triplicates without any dilution.

Conductivity measurements

The conductivity of the microemulsions was measured using YSI 3200 conductivity meter (Yellow Spring Instruments Co. Inc., Yellow Springs, OH, USA) coupled to YSI 3252 dip cell with a cell constant of 1.0 cm^{-1}. The instrument was calibrated using YSI conductivity calibrators. Samples were measured at ambient temperature.

Freeze fracture transmission electron microscopy (FFTEM)

The morphology of the W/O microemulsion was characterized by examination of freeze fracture replicas using transmission electron microscopy (TEM). A tiny drop of microemulsion was sandwiched between gold double-replica mounts and frozen in liquid nitrogen-cooled Freon. Next, the specimens were fractured in a Balzers BAF 400T freeze fracture device at a stage temperature of -100ºC under vacuum. The fractured surfaces were shadowed unidirectionally with evaporated platinum and stabilized by carbon evaporation. The resulting replicas and sample residues were rinsed in distilled water, followed by washing in a solution of 5% sodium dichromate in 50% sulfuric acid. Replicas were then transferred to distilled water, placed onto standard copper microscopy grids, examined, and photographed with a Zeiss EM 900 Transmission Electron Microscope at an accelerating voltage of 60 kV (Carl Zeiss, Thornwood, NY, USA).

2.3.4 Phase inversion behavior of W/O microemulsions

To investigate the phase inversion behavior of W/O microemulsions upon dilution, a lipophilic fluorescent marker BODIPY FL C12 was incorporated into a selected W/O microemulsion at the concentration of 0.1% by weight, followed by dilutions of 2-, 5-, 10-, 50-, and 250-fold by weight with water. The W/O microemulsion with BODIPY FL C12 before and after dilution were examined under a Nikon Eclipse TE 300 Fluorescence Microscope (Fryer Co. Inc., Huntley, IL, USA). The structure of the diluted sample was further investigated by TEM. The W/O microemulsion after a tenfold dilution in water was negatively stained as follows: a drop of diluted microemulsion in water was placed on a copper grid, followed by removal of excess sample with filter paper, and then a drop of 2% uranyl acetate was placed on the copper grid for 2 min and subsequently examined by TEM.

To elucidate the phase inversion behavior of samples across the microemulsion window, microemulsions incorporating 5% water and with varying amounts of oil and surfactants were diluted 100-fold in water by weight, and the appearance and particle size of diluted samples were assessed.

2.3.5 *In vitro* stability studies in modified simulated intestinal fluid

Modified simulated intestinal fluid (MSIF) was prepared based on USP 34 (*Solutions* / Test Solutions). Briefly, 0.68 g of monobasic potassium phosphate was dissolved in 75 mL of water and mixed with 7.7 mL of 0.2 N sodium hydroxide. Pancreatin (0.125 g) was added and mixed well. The pH was adjusted to 6.8 ± 0.1. Water was added to q.s. to 100 mL, and then 1 mL was taken and diluted with 999 mL phosphate buffer of pH 6.8 (10 mM) to a total of 1000 mL.

TAMRA-TAT microemulsion was prepared by incorporating a defined amount of the TAMRA-TAT water solution to the mixture of Miglyol 812, Capmul MCM, and Tween 80 to a final composition of Miglyol 812/Capmul MCM/Tween 80/TAMRA-TAT solution at the weight

ratio of 62.8/21.2/7/9 with TAMRA-TAT at 60 μg/g of the microemulsion. In the *in vitro* stability studies, 100 μL of MSIF was added to 50 mg of TAMRA-TAT microemulsion or TAMRA-TAT solution (Soln., 60 μg/g) and incubated at 37˚C. At specified time points, the incubation was terminated by adding 300 μL of acetone with 2% (v/v) of trifluoroacetic acid. The clear fraction containing TAMRA-TAT was taken after centrifugation at 16,000 × *g* at 4˚C for 10 min, and then lyophilized and reconstituted in acetonitrile/water with 0.1% trifluoroacetic acid (19/81, v/v). TAMRA-TAT in the reconstituted sample was determined by high-performance liquid chromatography (HPLC) with fluorescence detection. Briefly, TAMRA-TAT was detected using a reverse-phase column (Vydac 238 MS C18 5 μm, 4.6 × 250 mm, Grace Davison, Deerfield, IL, USA) on a Thermo Finnigan Surveyor Plus HPLC system with a FL Plus detector using a binary gradient elution. Mobile phase A consisted of 0.1% trifluoroacetic acid in acetonitrile and mobile phase B consisted of 0.1% trifluoroacetic acid in deionized water. The initial eluent contained 19% phase A and 81% phase B, and then phase A was increased to 37% in 14.5 min. The eluent composition was held at 37% phase A for 1 min and then changed back to the initial composition and equilibrated for 5 min before the next injection. The flow rate was kept constant at 1 mL/min. The sample injection volume was 10 μL and the excitation and emission wavelengths were 545 and 579 nm, respectively.

2.3.6 *In vivo* studies for intestinal delivery

C57/BL6 female mice were obtained from the Charles River Labs and maintained in specific pathogen-free conditions. All experiments involving mice were carried out according to the protocol approved by the UNC Institutional Animal Care and Use Committee at the University of North Carolina at Chapel Hill. Twelve-week-old C57/BL6 female mice (18-20 g) were fed with standard chow and grouped randomly and treated with TAMRA-TAT microemulsion (2.5 mg/kg) or TAMRA-TAT solution (2.5 mg/kg) or placebo

microemulsion. TAMRA-TAT microemulsion and TAMRA-TAT solution were prepared as described above with TAMRA-TAT concentration at 250 μg/g. Placebo microemulsion was prepared in the same manner but using water as the aqueous phase instead of TAMRA-TAT stock. All treatments were administered by oral gavage with a single dose. Mice were sacrificed 4 h later and intestinal tissue was harvested. Intestinal samples from duodenum, jejunum, ileum, and colon were snap frozen in O.C.T. Compound and cut into 7-μm-thick sections onto microscope slides. Tissue on the slides was counterstained with DAPI and examined using fluorescence microscopy on an Olympus I×70 Fluorescence Microscope (Olympus America). Fluorescence intensity (FI) was quantified using ImageJ and expressed as integrated density over the total field of each picture, the same region of interest (ROI). The background was subtracted from each picture by setting up a threshold value. Data are presented as mean ± SD. The statistical differences among the three treatments (TAMRA-TAT microemulsion, TAMRA-TAT solution, and placebo microemulsion) and different intestinal sections (duodenum, jejunum, ileum, and colon) were evaluated by linear regression. The statistical significance between the treatments for each intestinal section was assessed by one-way ANOVA with Bonferroni post-tests. A value of $p < 0.05$ was considered statistically significant.

2.4 Results and Discussion

2.4.1 Phase diagrams

The partial pseudoternary phase diagrams of Miglyol 812/Capmul MCM/Tween 80/water system were constructed and are presented in Figure 2.1. Miglyol 812 was the oil phase, Tween 80 was the surfactant, Capmul MCM was the co-surfactant, and water was the aqueous phase. Capmul MCM has an HLB value of 5.5-6.0. It was utilized since it has the same carbon chain length as Miglyol 812. Tween 80 is a water-soluble surfactant with an HLB value of 15. The combination of Capmul MCM and Tween 80 created a more flexible water/oil interface, which in turn stabilized the W/O microemulsions with an overall HLB value in the range from 7 to 9. The weight ratio of Miglyol 812 to Capmul MCM was kept constant at 4:1, 65:22, and 2:1 (w/w), respectively. The advantage for keeping the weight ratio of Miglyol 812 to Capmul MCM constant was that when the sample composition changed, the sample HLB value would change according to the Tween 80 to Capmul MCM ratio in each phase diagram. As described in the "**Materials and Methods**" section, the microemulsion window was defined as the region where formation of clear and transparent formulations upon visual examination occurs. During the visual examination process, the flow property of the samples was also considered when the Tween 80 concentration was higher than 50% by weight. Samples that were very viscous and unable to flow when the vial was turned upside down were excluded from the microemulsion window in this study. When comparing the area obtained from these three phase diagrams, the apparent microemulsion window was larger when the oil to co-surfactant ratio was lower. However, during the formulation screening process, a stable system with lower amount of surfactants and similar water incorporation capacity was preferred due to the potential lower cytotoxicity [149]. Meanwhile, since a lower viscosity was also preferred and microemulsion viscosity increases with the increase of Tween 80 concentration, the weight ratio of Miglyol 812/Capmul MCM at 65:22 (w/w) was selected. With this ratio, microemulsions with the

Tween 80 concentration at 10% by weight could incorporate up to around 9% water by weight. Clear samples inside the microemulsion window were stored at room temperature and monitored over time to assess whether precipitation, phase separation, or any clarity change occurred. All clear samples remained clear for at least six months at room temperature, which clearly demonstrated the excellent stability of the optimized systems.

A similar W/O microemulsion system has been reported by Constantinides and colleagues [138, 150, 151] for systemic peptide delivery. They reported greatly enhanced bioavailability of Calcein and a water-soluble RGD peptide using the system of Captex 355/Capmul MCM/Tween 80/Aqueous (65/22/10/3, in percent w/w). In current studies, Miglyol 812, which has more defined fatty acid distribution and different product specifications compared to Captex 355, served as the oil phase and up to 9% water was incorporated in the W/O microemulsions. The feasibility of these formulations for local intestinal delivery of peptides via oral administration was investigated both *in vitro* and *in vivo*.

2.4.2 Characterization of W/O microemulsions

Rheological properties and conductivity

The rheological properties of microemulsion samples in the microemulsion window were characterized by measuring their shear stress versus shear rate. Several representative samples across the microemulsion window incorporating 5% water and varying amounts of Tween 80 (Figure 2.2A) were measured. As shown in Figure 2.2B, all of the 11 microemulsion samples showed apparent Newtonian fluid behavior wherein there was a linear relationship between shear stress and shear rate. The viscosity of the 11 samples was obtained by linear regression, and the slope of each regression line was the apparent viscosity of each sample. As shown in Figure 2.2C, the viscosity of the microemulsion samples increased with an increase in Tween 80 concentration. The

viscosity data also indicated the presence of a threshold (at the line around 42% Tween 80). When the Tween 80 concentration was lower than this threshold, the effect of Tween 80 on the microemulsion viscosity was minor; however, when the Tween 80 concentration was above this threshold, the effect of Tween 80 on the microemulsion viscosity was more pronounced. This phenomenon indicated that there might be a microemulsion structure change when the Tween 80 concentration increased up to around 42% (wt. %) (Figure 2.2C), which was consistent with the results of the dilution studies discussed later. The detailed microstructure is not yet understood. We hypothesize that below this threshold, the W/O microemulsion droplets and micelles coexisted, and the enhanced viscosity was due to the increase of micelle number and size. Moreover, above this threshold, there was the existence of a bicontinuous microemulsion where Tween 80 and Miglyol 812 existed as two continuous phases with Capmul MCM dispersed in the interfacial layer and water dispersed in the continuous Tween 80 phase or associated with the polar head group of Tween 80 in the interfacial layer. Thus, the viscosity increase above this threshold was attributed to the increase of bulk Tween 80.

To elucidate the sample properties inside the microemulsion window, a series of microemulsion samples at different Miglyol 812/Capmul MCM (65:22, w/w) to Tween 80 ratio, such as 85:10, 70:25, 50:45, and 30:65, were prepared and characterized. The viscosity of these microemulsion samples is shown in Figure 2.3A. At each fixed oil to surfactant ratio, the viscosity increased slowly with increasing water content. This increase was most likely due to the increase in both droplets number and size which enhanced the dispersed phase droplet interaction. In addition, consistent with the results above, as the Tween 80 concentration increased, the viscosity increased accordingly.

Conductivity is an important parameter which might reflect the microstructure of the microemulsions [152]. The conductivity of series of microemulsion samples with different oil to surfactant ratios is shown in Figure 2.3B. With increasing water concentration at each

fixed oil to surfactant ratio, the conductivity increased accordingly, most likely due to the increase in both droplets number and size [153]. Related, with increasing Tween 80 concentration, the conductivity also gradually increased, which was probably due to the increased interaction between droplets which facilitated the ion exchange between droplets [153]. Overall, the low conductivity of these microemulsions was an indication of the formation of W/O microemulsions [154].

Photon Correlation Spectroscopy and FFTEM

Photon correlation spectroscopy was employed for microemulsion droplet size analysis. As shown in Figure 2.3C, samples in the microemulsion window with water concentration higher than 3% and Tween 80 concentration lower than 20% showed smaller polydispersity index (PI) with more uniform droplet diameter in the range of 10-40 nm (data not shown). While samples in the microemulsion window with Tween 80 concentration at 20% (w/w) or higher, or with water concentration lower than 3% (w/w) were polydisperse with a greater PI. The size analysis reports indicated that those samples with a larger PI (e.g., PI > 0.3) were too polydisperse for data analysis. The high PI values of the microemulsion samples were likely an indication of the presence of an excess amount of Tween 80 surfactant. Since samples with uniform size distribution were preferred, microemulsion samples with smaller PI (PI < 0.1) were identified for further evaluation.

To investigate the morphology and confirm the droplet size of the W/O microemulsions, FFTEM was utilized. Figure 2.4 shows the FFTEM results of one of the placebo microemulsion formulations of interest (Table 2.1), which was plotted and highlighted by a red circle and a red arrow in Figure 2.3C. The droplets were spherical with an average diameter around 20 nm, which was consistent with the results obtained by photon correlation spectroscopy.

2.4.3 Phase inversion behavior of W/O microemulsions

The W/O microemulsions developed in this work were primarily designed for oral delivery route. After oral administration, the W/O microemulsions will likely be phase-inverted into o/w emulsions and/or water-in-oil-in-water (w/o/w) double emulsions. Since the phase inversion behavior might affect the *in vivo* fate of the drug incorporated [155], it is important to investigate this behavior. The first experiment performed was a dilution study using fluorescence microscopy. A fluorescent fatty acid, BODIPY FL C12, was dissolved in a W/O microemulsion formulation (84% mixture of Miglyol 812/Capmul MCM (65:22, w/w), 10% Tween 80, and 6% water), and then diluted in water by different dilution factors. The purpose of this dilution study was: (1) to confirm the phase inversion behavior and (2) to find out the minimal dilution factor required for the phase inversion to occur. As expected, before dilution the microemulsion with BODIPY FL C12 appeared clear with strong green fluorescence (Figure 2.5A). However, upon a fivefold or more dilution, the W/O microemulsion was readily inverted into coarse o/w-type emulsions with large and polydisperse green fluorescent droplets (Figure 2.5C-F), while with a twofold dilution, the W/O microemulsion was only partially phase-inverted as large continuous green fluorescent area occupied close to half of the examined field (Figure 2.5B). This study visually demonstrated the occurrence of phase-inversion behavior of W/O microemulsions upon dilution.

To further examine the detailed structure of the resulting emulsion from dilution, a W/O microemulsion formulation (84% mixture of Miglyol 812/Capmul MCM (65:22, w/w), 10% Tween 80, and 6% water) diluted tenfold by weight in water was negatively stained using 2% uranyl acetate, and subsequently examined using TEM. The results showed that the large droplets seen under fluorescence microscope contained numerous smaller droplets associated together (Figure 2.6), and there was no clear indication of the formation of double or multiple emulsions. The dark area between those smaller droplets might be an

indication of the presence of aqueous phase, which may be able to host water-soluble drug molecules and protect the drug molecules from acidic and enzymatic degradation. The oil phase might also be able to bring the peptide to the proximity of mucosa surface quicker and so that the peptide stands more chance to be internalized before the degradation occurrence in the lumen. The phase inversion studies using fluorescence microscopy together with TEM provide a high resolution perspective of phase inversion from W/O microemulsions to coarse o/w emulsions upon dilution using aqueous phase.

To provide an overview of the phase inversion behavior of samples across the microemulsion window, samples with 5% water and different oil to surfactant ratios were diluted 100-fold in water by weight. The results showed that as the weight ratio of Miglyol 812/Capmul MCM (65:22, w/w) to Tween 80 was 40:55 (#7 in Figure 2.7A) or less, such as 40:60, 30:65, 20:75, 10:90 (corresponding to #8, 9, 10, and 11 in Figure 2.7A), the microemulsion was inverted to stable clear or translucent microemulsion (Figure 2.7A) with uniform size distribution (Figure 2.7B). However, when the weight ratio of Miglyol 812/Capmul MCM (65:22, w/w) to Tween 80 was 45:50 (#6 in Figure 2.7A) or higher, the microemulsion was inverted to turbid emulsions. These results were consistent with the viscosity data which showed the existence of a threshold around the line of 42% Tween 80. Together, the viscosity data and dilution data indicated there might be a microstructure change of microemulsions with Tween 80 concentration close to 42-50% by weight in the microemulsion window of the selected phase diagram. In addition, since the microemulsion with the weight ratio of Miglyol 812/Capmul MCM (65:22, w/w) to Tween 80 at 40:55 (#7 in Figure 2.7A) or lower exhibited similar dilution properties of self-microemulsifying drug delivery systems [156, 157], these microemulsions might find applications to enhance oral absorption of poorly water-soluble and/or poorly permeable drugs, which is beyond the scope of the current study.

2.4.4 *In vitro* stability studies in modified simulated intestinal fluid

MSIF was prepared using pancreatin from porcine pancreas, which contains a broad-spectrum of digestive enzymes, including amylase, trypsin, lipase, ribonuclease, and protease. The pancreatin from porcine pancreas contains similar enzymes as the pancreatic fluid which a drug might encounter when it enters the intestines following oral administration. To test the hypothesis that W/O microemulsion can provide protection to the water-soluble peptide incorporated from enzymatic degradation, the stability of TAMRA-TAT in microemulsion and TAMRA-TAT in solution in MSIF at 37ºC was determined by HPLC with fluorescence detection. The TAMRA-TAT peak in HPLC chromatogram was well separated from its degradation products. Spike-recovery studies of TAMRA-TAT in the presence of placebo microemulsion using the sample processing method described under "**Materials and Methods**" section was 100.11% ± 6.24% (*n* = 3). The kinetics of TAMRA-TAT degradation was determined by following the loss of TAMRA-TAT as a function of time [158]. As shown in Figure 2.8, the kinetics of TAMRA-TAT microemulsion and solution in MSIF followed pseudo-first-order rates, which were described by the equation $y = b \times e^{-kt}$. In this equation, y represents the percentage (normalized concentration) of TAMRA-TAT at time t, b is the initial TAMRA-TAT concentration (percentage), t is the reaction time in minutes, and k is the pseudo-first-order rate constant [158]. For TAMRA-TAT solution, the TAMRA-TAT degradation kinetics fit the equation $y = 96.78\ e^{-0.1034\ t}$ ($R^2 = 0.9977$), and the half-life ($t_{1/2}$) calculated from the resulting rate constant was 6.7 min. For TAMRA-TAT microemulsion, the TAMRA-TAT kinetics followed $y = 91.56\ e^{-0.0357\ t}$ ($R^2 = 0.991$) with a calculated $t_{1/2}$ of 19.4 min, which was nearly threefold greater than that of the TAMRA-TAT solution.

The HIV TAT (47-57) moiety in TAMRA-TAT contains positively-charged amino acids arginine and lysine, which makes it highly susceptible to proteolysis by tryptic enzymes [158]. A review article [159] pointed out seven potential trypsin cleavage sites (48, 49, 50, 51, 52,

54, and 56), and Grunwald *et al.* [158] also identified a few fragments by MS in *in vitro* TAT (47-57) proteolysis studies, which include GRKKRRQRRR, GRKKRRQRR, GRKKRRQR, YGRKKRRQR, and YGRKKRRQRR. In our study, the kinetics of TAMRA-TAT degradation was followed by the detection of the loss of parent TAMRA-TAT. The stability of the TAMRA-TAT was significantly enhanced by the W/O microemulsion when challenged by MSIF. A similar protective effect from a different W/O microemulsion system to a rhPTH1-34 peptide in the presence of pepsin and trypsin was also reported by Guo *et al.* [160] in an *in vitro* enzymatic stability study. Another study by Cheng *et al.* [137] stated that after their W/O microemulsion system was phase inverted following a 800-fold dilution, only 7% loaded peptide was detected in the aqueous phase and the rest of the peptide was still detected in the upper coarse emulsion after separation by centrifugation. Although, there was no direct evidence, it is possible that even after dilution, the peptide loaded to the microemulsion might be still associated with the coarse emulsion when phase inversion happens, which renders protection to the peptide loaded from enzymatic degradation. These peptide stability data further supported the results from the following *in vivo* mouse studies and the hypothesis that W/O microemulsion may provide protection to the peptide incorporated in the enzymatic environment compared to peptide water solution.

2.4.5 *In vivo* studies for intestinal delivery

The initial aim of this work was to develop and optimize a W/O microemulsion that has the potential to increase the delivery of a potent peptide to inflamed intestinal tissue. If successful, the W/O microemulsion could then be incorporated into enteric-coated hard gelatin capsules to further enhance the delivery where and when needed. Therefore, it was not the intention to develop a W/O microemulsion that would be given orally as an oral microemulsion drink. To facilitate the initial aim, a commercially available fluorescent TAMRA-TAT peptide was used as a model therapeutic peptide, considering it has similar

cationic content and cell-penetrating properties to 8K-NBD, a potent NF-κB inhibitor. TAMRA-TAT was loaded to one of the W/O microemulsion templates (Table 2.1) and orally gavaged to mice. TAMRA-TAT solution and placebo microemulsion were administered in parallel as controls. The physical properties of the W/O microemulsion with and without TAMRA-TAT are shown in Table 2.1. The actual TAMRA-TAT loading was 96.6 ± 1.69% (*n* = 5) compared to the theoretical loading as measured by HPLC.

The intestinal distribution of TAMRA-TAT was evaluated using a semiquantitative method, fluorescence microscopy. The FI was quantified using Image J and represented as integrated density over the same ROI. As shown in Figure 2.9, the FI from the treatment of TAMRA-TAT microemulsion in all the intestinal sections are significantly greater than that from the treatment of TAMRA-TAT solution or placebo microemulsion. Linear regression of FI versus treatments (TAMRA-TAT microemulsion, TAMRA-TAT solution. and placebo microemulsion) and FI versus intestinal sections (duodenum, jejunum, ileum, and colon) showed *p* values of 1.51×10^{-26} and 3.52×10^{-6}, respectively, which indicated FI was strongly correlated with the treatments, meanwhile, FI was associated with intestinal sections, but to a lesser extent. To compare the overall FI in the small intestines to that in the large intestine, the linear regression coefficients of FI versus treatments in each intestinal section were calculated. The average linear regression coefficient from the duodenum, jejunum, and ileum was 5.9-fold greater than that from the colon, which suggested that overall, the FI difference among three treatments in the small intestine was greater than that in the large intestine. Representative images from each intestinal section are shown in Figure 2.10.

In summary, the *in vivo* mouse experiment showed that FI resulting from the TAMRA-TAT microemulsion treatment was significantly greater than that from the TAMRA-TAT solution or placebo microemulsion treatment in all intestinal sections. Although a semiquantitative method was employed in these *in vivo* studies, it was likely that the

fluorescence observed was mostly due to intracellular fluorescence since the intestine tissue was washed before fluorescence imaging. Moreover, only intact TAMRA-TAT should be taken up intracellularly, so the presence of more fluorescence in the tissue was an indication of the presence of more intracellular TAMRA-TAT. Therefore, results from the *in vivo* studies showed that the TAMRA-TAT W/O microemulsion enhanced the intestinal delivery of TAMRA-TAT compared to the TAMRA-TAT solution and placebo micromeulsion. However, the overall FI in the small intestine was still greater than that in the large intestine after oral administration, which will be addressed by encapsulation of the W/O microemulsion into enteric-coated capsules to facilitate the local delivery to the target region of the intestinal tract, such as the colon. Some preliminary experiments on the compatibility of the W/O microemulsion and hard gelatin capsules were carried out. The results showed that hard gelatin capsules containing Miglyol 812, Capmul MCM, Tween 80, and the W/O microemulsion, respectively, remained stable at room temperature for at least 1 year. There were no obvious changes to capsule stiffness or shape. The W/O microemulsion inside the hard gelatin capsules stayed clear with the same particle size after 1 year at room temperature. The compatibility of the excipients in W/O microemulsions contained in hard gelatin capsules was also supported by a review [161]. After capsules containing W/O microemulsion were enteric coated, the microemulsion stayed clear and stable in enteric-coated capsules at room temperature or at 4˚C in a refrigerator for at least 1 week before being used for experiments. Results from the mouse experiments were also supported by the data from the TAMRA-TAT *in vitro* stability studies, which provided direct evidence on the protective effect of W/O microemulsion to the peptide incorporated when challenged by the enzyme-containing environment. Together, the *in vitro* and *in vivo* studies indicated that the W/O microemulsion system may serve as a viable oral delivery vehicle to enhance the intestinal delivery of water-soluble peptides.

Intestinal delivery of peptides and proteins have been reported [162], but most of the reports have focused on the improvement of systemic absorption. There are quite limited reports on the local intestinal delivery of peptides or proteins for the treatment of local pathologies, like IBDs. Coco *et al.* [32] investigated the potential of three polymeric nanoparticles for colon-specific protein delivery via *in vitro* and *ex vivo* approaches. Hong *et al.* [98] reported promising peptide local intestinal delivery using colon-targeted enteric-coated capsules. In our study, W/O microemulsions as a potential oral delivery vehicle for local intestinal delivery of a cell-permeable peptide was investigated. The hydrophobic oil phase, Miglyol 812, together with Capmul MCM served as a protective vehicle to shield the peptide from acidic and enzymatic attack and protect the peptide incorporated during transition. In addition, Miglyol 812 as medium-chain triglycerides might also be converted to monoglycerides in the presence of lipase and enhance intracellular delivery [163]. In our study, the protective effect of the W/O microemulsion to the peptide incorporated was clearly presented. Incorporation of therapeutic peptides into the W/O microemulsion developed in the current study followed by encapsulation into enteric-coated capsules will be evaluated in larger animal models, like pig colitis models and will be the focus of our future studies.

2.5 Conclusions

This work demonstrates the potential of using W/O microemulsions as an oral delivery vehicle to deliver a cell-permeable peptide to the local murine intestines. Water-in-oil microemulsions were developed, characterized, and evaluated. The *in vitro* peptide stability studies provided direct evidence of the protective effect from the W/O microemulsion to the peptide incorporated against the enzymatic degradation. The *in vivo* mouse studies exhibited enhanced intestinal delivery of the model peptide TAMRA-TAT to the mouse small and large intestines using the W/O microemulsion system. Since the W/O microemulsions developed in this work might exhibit dual mechanisms by providing both enhanced protection and intracellular delivery, their applications are not limited to cell-penetrating peptides. Meanwhile, the W/O microemulsions developed in this work were thermodynamically stable, and formed spontaneously at room temperature without the application of heating or high shear stress. These microemulsion systems may serve as a platform for oral intestinal delivery of water-soluble and heat-labile peptides or proteins by their incorporation into enteric-coated capsules.

Table 2.1 Characterization of placebo and TAMRA-TAT W/O microemulsions (*n* = 3).

W/O Microemulsions	Viscosity (cP)	Mean droplet diameter (nm)	Polydispersity index	Conductivity (μS/cm)
Placebo ME	43.7 ± 1.2	20.6 ± 2.3	0.023 ± 0.030	0.690 ± 0.013
TAMRA-TAT ME	43.2 ± 0.6	21.4 ± 3.3	0.059 ± 0.036	0.681 ± 0.017

Note:

This W/O microemulsion composition was Miglyol 812/Capmul MCM/Tween 80/Aqueous at the weight ratio of 62.8/21.2/7/9. The aqueous for placebo microemulsion (ME) is water and for TAMRA-TAT microemulsion is TAMRA-TAT stock.

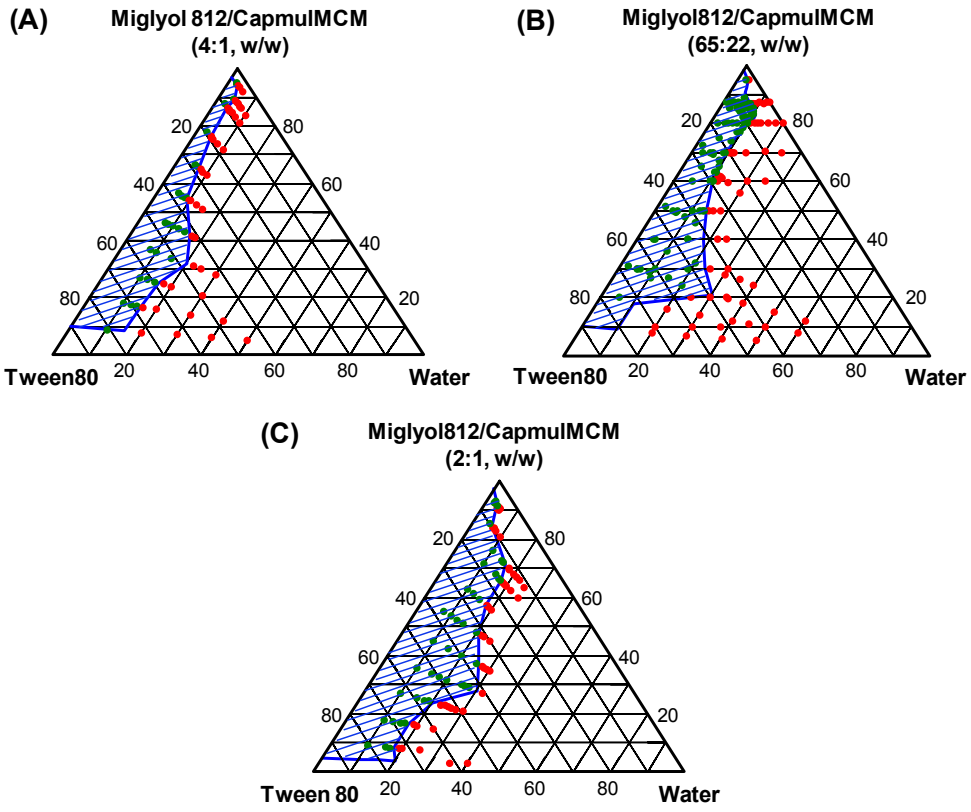

Figure 2.1 Partial pseudo-ternary phase diagrams of the system comprising Miglyol 812/Capmul MCM/Tween 80/Water for the development of W/O microemulsions. The weight ratio of Miglyol 812/Capmul MCM was kept constant at (A) 4:1; (B) 65:22; and (C) 2:1, respectively. The green dots represent clear samples, the red dots represent turbid samples and the shaded area is the microemulsion window.

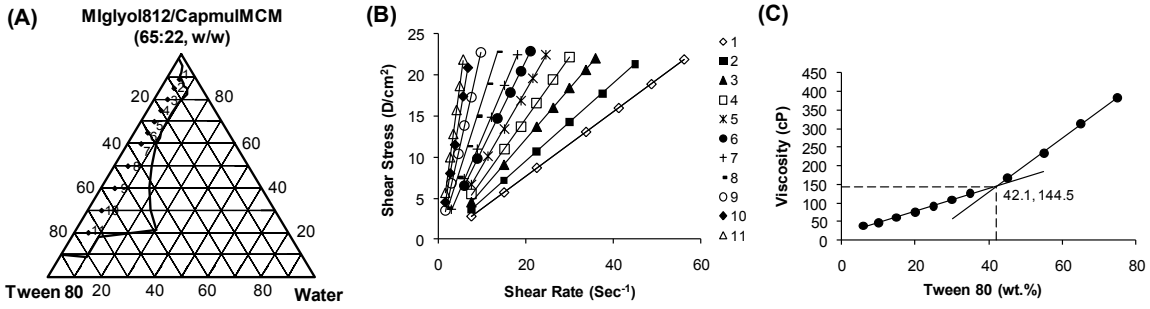

Figure 2.2 The mapping (A), rheological property (B) and viscosity (C) of 11 microemulsion samples containing 5% water inside the microemulsion window for characterization. The sample numbers on the legend of B correspond to the samples shown in A.

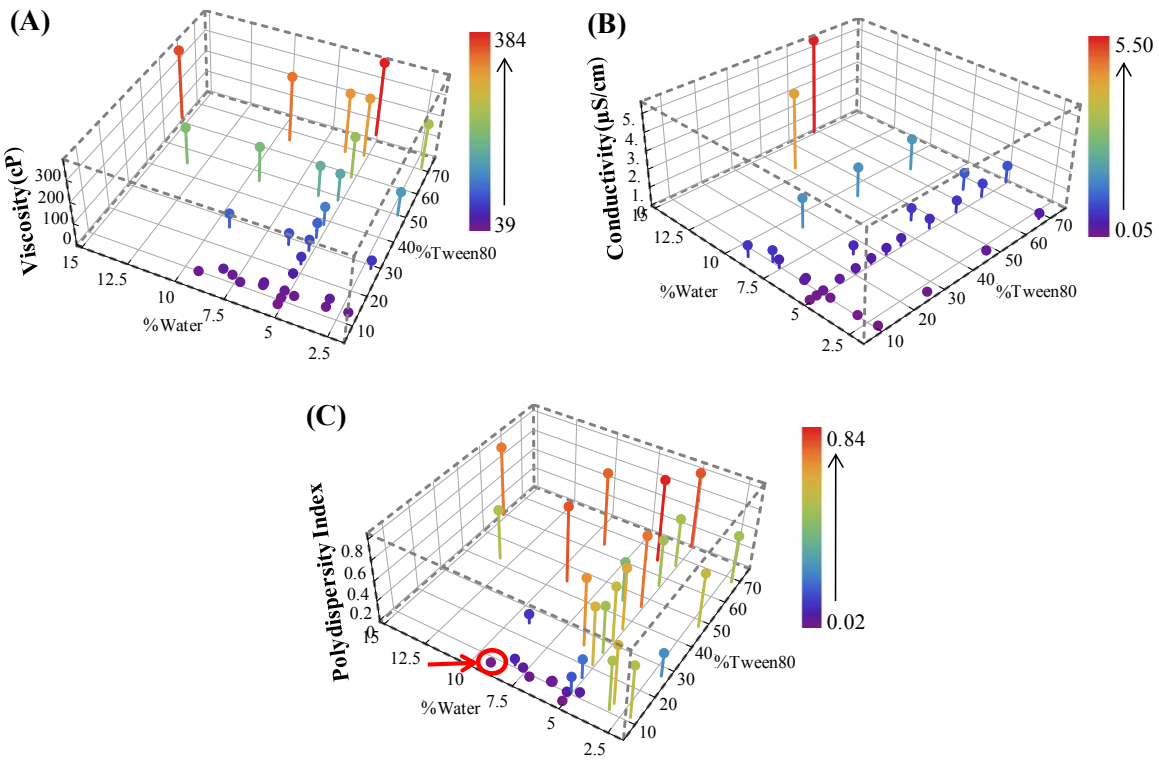

Figure 2.3 The viscosity (A), conductivity (B) and polydispersity index (C) of microemulsion samples across the microemulsion window with the weight ratio of Miglyol 812/Capmul MCM at 65:22 (w/w). Each data point is color coded and the height of each bar also indicates the relative value of each data. The circled data point with a red arrow corresponds to the placebo microemulsion shown in Table 2.1.

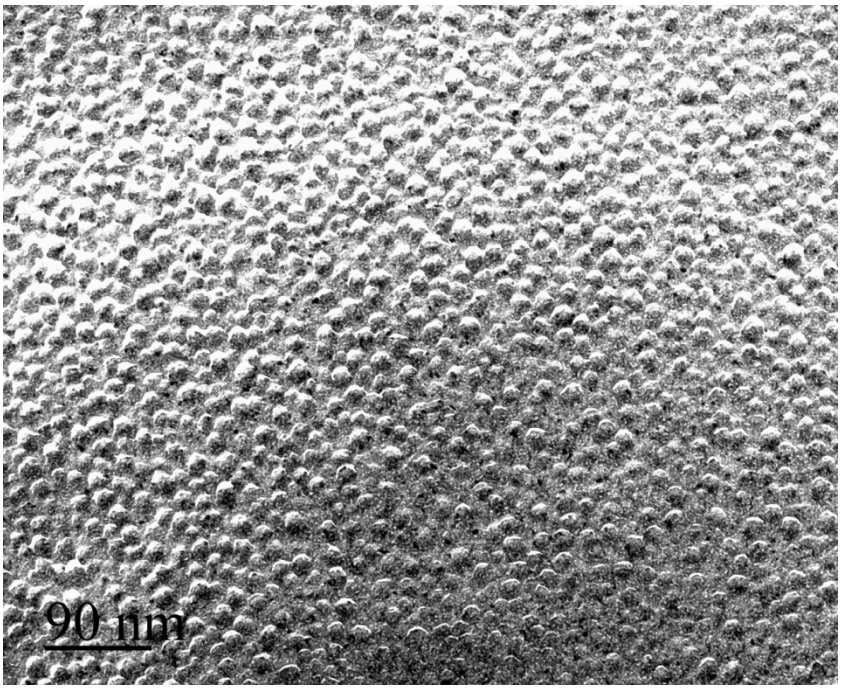

Figure 2.4 The FFTEM of a selected placebo water-in-oil (W/O) microemulsion.

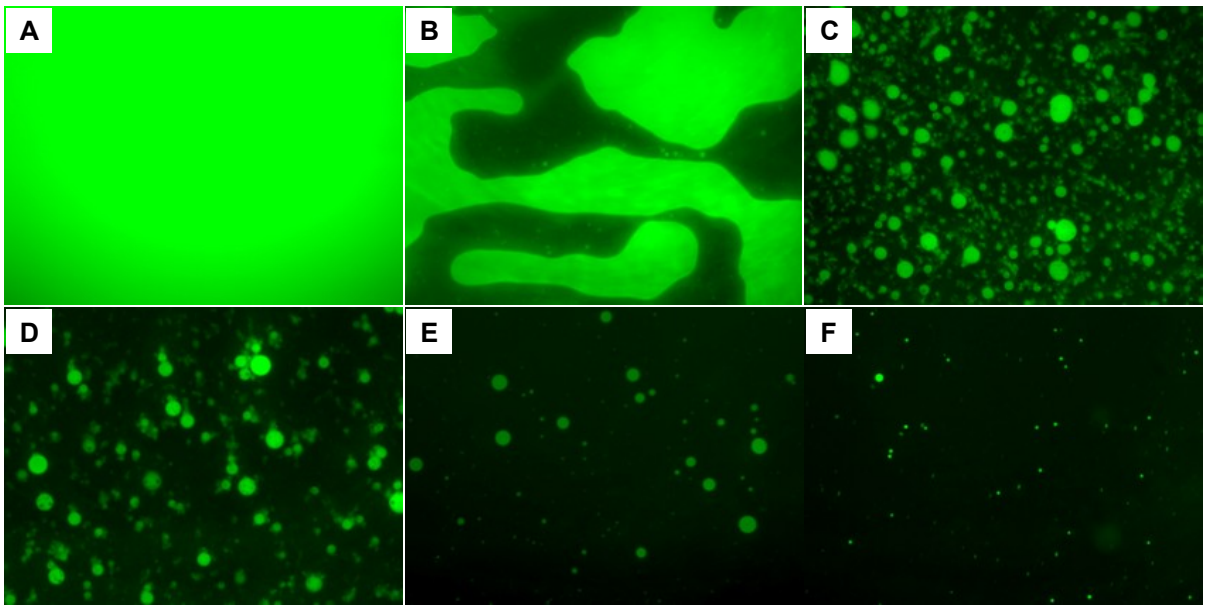

Figure 2.5 Fluorescence microscopy of water-in-oil (W/O) microemulsion upon dilution in DI water. (A) W/O microemulsion with BODIPY FL C12, (B) W/O microemulsion with BODIPY FL C12 by a twofold dilution, (C) fivefold dilution, (D) tenfold dilution, (E) 50-fold dilution, and (F) 250-fold dilution, respectively. The composition of the W/O microemulsion was Miglyol 812/Capmul MCM/Tween 80/water at the weight ratio of 62.8/21.2/10/6. All the images shown were taken with ×10 objective lens (with a total of ×100 magnification).

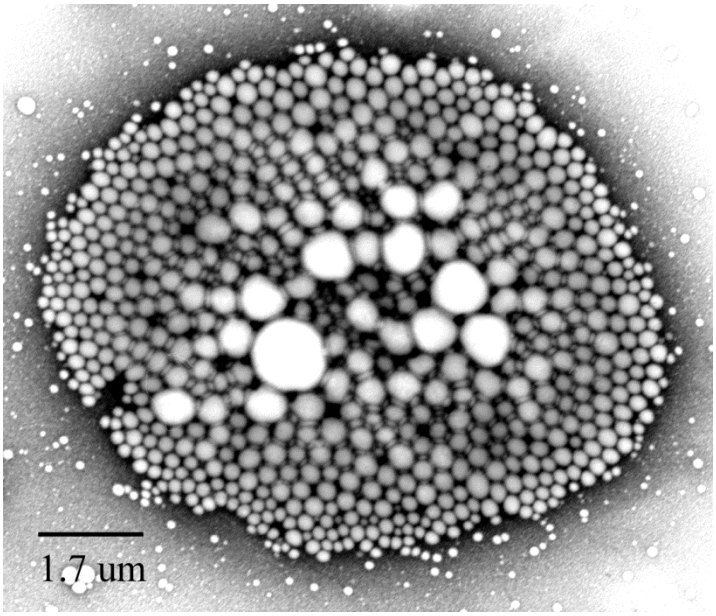

Figure 2.6 TEM of a W/O microemulsion sample after a tenfold dilution. The W/O microemulsion composition was the same as stated under Figure. 2.5.

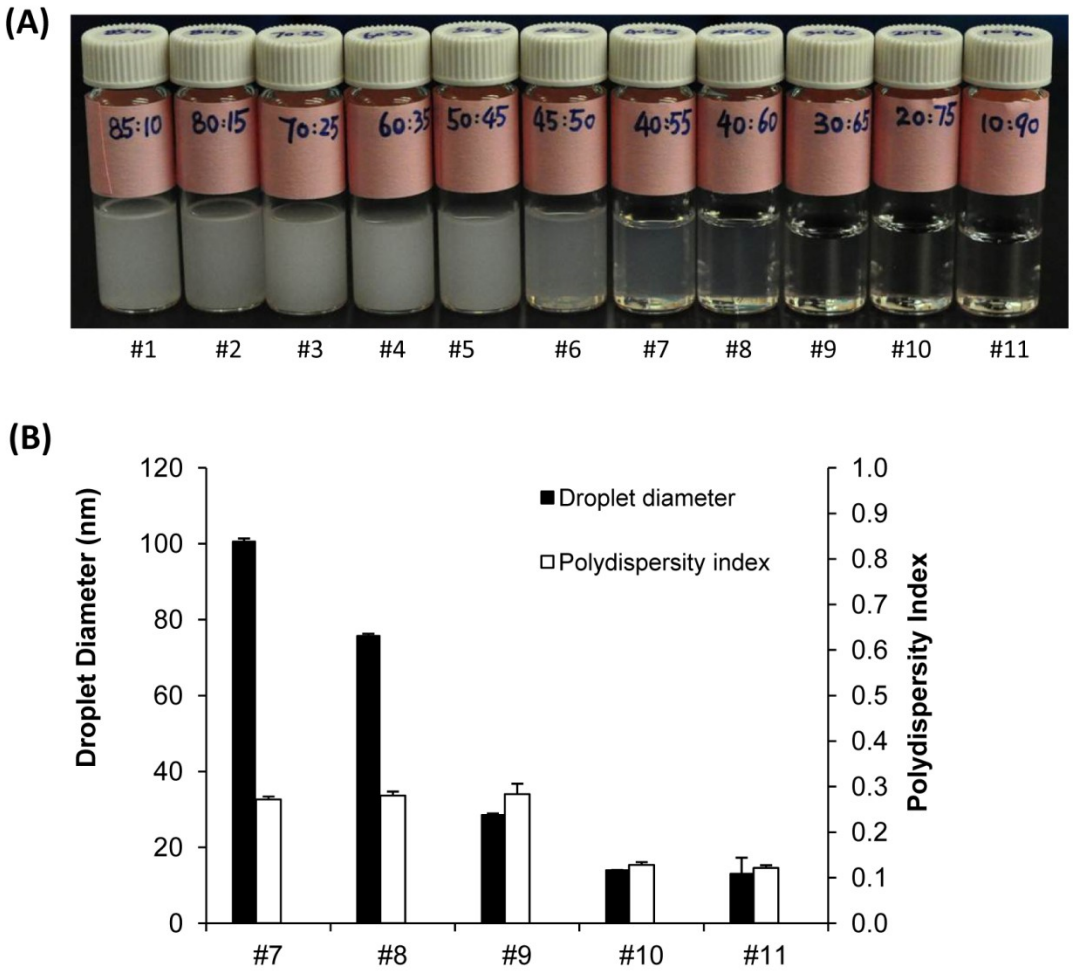

Figure 2.7 The phase inversion behavior of W/O microemulsions. (A) The picture shows the phase inversion behavior of samples across the microemulsion window. Eleven microemulsion samples with the weight ratio of Miglyol 812/Capmul MCM (65:22, w/w) to Tween 80 at 85:10, 80:15, 70:25, 60:35, 50:45, 45:50, 40;55, 40:60, 30:65, 20:75, and 10:90 were diluted 100-fold by weight with water, respectively. (B) The droplet size analysis of diluted samples corresponds to samples labeled in Figure. 2.7A.

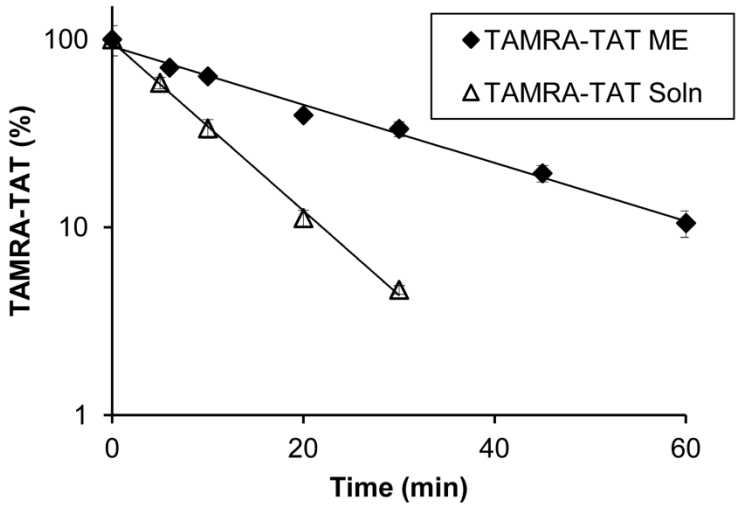

Figure 2.8 The stability of TAMRA-TAT microemulsion versus TAMRA-TAT solution (Soln.) in MSIF at 37˚C. The remaining TAMRA-TAT was normalized with respect to the initial concentration. Three samples were prepared for each time points for both TAMRA-TAT microemulsion and TAMRA-TAT solution. Data are presented as mean ± SD (*n* = 3) on a logarithmic scale. The degradation profiles of TAMRA-TAT in microemulsion and solution in MSIF at 37˚C were described by pseudo-first-order kinetics.

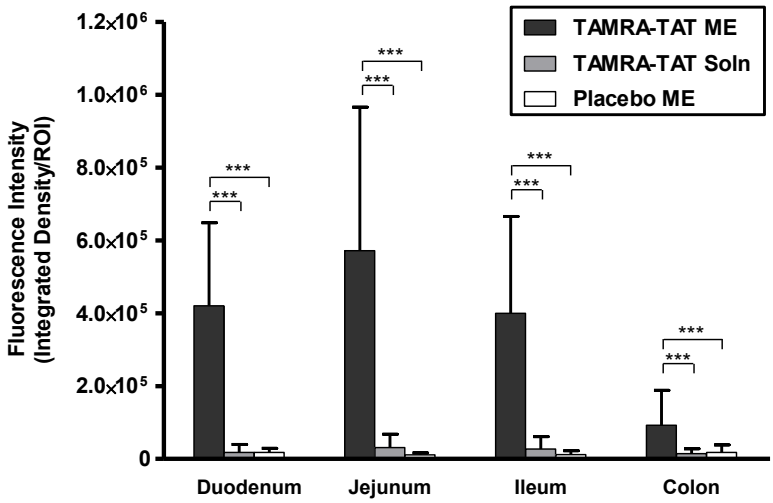

Figure 2.9 The fluorescence intensity in different mouse intestinal sections after oral administration of TAMRA-TAT microemulsion (*n* = 4 mice), TAMRA-TAT solution (Soln.; *n* = 4 mice) and placebo microemulsion (*n* = 3 mice). The data are presented as mean ± SD. *** $p < 0.001$, comparisons.

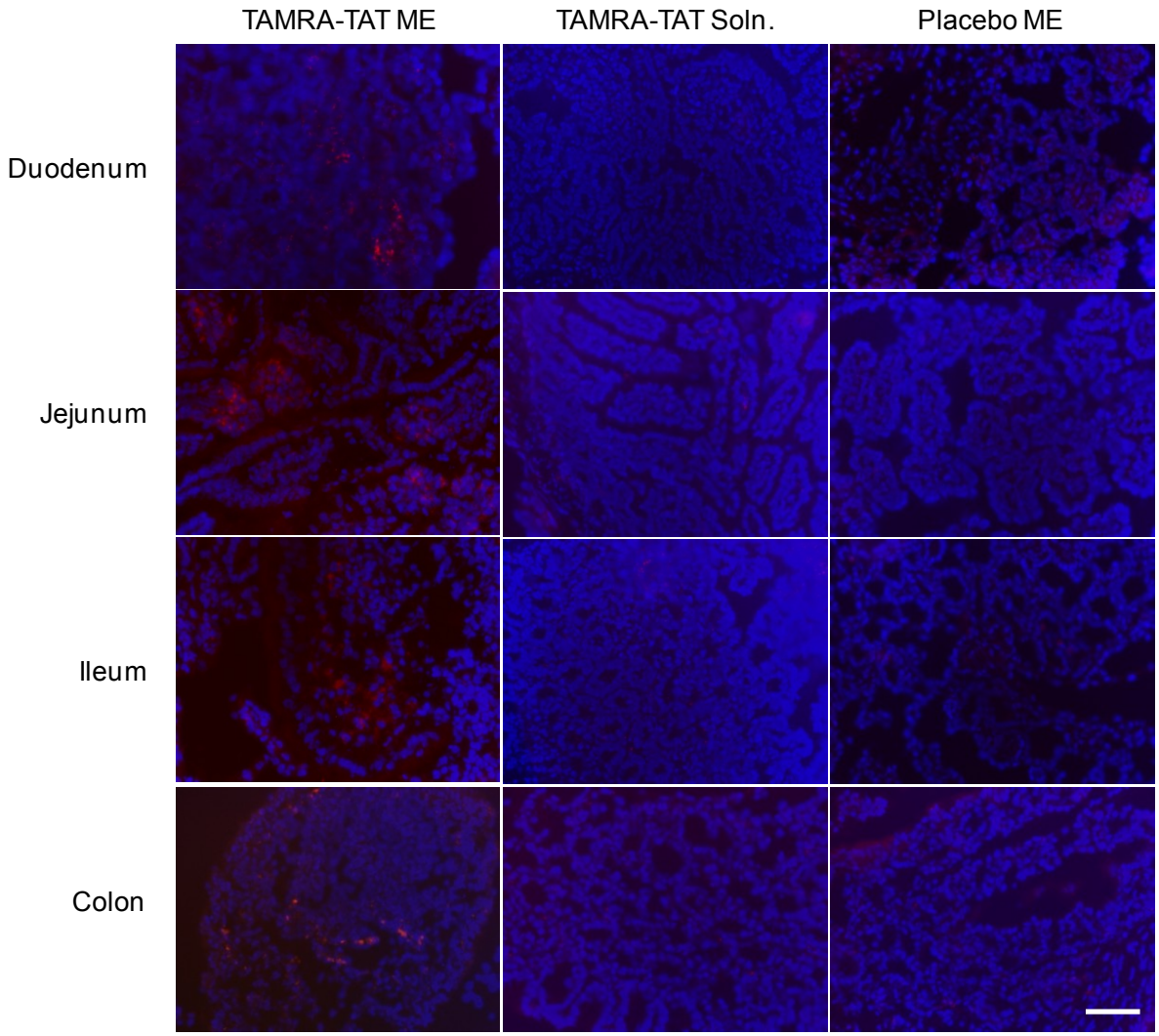

Figure 2.10 Representative fluorescence microscopic images from intestines of C57/BL6 mice treated with TAMRA-TAT microemulsion, TAMRA-TAT solution (Soln.) and placebo microemulsion (ME) 4 h after oral gavage. Scale bar represents 50 μm.

Chapter III

Hydrogel Nanoparticles in Water-in-Oil Microemulsions for Peptide Oral Delivery: Formulation Optimization and *In Vitro* Evaluation

3.1 Summary

The objective of the current studies was to develop hydrogel nanoparticles in water-in-oil (W/O) microemulsions (MEs) for improved oral intestinal delivery of peptide drugs. An amphiphilic triblock copolymer Pluronic F127 (PF127) was selected based on its thermoreversible gelation property and its wide applications in the drug delivery field. 14% PF127 (w/w) was selected as the intial concentration to prepare hydrogel nanoparticles based on its viscosity as a function of temperature. A pseudo-ternary phase diagram of Miglyol 812/Capmul MCM/Tween 80/14% PF127 was constructed and facilitated the formulation screening process. Several W/O MEs with 14% PF127 in the ME window were characterized in terms of viscosity, droplet diameter, polydispersity index (PI), turbidity, conductivity and freeze-etch electron microscopy (FEEM). A selected formulation of W/O ME with 14% PF127 was further evaluated in *in vitro* enzymatic stability studies using TAMRA-TAT as a model peptide. The half-life ($t_{1/2}$) of TAMRA-TAT in the W/O ME with 14% PF127 was two-fold greater than that in water solution, while the $t_{1/2}$ of TAMRA-TAT in the W/O ME without PF127 was three-fold greater than that in the water solution in the presence of MSIF at 37°C. The less protective effect from the W/O ME with 14% PF127 was explained based on the physical/chemical characterization data. The increased droplet diameter from around 30 nm to around 3 μm along with greatly increased turbidity, PI, and

decreased conductivity suggested that PF127 aggregated and precipitated out from the water droplets of the W/O ME at 37°C, which exposed the TAMRA-TAT associated with it directly to enzymic degradation, resulting in a compromised protective effect compared to the W/O ME without PF127. To find out whether a W/O ME with PF 127 that could stay clear at 37°C was more protective or not, a W/O ME with 8% PF127 was characterized and evaluated in an *in vitro* enzymatic stability study. The W/O ME with 8% PF127 appeared clear with a small droplet size increase (29 nm to 55 nm) when temperature increased to 37°C, which rendered a superimposable TAMRA-TAT degradation profile compared to the W/O ME without PF127. The similar protective effect supported the earlier explanation of why the W/O ME with 14% PF127 was less protective, but also indicated the concentration of 8% PF127 was probably too low to form hydrogel nanoparticles in the W/O MEs. Therefore, the hydrogel formation of PF127 in the nano-sized water droplets in the W/O ME system was yet achieved. More efforts are necessary to provide some insight into the polymer gelation process in the ME microenvironment, and to develop an improved hydrogel nanoparticle in ME-based formulation for peptide intestinal delivery.

3.2 Introduction

3.2.1 Peptide and protein oral delivery

Oral delivery of peptide and protein drugs has been an attractive alternative to their parenteral delivery, but remains a challenge in the drug delivery field. Some issues associated with peptide and protein oral delivery mainly include the following [2]: (1) peptides and proteins are large molecular weight biopolymers with poor permeability through various biological membranes; (2) most peptides and proteins are susceptible to acid-induced hydrolysis in the stomach and enzymatic degradation throughout the GI tract by digestive enzymes and/or luminal microorganisms. Many strategies have been pursued to overcome these barriers [1, 2, 4, 129, 164, 165] and to develop safe and effective oral delivery systems for peptides and proteins. Among the various formulation approaches, microemulsions have attracted much attention in the past decades.

3.2.2 Microemulsion

Microemulsions [166] are defined as "a system of water, oil and an amphiphile which is a single optically isotropic and thermodynamically stable liquid solution". Microemulsions were first introduced by Hoar and Schulman in 1943 [167, 168] and since then, different theories of microemulsion formation and stability have been proposed, mainly including interfacial or mixed film theories [169], solubilization theories [170, 171], and thermodynamic theories [172, 173]. A simplified version of the thermodynamic theories is presented as follows. The free energy of microemulsion formation can be expressed using the Equation 3.1:

$$\Delta G_{form} = \Delta A \bullet \gamma - T \bullet \Delta S \qquad \text{(Equation 3.1)}$$

In this equation, the ΔG_{form} is the free energy of formation, ΔA is the change in the interfacial area on microemulsification, γ is the interfacial tension of the oil and water interface at temperature T (Kelvin), ΔS is the change in entropy of the system, and T is the

temperature. When a microemulsion is formed, the change in ΔA is very large due to the formation of a large number of very small droplets, and ΔS is positive as well. As long as the surfactants can produce extremely low interfacial tension (approximately 0.01 mN/m), the condition $\Delta A \bullet \gamma \leq T \bullet \Delta S$ will be fulfilled, which will result in a negative free energy of formation ($\Delta G_{form} < 0$). In such cases, microemulsion will be formed spontaneously and the resulting microemulsion is thermodynamically stable [136].

The most common microemulsions are: (a) oil-in-water; (b) bicontinuous; and (c) water-in-oil microemulsion (Figure 3.1). For oil-in-water (o/w) type of microemulsion, oil droplets are dispersed in water and the volume fraction of oil is generally low. Conversely, for water-in-oil (W/O) type of microemulsion, water droplets are dispersed in oil phase and likely the volume fraction of water is low. For a bicontinuous microemulsion, the volume fractions of water and oil are similar, and both water and oil exist as a continuous phase. The microemulsion type or structure is essentially determined by the nature of the surfactant, cosurfactant and oil. Microemulsons have been investigated over years in the drug delivery field [139, 150, 156, 174, 175]. Oil-in-water microemulsions have been researched for the delivery of hydrophobic molecules [139, 176, 177], while W/O microemulsions have aroused interest for the delivery of water-soluble molecules, like heat-labile peptides and proteins [137, 150].

In our earlier study [178], we developed W/O microemulsions for oral local intestinal delivery of water-soluble peptides and demonstrated promising enhanced local peptide delivery. However, this W/O microemulsion system bears the same dilution issues as all other W/O microemulsions, i.e., phase inversion upon addition of excess amount of aqueous phase, which can affect the drug release both *in vitro* and *in vivo* [155]. This phase inversion behavior has been studied *in vitro*, but *in vivo* how quick and to what extent it will happen are hard to predict. To overcome this drawback, an improved formulation, hydrogel nanoparticles in the W/O microemulsions was designed. Hydrogel nanoparticles formed in

the nanosized droplets will provide further protection in addition to the W/O microemulsion. Therefore, the incorporated peptide will still be protected in the gel matrix even when phase inversion occurs.

3.2.3 Pluronic F127

Based on prior research [179, 180], an amphiphilic polymer of Pluronic F127 was pursued. Pluronic F127 is a triblock copolymer of poly(ethylene oxide)-poly(propylene oxide)-poly(ethylene oxide) (PEO-PPO-PEO) as shown in Figure 3.2. It contains 70-79% polyoxyethylene with a nominal molecular weight of 12,600 and an HLB ranges from 18-23. Pluronic F127 is a registered trademark of BASF Corporation and also known as Poloxamer 407.

The Pluronics are available in a range of molecular weights as presented in Figure 3.3 [180]. These Pluronic PEO-PPO-PEO copolymers vary in the PPO/PEO ratio, the PEO block length, the PPO block length, and the total chain length, which result in different properties of average molecular weight, melting point, viscosity, surface tension, cloud point, hydrophilic-lipophilic-balance. Therefore, they meet widespread pharmaceutical and cosmetic applications as detergents, foaming agents, emulsifying agents, and lubricating agents. The critical micellization concentration (CMC) and thermoreversible gelation process are important properties related to many of their applications, which have been investigated by various groups [181-184]. Typically, a PEO-PPO-PEO copolymer exists as unimers in water at a low temperature and/or concentration, and forms micelles when the temperature is above its critical micellization temperature (CMT) or the copolymer concentration is above its CMC. This micellization happens through the hydrophobic association of the PPO blocks. In other words, at low temperatures, the PPO blocks are less hydrophobic and can be dissolved in water through hydrogen bonding or just surrounded by water molecules. However, at high temperatures (above CMT), the

hydrophobic PPO blocks squeeze out water molecules and associate together to form micelles. When the micelle concentration approaches the volume fraction of 0.53, the micellar liquid may freeze into a cubic crystal and gelation occurs [185]. At even higher temperatures, the gel may "dissolve" again [180]. Vadnere *et al.* investigated the gelation process of nine Pluronic PEO-PPO-PEO copolymers [181]. Two trends were noted: (1) The concentration required for gel formation was similar to coplolymers with the same weight of PPO blocks; (2) While for a given PPO/PEO ratio, the polymer concentration required for gel formation decreased with inceasing molecular weight at a given temperature.

In the Pluronic family, Pluronic F127 is the most extensively studied member [179, 183, 184, 186-188]. It has a relatively large average molecular weight (*Mw* = 12,600), and an appropriate PPO/PEO ratio with about 70% ethylene oxide content, which renders both good water solubility through the high PEO content and a capacity of hydrophobic association through the long PPO block. Compared to other Pluronics, Pluronic F127 requires the lowest concentration for gel formation at a given temperature, and shows the lowest gelation temperature at the same copolymer concentration [181]. Its special thermoreversible gelation profile attracted lots of research interest for many pharmaceutical applications. The effect of additives on the gelation properties of Pluronic F127 has also been studied by several groups [183, 184, 186, 189, 190]. The gel-sol transition temperature decreased as the benzoic acid concentration increased [189]. When adding a homologous series of para-hydroxybenzoate esters, methyl, ethyl, propyl and butyl, the more lipophilic esters resulted in a greater decrease in Pluronic F127 gel-sol transition temperature for all the concentrations studied. Conversely, the addition of PEG increased the gelation temperature and the extent of the increase depended on the the PEG chain length and concentration. The effects of polymers and solutes were also investigated by Malmsten *et al.* [183, 184]. The homopolymer PEO of intermediate molecular weight induced the gel to "melt", while the addition of PPO homopolymer tended to increase the

stability region of the gel, depending on the PPO molecular weight [184]. The gel formation of Pluronic F127 was also affected by the presence of salts. Sodium chloride (NaCl) shifted the whole gel region to lower temperatures, while the presence of NaSCN displaced the whole gel region to higher temperatures [183]. It has also been reported that the addition of Na_2HPO_4, NaH_2PO_4 [191, 192], benzalkonium chloride [193], sodium alginate, and carbopol [194] lowered the gelation temperature of Pluronic F127, while cyclodextrins in Pluronic F127 solution increased the gelation temperature [195].

Pluronic F127 is generally considered to be a nontoxic and nonirritant material [196] and has been included in the FDA inactive ingredient database for oral, topical, ophthalmic and periodontal products [147]. It has also been investigated in rectal [194, 197] and local injectable formulations [198]. Studies indicated that Pluronic F127 promoted stabilization of peptides and proteins [199-203]. Based on its thermoreversible gelation profile and wide applications as a nontoxic pharmaceutical excipient, Pluronic F127 was selected for the current study to develop hydrogel nanoparticles in the W/O microemulsions. Figure 3.4 depicts (A) an illustration of the W/O microemulsion developed earlier; (B) the W/O microemulsion with the aqueous phase replaced by a Pluronic F127 solution; and (C) the temperature-induced thermo-gelation of Pluronic F127 inside the nanosized water droplets of W/O microemulsions. The concept is that even when the W/O microemulsion with Pluronic F127 undergoes potential phase inversion after oral administration, the peptide incorporated in the W/O microemulsion may still be protected by the gel matrix of Pluronic F127. Therefore, it was hypothesized that peptides would be better protected in the W/O microemulsion with Pluronic F127 compared to that in the W/O microemulsion without Pluronic F127 or an aqueous solution.

In this study, we first measured the viscosity of Pluronic F127 in water as a function of temperature and concentration, and then constructed a pseudo-ternary phase diagam using one of the Pluronic F127 solutions as the aqueous phase. Several formulations of

W/O microemulsion with Pluronic F127 were characterized, and selected formulations were further evaluated via conductivity measurements, freeze-etch electron microscopy, and *in vitro* enzymatic stability studies using TAMRA-TAT as a model peptide.

3.3 Materials and Methods

3.3.1 Materials

Miglyol 812 (Caprylic/Capric triglycerides, neutral) was provided by Sasol Germany GmbH (Eatontown, NJ, USA). The fatty acid distribution of Miglyol 812 according to the manufacturer is 57.7% caprylic acid (C_8), 41.6% capric acid (C_{10}), 0.2% caproic acid (C_6), and 0.3% lauric acid (C_{12}). Capmul MCM NF (C_8/C_{10} mono- and di-glycerides) was supplied by Abitec Corporation (Janesville, WI, USA). Capmul MCM contains 53.6% of monoglycerides with 6.3% free glycerol and its fatty acid distribution is 82.6% caprylic acid and 17.4% capric acid. Tween 80 (polyoxyethylene sorbitan monooleate, NF grade) was purchased from Spectrum Chemical MFG. Corporation (Gardena, CA, USA). 5-(and-6)-Carboxytetramethylrhodamine-labeled TAT peptide (sequence: TAMRA-YGRKKRRQRRR) was purchased from ANASPEC Inc. (Fremont, CA, USA). Pluronic F127 (Poloxamer 407; polyethylene-polypropylene glycol, NF grade) was purchased from Spectrum Chemical MFG. Corporation (Gardena, CA, USA). Pancreatin from porcine pancreas (8 × USP specifications) was purchased from Sigma-Aldrich Corporation (St. Louis, MO, USA). Purified deionized water from a Milli-Q Advantage System was used for all of the sample preparation. All other chemicals were of analytical grade.

3.3.2 Viscosity studies of Pluronic F127 as a function of concentration and temperature

Pluronic F127 was weighed out and added to deionized water, followed by magnetic stirring at 4˚C until Pluronic F127 was completely dissolved. Pluronic F127 water solutions

at the concentrations of 5, 8, 10, 11, 12, 13, 14, 14.5, 15, 16, and 17% by weight were prepared. The viscosity of each sample was measured using a Brookfield RVDV-III Ultra Cone and Plate Rheometer (Brookfield Engineering Laboratories, Inc., Middleboro, MA, USA) with cone spindles CPE-40, CPE42, or CPE-52 according to the viscosity range of the samples. Each sample was equilibrated to the desired temperature for 20 min before measurements. The sample temperature during measurement was controlled by connecting to a Brookfield TC-502 Programmable Controller Water Bath. The accuracy of the RVDV-III Ultra CP Rheometer was verified using Brookfield Viscosity Standard Fluids. The viscosity of Pluronic F127 solutions was measured as a function of temperature.

3.3.3 Phase diagram construction

Based on our earlier work [178], a pseudo-ternary phase diagram was constructed using Miglyol 812, Capmul MCM, Tween 80, and 14% (w/w) Pluronic F127 water solution. Miglyol 812 and Capmul MCM were mixed at the weight ratio of 65:22. Each sample was prepared by weighing out appropriate amounts of Miglyol 812/Capmul MCM (65:22, w/w), Tween 80, and 14% Pluronic F127 into screw-capped scintillation vials. The mixtures were thoroughly mixed at room temperature by magnetic stirring. After equilibration at room temperature for at least 48 h, samples were examined in terms of clarity upon visual inspection. The microemulsion window was defined as the region where clear and transparent formulations were obtained. All samples were stored at room temperature and the stability of each sample was further accessed in terms of clarity over time.

3.3.4 Characterization of W/O microemulsions with Pluronic F127

Based on the phase diagram constructed, several formulations containing 5 or 6% aqueous phase in the microemulsion window were prepared and characterized in terms of viscosity, droplet diameter, polydispersity index (PI), absorbance at 750 nm and appearance.

The sample viscosity was measured using the same instrument and method as described under "**Materials and Methods – 3.3.2**".

Photon Correlation Spectroscopy

The droplet diameter of W/O microemulsion with or without Pluronic F127 was measured by Photon Correlation Spectroscopy (PCS) using a Zetasizer Nano ZS (Malvern Instruments Inc., Worcestershire, UK) by backscattering at a fixed angle of 173°. Samples were pre-incubated to the desired temperature in a water bath, and then equilibrated and measured in the temperature-controlled Malvern Zetasizer. All the samples were measured in triplicates without dilution.

Conductivity

The conductivity of the microemulsions was measured using YSI 3200 Conductivity Instrument (Yellow Spring Instruments Co. Inc., Yellow Springs, OH, USA) coupled to YSI 3252 Dip Cell with a cell constant of 1.0 cm^{-1}. The instrument was calibrated using YSI conductivity calibrators. Conductivity measurements were made after samples were equilibrated to the desired temperature.

Turbidity at absorbance of 750 nm

The absorbance at 750 nm was used as an indication of sample turbidity. The measurements were performed at 25 and 37˚C, respectively, using a Beckman Coulter DU® 800 UV-Vis Spectrophotometer coupled with a Beckman Coulter Peltier Temperature Controller. Samples were incubated to the desired temperature and then loaded to the spectrophotometer and equilibrated for 20 min before measurement. An average value of 8 readings for each sample was reported.

Freeze-Etch Electron Microscopy

Several microliters of W/O microemulsion with Pluronic F127 were positioned on gold freeze-etch mounts and frozen in liquid nitrogen-cooled freon and held in liquid nitrogen. The specimens were transferred to the stage of a Balzers BAF400T Freeze-Fracture Plant at liquid nitrogen temperature with a high vacuum established in the unit. The temperature of the specimen stage was raised to -100˚C and the microtome arm was cooled to -170˚C. The frozen droplets of the specimen were shaved with a liquid nitrogen-cooled blade which was retracted a short distance following the last cutting cycle and positioned over the fractured specimens for a five-minute etch interval. After etching, the microtome was cycled out of position and an evaporative coat of platinum/carbon was applied to the fractured and etched surfaces at an angle of 30°. A support layer of carbon was then evaporated over the specimens from an angle of 90°. The specimens were removed from the unit and replicas were floated onto a distilled water surface and subsequently washed in 5% sodium dichromate in 50% sulfuric acid. The replicas were retrieved from distilled water onto 300 mesh copper grids and examined and photographed using a Zeiss EM900 Transmission Electron Microscope and Gatan Digital Camera.

3.3.5 *In vitro* enzymatic stability studies

Modified Simulated Intestional Fluid (MSIF)

MSIF was prepared as described previously [178]. Briefly, pancreatin from porcine pancreas (8 × USP specifications) was dissolved in potassium phosphate buffer of pH 6.8 according to USP 34 (*Solutions*/Test Solutions), and then diluted in phosphate buffer of pH 6.8 (10 mM) by 1,000-fold.

Sample preparation

Lyophilized TAMRA-TAT was reconstituted in deionized water and weighed out into an amber vial. Then, a defined amount of Pluronic F127 was added and dissolved in TAMRA-TAT solution in an icy water bath. Miglyol 812, Capmul MCM and Tween 80 were added and mixed well to form TAMRA-TAT W/O microemulsion with Pluronic F127. TAMRA-TAT W/O microemulsion was prepared with the same oil and surfactant weight ratio but using TAMRA-TAT stock solution as the aqueous phase instead of the TAMRA-TAT solution with Pluronic F127. TAMRA-TAT solution with equivalent TAMRA-TAT concentration by weight served as the control.

In vitro stability studies

The enzymatic *in vitro* stability study was designed similarly to our previous studies [178]. TAMRA-TAT microemulsion with Pluronic F127 was weighed out into centrifuge tubes (~58 mg/tube), and equilibrated to 37˚C in a water bath. Then, 116 mL of MSIF at 37˚C was added and the mixture was incubated at 37˚C. At predetermined time points, the sample was put on ice, and the reaction was stopped by adding 300 µL of acetone with 2% (v/v) trifluoroacetic acid. The clear TAMRA-TAT fraction was collected after centrifugation at 16,000 × *g* for 10 min at 4˚C, and then frozen on dry ice, lyophilized (see Table 3.1) and reconstituted in acetonitrile/water with 0.1% (v/v) trifluoroacetic acid (19/81, v/v). TAMRA-TAT in the reconstituted sample was determined by HPLC with fluorescence detection [178]. Briefly, TAMRA-TAT was detected using a reverse-phase column (Vydac 238 MS C18 5 µm, 4.6 × 250 mm, Grace Davison, Deerfield, IL, USA) on a Thermo Finnigan Surveyor Plus HPLC system with a FL Plus detector using a binary gradient elution. Mobile phase A was 0.1% trifluoroacetic acid in acetonitrile and mobile phase B was 0.1% trifluoroacetic acid in deionized water. The initial eluent contained 19% phase A and 81% phase B, and then phase A was increased to 37% in 14.5 min. The flow rate was kept constant at 1 mL/min.

The sample injection volume was 10 µL and the excitation and emission wavelengths were 545 and 579 nm, respectively.

Sample processing recovery studies

To determine whether TAMRA-TAT in W/O microemulsion (ME) with Pluronic F127 can be recovered using the sample processing method described under "***in vitro* stability studies – 3.3.6**", a total of three recovery studies were designed and preformed.

In the first study, the recovery of TAMRA-TAT in ME with 14% Pluronic F127 after the sample extraction, lyophilization, and reconstitution process was examined. Placebo W/O ME with Pluronic F127 was prepared, and added to a known amount of TAMRA-TAT stock solution to make a final TAMRA-TAT W/O ME with 14% Pluronic F127. Then, 100 mg of TAMRA-TAT ME with 14% Pluronic F127 was incubated at 37˚C for 5 min, and diluted with 200 µL of phosphate buffer of pH 6.8. Next, acetone with 2% trifluoroacetic acid was added to stop the reaction. After centrifugation at 16,000 × *g* for 10 min at 4˚C, the TAMRA-TAT fraction was collected, lyophilized, reconstituted and detected by HPLC.

In the second study, the recovery of TAMRA-TAT in ME with 14% Pluronic F127 after different incubation time at 37˚C was determined. In this study, TAMRA-TAT ME with 14% Pluronic F127 was weighed out (50 mg/tube), and incubated with 100 µL of phosphate buffer of pH 6.8 at 37˚C for 5, 10, 20, 30, 45 and 60 min, respectively. Then, acetone with 2% trifluoroacetic acid was added, and the sample was processed in the same way as described above and detected by HPLC.

In the third study, the recovery of TAMRA-TAT from 14% Pluronic F127 after incubation at 37˚C for different amount of time was determined. TAMRA-TAT in 14% Pluronic F127 was weighed out (50 mg/tube) and incubated with 100 µL of phosphate buffer of pH 6.8 at 37˚C for 5, 10, 20, 30, 45 and 60 min, respectively. After incubation,

acetone with 2% trifluoroacetic acid was added, and the sample was processed in the same way as described above and detected by HPLC.

In all three studies, TAMRA-TAT stock solution diluted in acetonitrile/water with 0.1% (v/v) trifluoroacetic acid (19/81, v/v) served as the control (n = 3).

3.4 Results and Discussion

3.4.1 Viscosity study of Pluronic F127

Pluronic F127 shows thermoreversible micellization and gelation properties as illustrated in Figure 3.5 and Figure 3.6. Its gelation process is both temperature and concentration dependent. To find a suitable Pluronic F127 concentration for hydrogel nanoparticle formation in the W/O microemulsion, the viscosity of Pluronic F127 was measured as a function of temperature and concentration. As shown in Figure 3.7, when the Pluronic F127 concentration was lower than 14% (wt %), the viscosity did not increase much as the temperature increased, and for 13% Pluronic F127, the viscosity was only 57 cP at 37˚C. However, when the Pluronic F127 concentration was at or above 14%, the viscosity increased more dramatically when the temperature increased (Figure 3.7A). Based on these results, 14% Pluronic F127 was selected as the starting concentration to engineer hydrogel nanoparticles in the W/O microemulsion.

3.4.2 Phase diagram

Figure 3.8 shows the pseudo-ternary phase diagram constructed with Miglyol 812/CapmulMCM/Tween 80/14% Pluronic F127. In this phase diagram, the weight ratio of Miglyol 812 and Capmul MCM was kept at 65:22, based on earlier work [178]. Miglyol 812 was the oil phase, Tween 80 was the water-soluble surfactant, Capmul MCM was the oil-soluble cosurfactant, 14% Pluronic F127 in water was the aqueous phase. Similarly, the red dots are turbid samples and the green dots represent clear samples, and the blue shaded

area is the microemulsion window defined at room temperature for this system. When compared to the microemulsion window from our previous study with the same Miglyol 812/Capmul MCM weight ratio (65:22) [178], the microemulsion window shifted more toward the center of the phase diagram. There was a narrow gap region between the side opposite to the 14% Pluronic F127 apex and the microemulsion window, where the weight percentage of 14% Pluronic F127 in each sample was low and samples appeared turbid. This turbid region became wider with the increase of Tween 80 concentration. There was no clear explanation for this phenomenon. It was speculated that when 14% Pluronic F127 was added to the Tween 80-rich oil and surfactant mixture, very small water droplets formed spontaneously, and when the water droplet size was smaller than the size of the Pluronic F127 micelle (approximately 10 nm in hydrodynamic radius [180]), Pluronic F127 became insoluble and precipitated out. This would be the case when the water fraction was very small.

3.4.3 Formulation characterization

The goal of this study was to find an optimal W/O microemulsion with a certain amount of Pluronic F127 that is more protective to the peptide incorporated than the W/O microemulsion when challenged by an enzyme-containing system. Based on the phase diagam constructed, several microemulsion formulations with 14% Pluronic F127 were prepared and characterized as shown in Table 3.2. Formulations of F1 to F5 contained 5% (wt.%) water, and the formulation F6 contained 6% (wt.%) water. They were all Newtonian fluids with a low viscosity ranging from 56-73 cP at 25˚C. Formulations of F1-4 and F6 showed uniform size distribution ranging from 30-60 nm in diameter with small polydispersity indices, while F5 was more polydispersed with a relatively larger PI.

The turbidity of the F1-6 was evaluated via absorption measurements at 750 nm. The absorbance of F1-4 and F6 at 750 nm was all negligible, while the absorbance of F5

was one order of magnitude larger than others at 25°C. Turbidity is the cloudiness or haziness of a fluid caused by particles in a sample. In the absence of a turbidimeter, the sample turbidity was estimated by measuring absorbance in a UV-Vis Spectrophotometer [204, 205]. The particles in the sample block the photons and appear as absorbance. Goodner [204] developed a model to evaluate the correlation of UV-Vis absorption and turbidity, and observed a linear relationship between turbidity and absorbance at 750 nm, which confirmed that the absorption at 750 nm could be used as a valid indication of sample turbidity. In combination with visual examination, the absorbance at 750 nm in this study was used to compare the turbidity of various formulations at different temperatures, which was an important piece of data to help formulation optimization and interpret the following *in vitro* stability data.

Based on the appearance, absorption at 750 nm, and the Photon Correlation Spectroscopy (PCS) results at 25˚C, F3 and F6 were selected for the current stage and their viscosity, particle size and absorption at 750 nm were further examined at 37˚C. Results (Table 3.2) showed that the viscosity of both F3 and F6 decreased somewhat when the temperature increased to 37˚C. However, significant changes occurred with particle size. The droplet diameter of both formulations of F3 and F6 increased from nanometer size to micrometer size, which was sort of consistent with their dramatic absorption increase at 750 nm.

In addition, F3 and F6 were characterized via Freeze-Etch Electron Microscopy (FEEM). Gold nanoparticles were processed via the same procedure to validate the FEEM method in this study. As shown in Figure 3.9, both formulations appeared to be spherical droplets/particles, and their droplet/particle diameters were consistent with the corresponding PCS results, i.e., around 40 and 50 nm in diameter for F3 and F6, respectively. The images obtained from FEEM were metal replicas of samples after they

were frozen in liquid nitrogen and etched at -170°C. Due to the special sample processing technique, it was hard to obtain images representing their morphology at 37°C.

The formulation of F6 was selected for further *in vitro* evaluation. Its viscosity and conductivity were both measured as a function of temperature compared to the corresponding W/O microemulsion without Pluronic F127. Results (Figure 3.10A) showed that the viscosity of both W/O microemulsion with 14% Pluronic F127 and without Pluronic F127 decreased with the temperature increase. The conductivity (Figure 3.10B) of the W/O microemulsion increased gradually with the increase of temperature, while the conductivity of W/O microemulsion with 14% Pluronic F127 decreased as the temperature increased.

3.4.4 *In vitro* enzymatic stability studies

After initial formulation screening, W/O microemulsion with 14% Pluronic F127 was evaluated *in vitro* using TAMRA-TAT as a model peptide [178]. Similarly, Modified Simulated Intestinal Fluid (MSIF) was used as the enzyme-containing medium and the same sample processing and detection method was applied.

Recovery studies

To make sure the TAMRA-TAT in W/O microemulsion with Pluronic F127 can be well recovered even when hydrogel nanoparticles are formed at 37°C, a total of three recovery studies were carried out. The first recovery study examined the spike-recovery of TAMRA-TAT in the presence of W/O microemulsion with 14% Pluronic F127 after the same sample processing method described under "**Materials and Methods**" and showed an average recovery of 97.61 ± 1.14% (n = 3) (Table 3.3). The second recovery study examined the influence of different incubation time on the recovery of TAMRA-TAT in W/O microemulsion with Pluronic F127 at 37°C. The results (Figure 3.11A) showed an average recovery of 89.02% from all seven time points, and no significant difference was observed across the

recoveries after different incubation time. The third recovery study investigated the influence of pure 14% Pluronic F127 and different incubation time on the recovery of TAMRA-TAT, and similar results (Figure 3.11B) were obtained, which showed an average recovery of 83.82% from all seven time points with no significant difference observed for the recovery after different incubation time. These recovery studies supported the feasibility of the sample processing method in this study.

Stability studies to evaluate W/O MEs with 14% Pluronic F127

During the *in vitro* stability studies, the degradation profiles of TAMRA-TAT in microemulsion with 14% Pluronic F127, TAMRA-TAT in W/O microemulsion and TAMRA-TAT in solution in the presence of MSIF at 37˚C were compared. The kinetics of TAMRA-TAT followed pseudo-first-order rates in all three preparations. As shown in Figure 3.12A and Table 3.4, the half life ($t_{1/2}$) calculated from the resulting rate constant was 6.7, 19.4 and 13.2 min for TAMRA-TAT in solution, W/O microemulsion and microemulsion with 14% Pluronic F127, respectively. These results were different from what we had expected based on our hypothesis. To confirm these results, the stability experiment was repeated. Similar trends were obtained as shown in Figure 3.12B and Table 3.5. The $t_{1/2}$ of TAMRA-TAT in solution and the W/O microemulsion and microemulsion with 14% Pluronic F127 was 5.7, 14.7 and 10.8 min, respectively. It was noticed that the $t_{1/2}$ of TAMRA-TAT in all three preparations was a little less than that from the first experiment, which was probably due to the activity difference in the MSIF used. Both the W/O microemulsion and microemulsion with 14% Pluronic F127 were more protective to the TAMRA-TAT incorporated compared the naked solution. However, the $t_{1/2}$ of TAMRA-TAT in the microemulsion with 14% Pluronic F127 was less than that in the W/O microemulsion. We then sought to explain these findings by investigating the physical/chemical properties of the systems. The W/O microemulsion with 14% Pluronic F127 (F6) contained 6% (wt.%) of aqueous phase, which

was 14% Pluronic F127 in water. The droplet diameter of F6 increased from around 50 nm to around 3 μm when the temperature increased from 25˚C to 37˚C, which suggested when the temperature increased to near 37˚C, the droplets containing Pluronic F127 might aggregate together and Pluronic F127 precipitated out. This speculation was further supported by the absorption increase at 750 nm and the viscosity and conductivity measurements as well. Figure 3.10A shows that the viscosity of ME with 14% Pluronic F127 was always higher than the corresponding W/O ME without Pluronic F127 until the temperature reached near and beyond 37˚C. Figure 3.10B observed a conductivity decrease for the ME with 14% Pluronic F127 when the temperature increased to 37˚C, which was opposite to the conductivity change of the corresponding W/O ME without Pluronic F127. If Pluronic F127 precipitation happened, both the viscosity and the conductivity would be lower than expected. During the precipitation process, some of the TAMRA-TAT in the W/O ME with 14% Pluronic F127 could fall out of the microemulsion droplets by association with the Pluronic F127 precipitates, and thus would be exposed to the challenging enzyme system and degraded more rapidly. Therefore, the protective effect from the W/O ME with 14% Pluronic F127 was decreased compared to the W/O ME without Pluronic F127.

Stability studies to evaluate W/O MEs with 8% Pluronic F127

Based on the above results, it was speculated that if the W/O ME with an appropriate amount of Pluronic F127 could stay clear at 37˚C without precipitation, it might provide better protection if hydrogels are formed inside the water droplets or at least similar protective effect if no hydrogels are formed in the W/O ME. To confirm this idea, several W/O MEs with different amount of Pluronic F127 were prepared and characterized. The purpose was to find a W/O ME with as much Pluronic F127 as possible, which could still stay clear when the temperature was increased to around 37˚C, and then the selected

formulation would be further evaluated using *in vitro* stability studies as described earlier. As shown in Table 3.6, W/O ME without Pluronic F127, with 5, 8, 9, 10 and 12% of Pluronic F127 by weight were prepared and characterized in terms of viscosity, droplet diameter, PI, absorption at 750 nm and physical appearance at both 25 and 37˚C. Water-in-oil ME with 8% Pluronic F127 showed to be the one with the highest Pluronic F127 amount that could still stay clear and stable at both temperatures. This formulation was further evaluated via viscosity and conductivity measurements, respectively. Its viscosity (Figure 3.13A) decreased with temperature increase similar to the W/O ME, and stayed a little bit higher than the viscosity of the W/O ME at all the temperature included. Its conductivity (Figure 3.13B) increased with the increase of temperature, which was similar to the W/O ME as well.

Water-in-oil ME with 8% Pluronic F127 was further evaluated using TAMRA-TAT as the model peptide and challenged by MSIF at 37˚C. Results are shown in Figure 3.12C and Table 3.5. The degradation profile of TAMRA-TAT in the ME with 8% Pluronic F127 almost overlapped with that in the W/O ME, and the estimated $t_{1/2}$ of TAMRA-TAT was very close to that in the W/O ME as well. This result supported our earlier speculation that the shorter $t_{1/2}$ of TAMRA-TAT in the ME with 14% Pluronic F127 compared to the W/O ME was indeed due to the formation of precipitation at 37˚C. Without precipitation, the protective effect of the W/O ME was not compromised by the addition of Pluronic F127. However, W/O ME with 8% Pluronic F127 did not provide better protective effect to the TAMRA-TAT incorporated compared to the W/O ME without Pluronic F127, which indicated that the Pluronic F127 concentration might be too low to form hydrogels in the W/O MEs.

The thermoreversible gelation process of Pluronic F127 is a complex process influenced by temperature, polymer concentration and the presence of many additives like salts or other polymers. Yang *et al.* reported that higher molar ratio of Tween 80 in a mixed micelle gel led to higher gel formation temperature when the molar ratio of Pluronic F127 to Tween 80 changed from 1:2 to 1:6 [190]. In our W/O ME with 8% Pluronic F127 system, the

weight percentage of Tween 80 was more than 20-fold higher than that of Pluronic F127, which might have influenced the gellation process of Pluronic F127. On the other hand, in the W/O ME with Pluronic F127, the hydrogel formation was expected to be confined to the tiny nano-sized water droplets, and how does the gelation process happen in the W/O ME system is not clear yet. It has been reported that [206] the hydrodynamic micellar radius of Pluronic F127 in water, as calculated from diffusion data at the CMC, was around 10.2 nm over the temperature range of 35-45˚C. However, the droplet diameter of our W/O ME with Pluronic F127, as measured by PCS, was in the range of 20-60 nm; the gelation capacity might be limited by how many micelles each water droplet could hold. It is not clear whether the space inside each droplet of the W/O ME system is large enough for the Pluronic F127 gel formation.

Originally, Pluronic F127 was thought to stay inside the water droplets after being incorporated into the W/O MEs considering it is a water-soluble polymer. However, Pluronic F127 is amphiphilic with an HLB value of 18-23, so some of the Pluronic F127 could possibly partition into or be associated with the surfactant layer. It has been reported that when temperature increased, the micelles of Pluronic F127 progressively became dehydrated [206], and the apparent micellar radius increased [180]. Therefore, it was possible that when temperature increased to around 37°C, the micellar size of Pluronic F127 became larger than the water droplet size, and Pluronic F127 micelles between droplets interacted and aggregated together, causing the disruption of the W/O ME system.

3.4.5 Attempts with other polymers in the W/O ME system

During the formulation development process, we also explored the feasiblility of using several other polymers for the purpose of nanoparticle formation in the W/O MEs, such as hydroxypropylcellulose (HPC) and poly(N-isopropylacrylamide) (PNIPAM). HPC is a nonionic water-soluble cellulose ether with a versatile of properties and wide applications

in the pharmaceutical field [207]. It is soluble in water below 38˚C and insoluble in water above 45˚C. The idea was to dissolve a certain amount of HPC in the aqueous phase of the W/O ME, and when the temperature increased to the HPC precipitation temperature, HPC would become insoluble and form HPC nanoparticles inside the W/O ME droplets. KLUCEL® HPC of different average molecular weight at 80,000, 95,000, 140,000, 370,000, and 850,000, corresponding to KLUCEL® grades of EF, LF, JF, GF, and MF, at the concentration of 0.5% (wt.%) in water were titrated into the mixture of Miglyol 812/Capmul MCM/Tween 80 (62.8/21.2/11, w/w). At different grades, around 6-7% of HPC could be incorporated to form clear W/O ME. However, all the clear W/O MEs with HPC became cloudy when the temperature increased to their precipitation temperature, i.e., around 38-40˚C, indicating HPC might have aggregated and precipitated out of the water droplets of the W/O MEs. The viscosity of these HPC solutions was quite low and ranged from 1.1to 7.3 cP at 25˚C, so the capacity of incorporating various grades of HPC into our W/O ME system seemed quite limited.

PNIPAM is a thermosensitive water-soluble polymer that exhibits a cloud point at approximately 32˚C [208]. At temperature below the cloud point, PNIPAM is hydrophilic, while at temperature above the cloud point the polymer becomes hydrophobic and collapses into globules or aggregates, and for samples with high polymer concentration precipitation or gelation is observed [209]. PNIPAM with a weight average molecular weight (M_w) in the range of 19,000-30,000 (Sigma-Aldrich Co., St. Louis, MO, USA) at the concentration of 0.5, 1, 2, and 5% (wt.%) was investgated in this work. The PNIPAM solution at each concentration was titrated into the mixture of Miglyol 812/Capmul MCM/Tween 80 (63.5/21.5/15, w/w) to form a clear W/O ME. Results showed samples titrated with 5% and 2% of PNIPAM always appeared cloudy, and samples titrated with 1% and 0.5% of PNIPAM looked clear when the weight percentage of PNIPAM solution was lower than 1.6% and

2.5%, respectively. Overall, the W/O ME system could not incorporate a sufficient amount of PNIPAM in the system.

Thermal reversible gelation is observed in several nonionic polymer systems, such as hydroxypropylmethylcellulose [210, 211], hydroxypropylcellulose [212], poly(N-isopropylacrylamide) and derivatives [213, 214], and Pluronics [180, 215]. These polymers contain both hydrophilic and hydrophobic segments, and can form structures like a hydrophobic core surrounded by a hydrophilic shell. The mechanisms behind thermal gelation have been investigated by many groups and several mechanisms reported include partial crystallization, coil-to-helix transition, hydrophobic association, and micelle packing [209, 216-218]. However, these mechanisms were proposed based on various instrumental techniques and observations, and this field is overall still controversial. The gel formation is a macroscopic property, and gels are defined as three-dimentional polymeric networks with increased viscosity and a solid like behavior under small deformation. The minimum molecule number and polymer density required for gel formation in the W/O ME with nanosized water droplets is hard to define based on the current understanding. The overall impression is that the small size of the water droplets in the W/O MEs might be one of the limiting factors for a stable macroscopic hydrogel formation, but there is no direct evidence to prove or connect the microenvironment to the macroscopic gel phase yet.

3.5 Summary

In summary, to develop improved formulations for peptide oral local intestinal delivery, a thermal reversible gelling polymer Pluronic F127 was investigated to engineer hydrogel nanoparticles in W/O MEs. Various characterization techniques and tools were utilized in this work. Water-in-oil MEs with different amount of Pluronic F127 was evaluated based on Pluronic F127 viscosity studies, phase diagram construction, conductivity

measurement, turbidity measurement, photon correlation spectroscopy, freeze-etch electron microscopy (FEEM), and *in vitro* enzymatic stability studies.

The FEEM study was a good technique to examine the morphology of W/O MEs with different amount of Pluronic F127 at low temperature, but not able to capture their temperature-dependent morphology at higher temperatures like at 37˚C. The *in vitro* enzymatic stability studies showed the W/O ME with 14% Pluronic F127 could not provide better protective effect to the model peptide incorporated compared to the W/O ME. Meanwhile, the W/O ME with 8% Pluronic F127 showed same protective effect compared to the W/O ME. So far, the engineering of hydrogel nanoparticles in the W/O MEs was still at the development and discovery stage. More experiments are needed to better understand the temperature-dependent microstructure of W/O MEs with Pluronic F127 and/or other polymers, and to further improve the formulation.

Table 3.1 Lyophilization cycle of TAMRA-TAT samples.

Thermal Treatment				
Step 1	-40˚C	30 min	Hold	
Freeze, Condenser, Vacuum phases				
Freeze			- 40˚C	
Additional Freeze			0	
Condenser			- 60˚C	
Vacuum			100 mTorr	
Drying Cycle Steps				
	Temperature (ºC)	**Time (min)**	**R/H**	**Vacuum (mTorr)**
Step 1	-35	30	Hold	100
Step 2	-30	30	Hold	100
Step 3	-25	30	Hold	100
Step 4	-20	30	Hold	100
Step 5	-15	60	Hold	100
Step 6	-10	180	Hold	100
Step 7	-5	60	Hold	100

Note:

A bench-top VirTis AdVantage Freeze Dryer 2.0 liter XL (SP Industries VirTis, Gardiner, NY, USA) was used for the sample lyophilization.

Table 3.2 Composition and physical characterization of different W/O microemulsions with 14% Pluronic F127 (PF127).

	Formulations	F1 (%,w/w)	F2 (%,w/w)	F3 (%,w/w)	F4 (%,w/w)	F5 (%,w/w)	F6 (%,w/w)
	Miglyol 812/Capmul MCM (65:22, w/w)	80.0	81.5	82.5	83.5	85.0	83.0
	Tween 80	15.0	13.5	12.5	11.5	10.0	11.0
	14% PF127	5.0	5.0	5.0	5.0	5.0	6.0
25˚C	**Viscosity (cP)**	72.8	66.4	65.8	59.8	56.5	62.0
	Droplet diameter (nm)	39.4 ± 0.3	44.0 ± 1.2	43.5 ± 0.8	52.3 ± 1.3	288.9 ± 289.1	48.3 ± 0.9
	Polydispersity Index	0.195 ± 0.030	0.048 ± 0.053	0.034 ± 0.029	0.220 ± 0.073	0.534 ± 0.048	0.082 ±0.062
	Absorbance at 750 nm	0.0010	0.0006	0.0011	0.0000	0.0218	0.0030
37˚C	**Viscosity (cP)**	–	–	36.1	–	–	33.1
	Droplet diameter (nm)	–	–	1998.0 ± 86.6	–	–	2762.0 ± 135.5
	Polydispersity Index	–	–	1.000	–	–	1.000
	Absorbance at 750 nm	–	–	0.0425	–	–	0.2046

Table 3.3 TAMRA-TAT recovery from W/O microemulsion with 14% PF127.

	Theoretical value (µg/mL)	Experimental value (µg/mL)	Recovery (%)	Mean recovery (%)	SD
Sample 1	0.7522	0.7263	96.56		
Sample 2	0.7522	0.7332	97.47	97.61	1.14
Sample 3	0.7522	0.7433	98.82		

Table 3.4 Parameters of TAMRA-TAT kinetic profile in MSIF (the first study).

Formulations	Equation	R^2	$t_{1/2}$ (min)
TAMRA-TAT Soln.	$y = 96.78\ e^{-0.1034\ t}$	0.9977	6.7
TAMRA-TAT ME	$y = 91.56\ e^{-0.0357\ t}$	0.9910	19.4
TAMRA-TAT ME 14% PF127	$y = 96.46\ e^{-0.0526\ t}$	0.9886	13.2

Note:

The composition of TAMRA-TAT ME was Miglyol 812/Capmul MCM/Tween 80/TAMRA-TAT water solution at the weight ratio of 62.8/21.2/7/9. The TAMRA-TAT ME with 14% PF127 contained Miglyol 812/Capmul MCM/Tween 80/TAMRA-TAT PF127 solution at the weight ratio of 60.5/20.5/12/7. TAMRA-TAT Soln. contained an equivalent concentration of TAMRA-TAT by weight compared to TAMRA-TAT ME and TAMRA-TAT ME with 14% PF127.

Table 3.5 Parameters of TAMRA-TAT kinetic profile in MSIF (the second study).

Formulations	Equation	R^2	$t_{1/2}$ (min)
TAMRA-TAT Soln.	$y = 89.11\ e^{-0.1216\ t}$	0.9868	5.7
TAMRA-TAT ME	$y = 95.31\ e^{-0.0470\ t}$	0.9888	14.7
TAMRA-TAT ME 14% PF127	$y = 97.82\ e^{-0.0641\ t}$	0.9876	10.8
TAMRA-TAT ME 8% PF127	$y = 99.78\ e^{-0.0489\ t}$	0.9955	14.2

Note:

The composition of TAMRA-TAT ME was Miglyol 812/Capmul MCM/Tween 80/TAMRA-TAT solution at the weight ratio of 62/21/11/6. For TAMRA-TAT ME with 14% PF127 and with 8% PF127, the TAMRA-TAT solution was replaced by TAMRA-TAT in 14% PF127 or TAMRA-TAT in 8% PF127, respectively. TAMRA-TAT Soln. contained an equivalent concentration of TAMRA-TAT by weight as all other TAMRA-TAT preparations.

Table 3.6 Characterization of W/O microemulsion with different amount of Pluronic F127.

Temperature	Formulations	Viscosity (cP)	Droplet diameter (nm)	Polydispersity index	Absorbance 750 nm	Appearance
25˚C	W/O ME	55.1 ± 0.1	21.8 ± 0.5	0.063 ± 0.019	0.0000	clear
	W/O ME 5% PF127	56.8 ± 0.2	26.7 ± 0.8	0.275 ± 0.190	0.0014	clear
	W/O ME 8% PF127	58.2 ± 0.2	29.0 ± 0.1	0.039 ± 0.025	0.0091	clear
	W/O ME 9% PF127	58.6 ± 0.2	31.1 ± 0.5	0.031 ± 0.025	0.0054	clear
	W/O ME 10% PF127	54.3 ± 0.2	38.5 ± 1.4	0.082 ± 0.057	0.0036	clear
	W/O ME 12% PF127	58.6 ± 0.3	43.8 ± 0.3	0.017 ± 0.010	0.0104	clear
37˚C	W/O ME	33.1 ± 0.2	30.0 ± 0.6	0.037 ± 0.035	0.0015	clear
	W/O ME 5% PF127	34.3 ± 0.1	38.0 ± 0.7	0.042 ± 0.040	0.0059	clear
	W/O ME 8% PF127	34.4 ± 0.5	55.2 ± 1.1	0.132 ± 0.088	0.0089	clear
	W/O ME 9% PF127	36.3 ± 0.2	57.7 ± 1.3	0.146 ± 0.164	0.0565	almost clear
	W/O ME 10% PF127	34.7 ± 0.2	104.3 ± 52.6	0.522 ± 0.414	0.0676	a little hazy
	W/O ME 12% PF127	35.7 ± 0.1	1688.7 ± 223.7	1.000	0.2131	turbid

Note:

The composition of W/O ME was Miglyol 812/Capmul MCM/Tween 80/water at the weight ratio of 62/21/11/6. For W/O ME with different amount of PF127, the water fraction was replaced by 5, 8, 9, 10, and 12% (w/w) of PF127, while the other components were kept at the same weight ratio as the W/O ME.

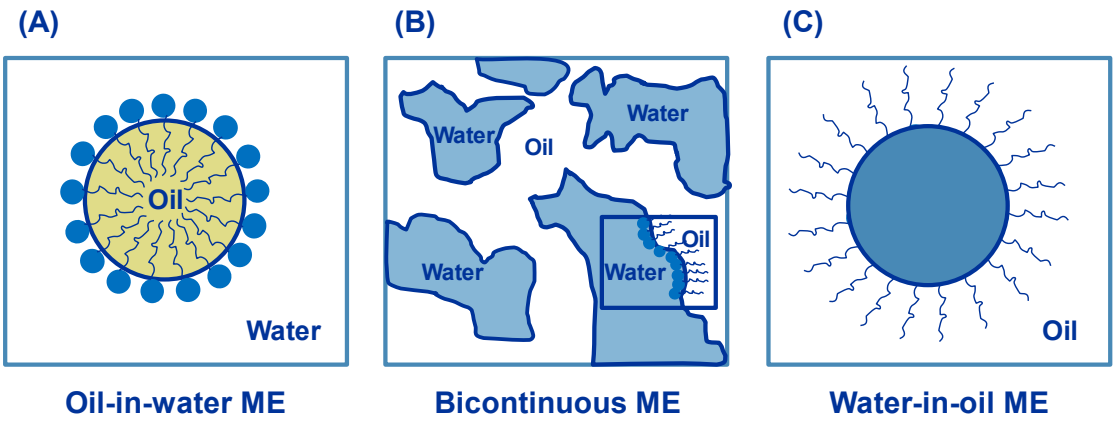

Figure 3.1 Schematic representation of three common microemulsions: (A) oil-in-water; (B) bicontinuous; and (C) water-in-oil microemulsion. (Modified from reference [136]).

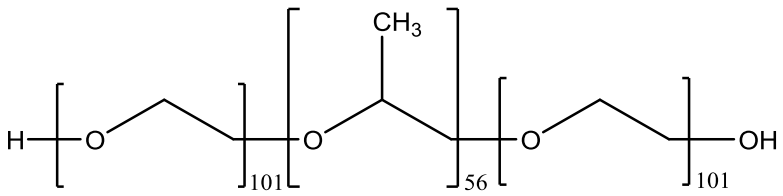

Figure 3.2 Chemical structure of Pluronic F127.

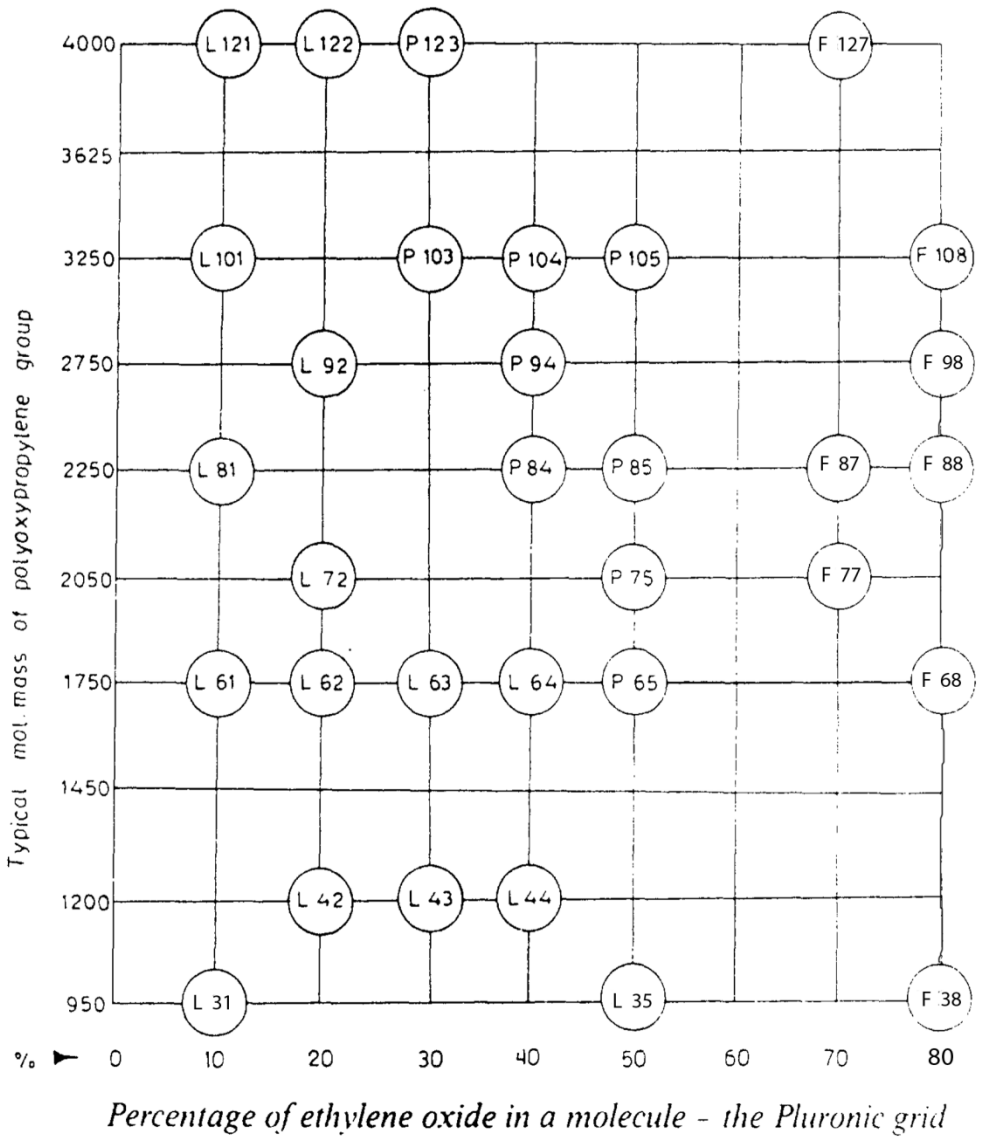

Figure 3.3 Pluronic PEO-PPO-PEO copolymers arranged in the “Pluronic grid” (Reprinted with permission from reference [180]. Copyright © 1995, Elsevier).

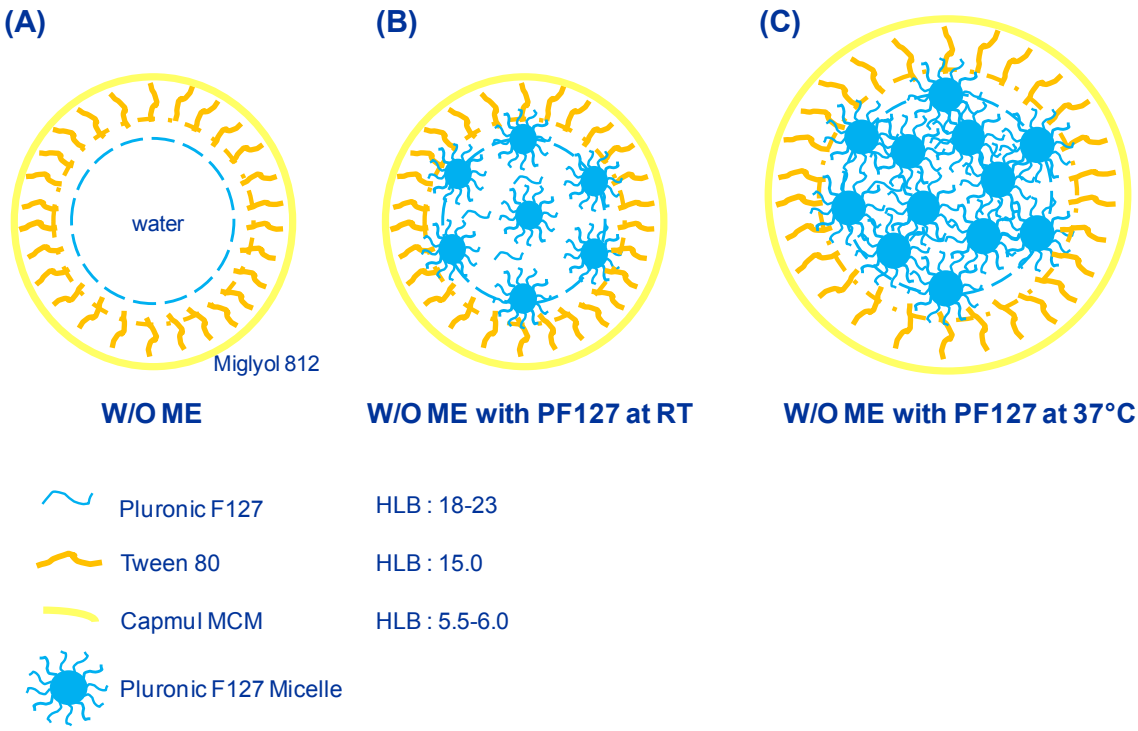

Figure 3.4 An illustration of the formation of hydrogel nanoparticles in the W/O ME at 37°C in the proposed hypothesis. (A) a W/O ME droplet; (B) a W/O ME droplet with a defined amount of PF127 at room temperature (RT); (C) PF127 hydrogel formation inside a water droplet of the W/O ME at 37°C.

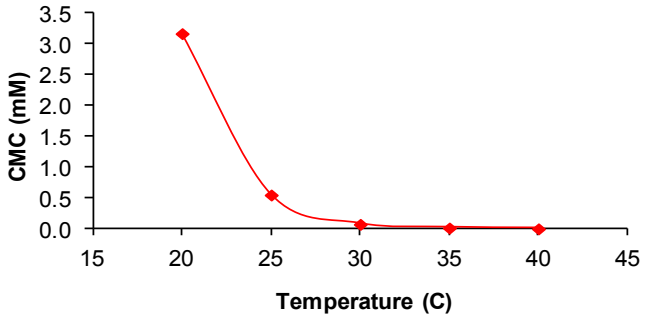

Figure 3.5 Temperature-dependent critical micellization concentration (CMC) of Pluronic F127 (constructed from the data in reference [219]).

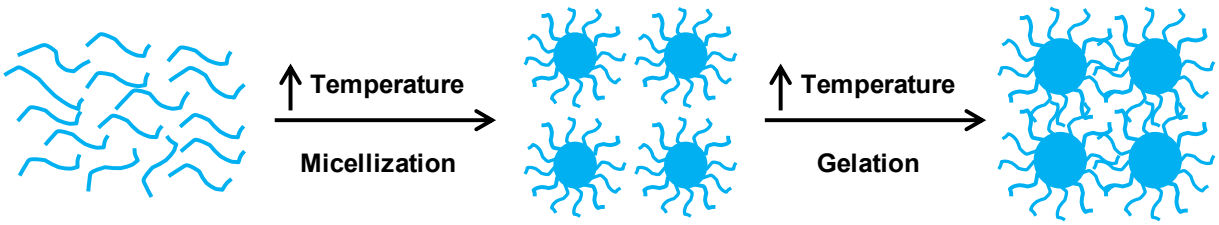

Figure 3.6 An illustration of the Pluronic F127 thermal gelling process.

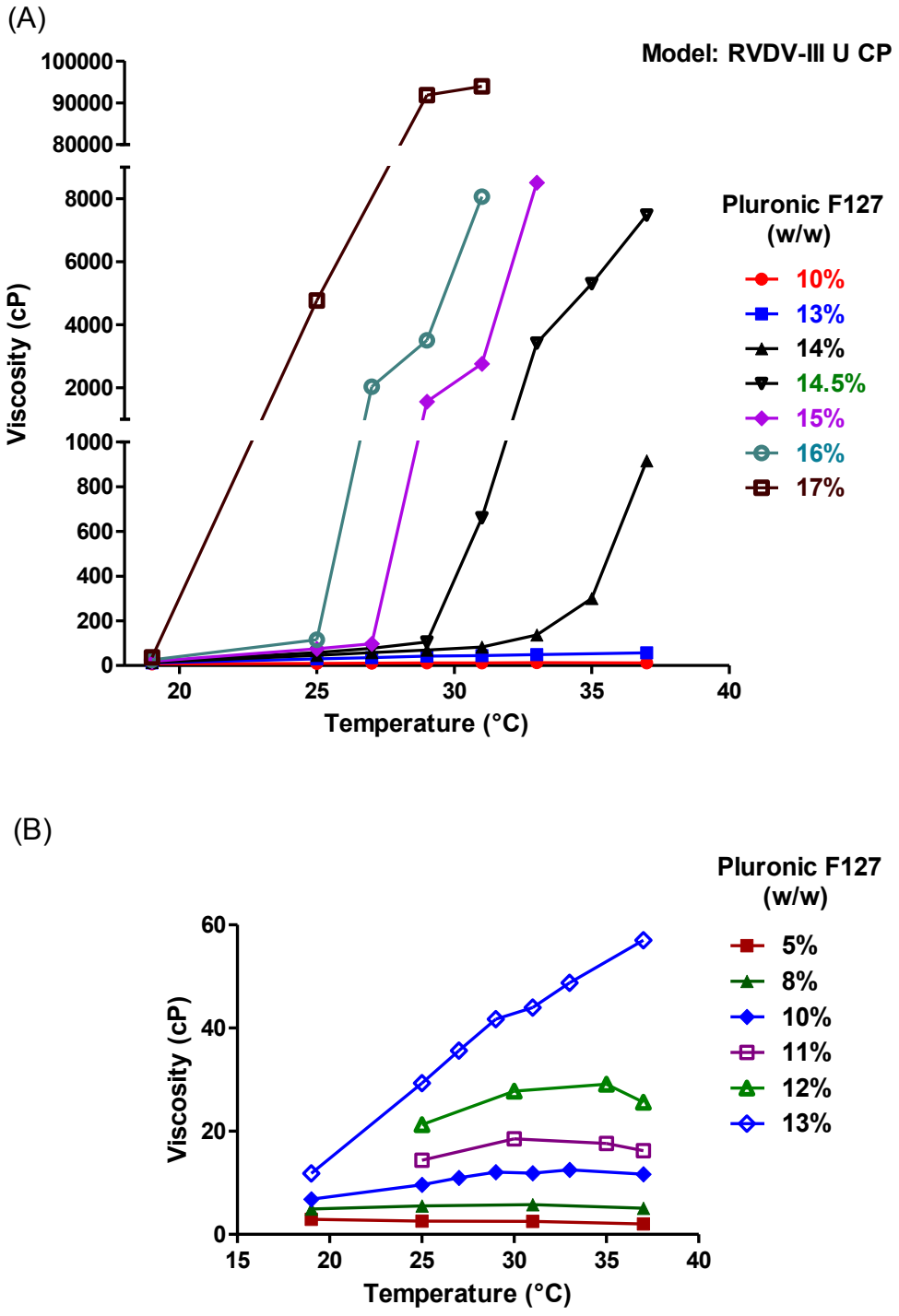

Figure 3.7 Viscosity of Pluronic F127 as a function of temperature and concentration. (A) the viscosity of Pluronic F127 at the concentrations of 10, 13, 14, 14.5, 15, 16, and 17% (w/w); (B) the viscosity of Pluronic F127 at the concentrations of 5, 8, 10, 11, 12, and 13% (w/w).

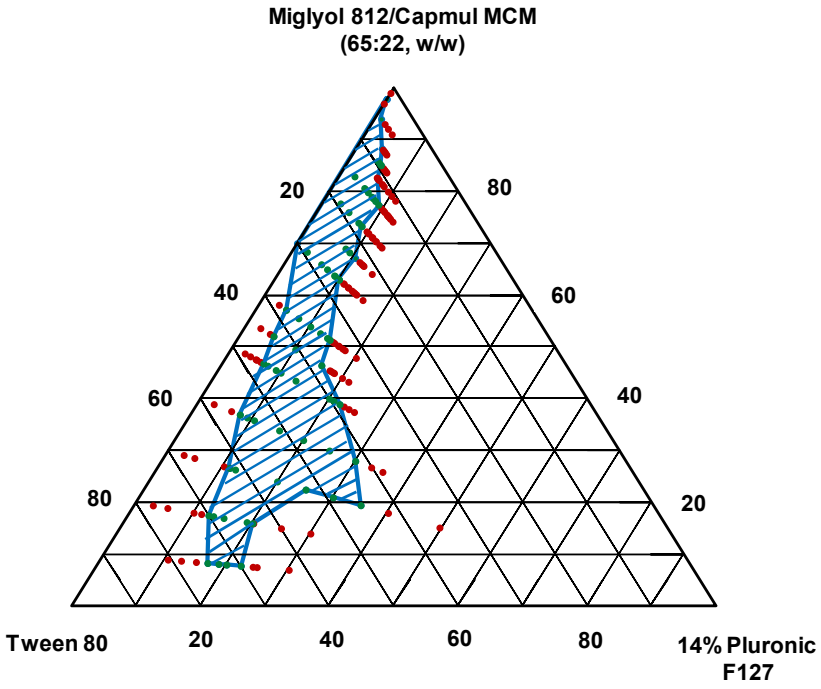

Figure 3.8 A pseudo-ternary phase diagram of Miglyol 812/Capmul MCM/Tween 80/14% Pluronic F127.

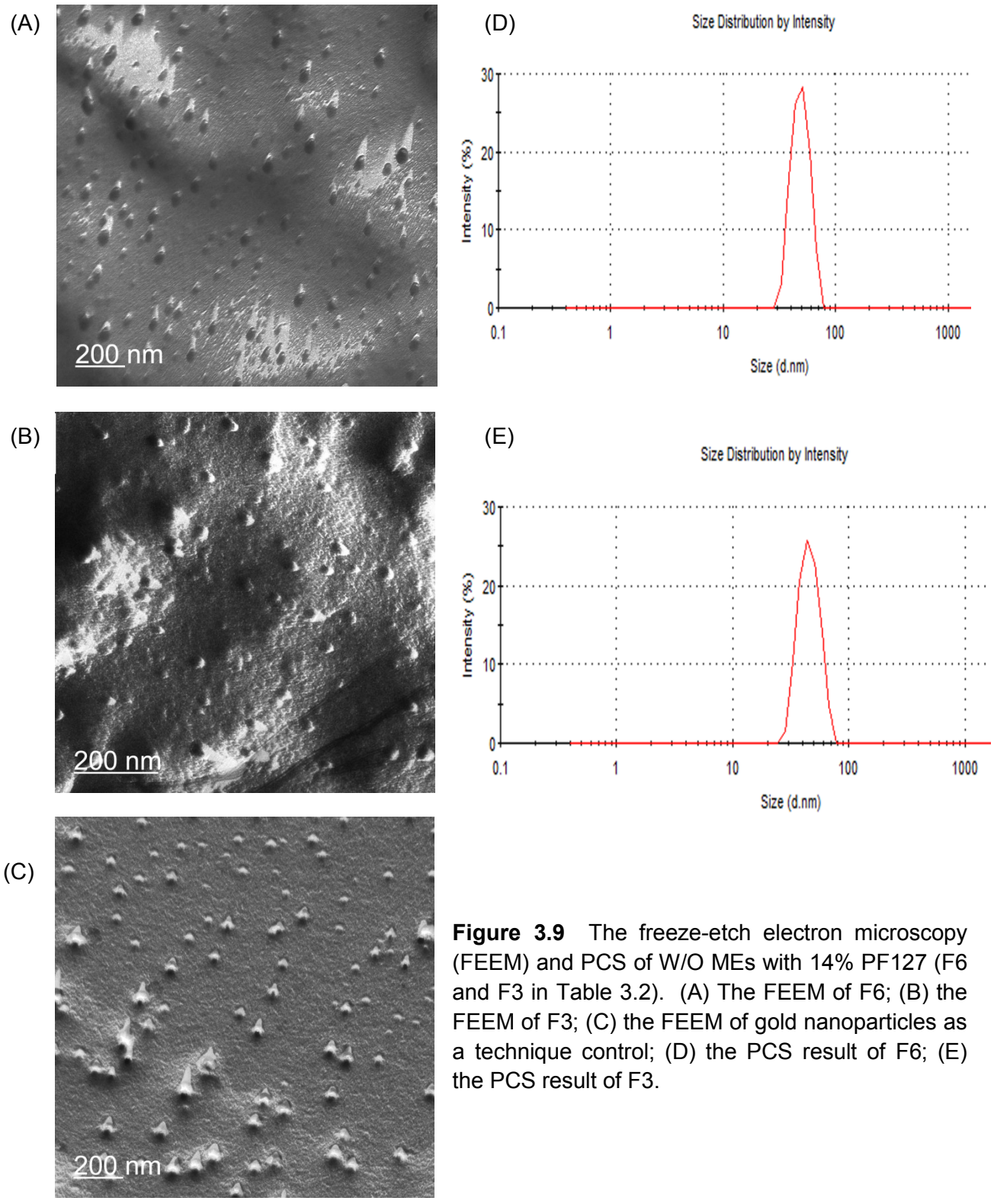

Figure 3.9 The freeze-etch electron microscopy (FEEM) and PCS of W/O MEs with 14% PF127 (F6 and F3 in Table 3.2). (A) The FEEM of F6; (B) the FEEM of F3; (C) the FEEM of gold nanoparticles as a technique control; (D) the PCS result of F6; (E) the PCS result of F3.

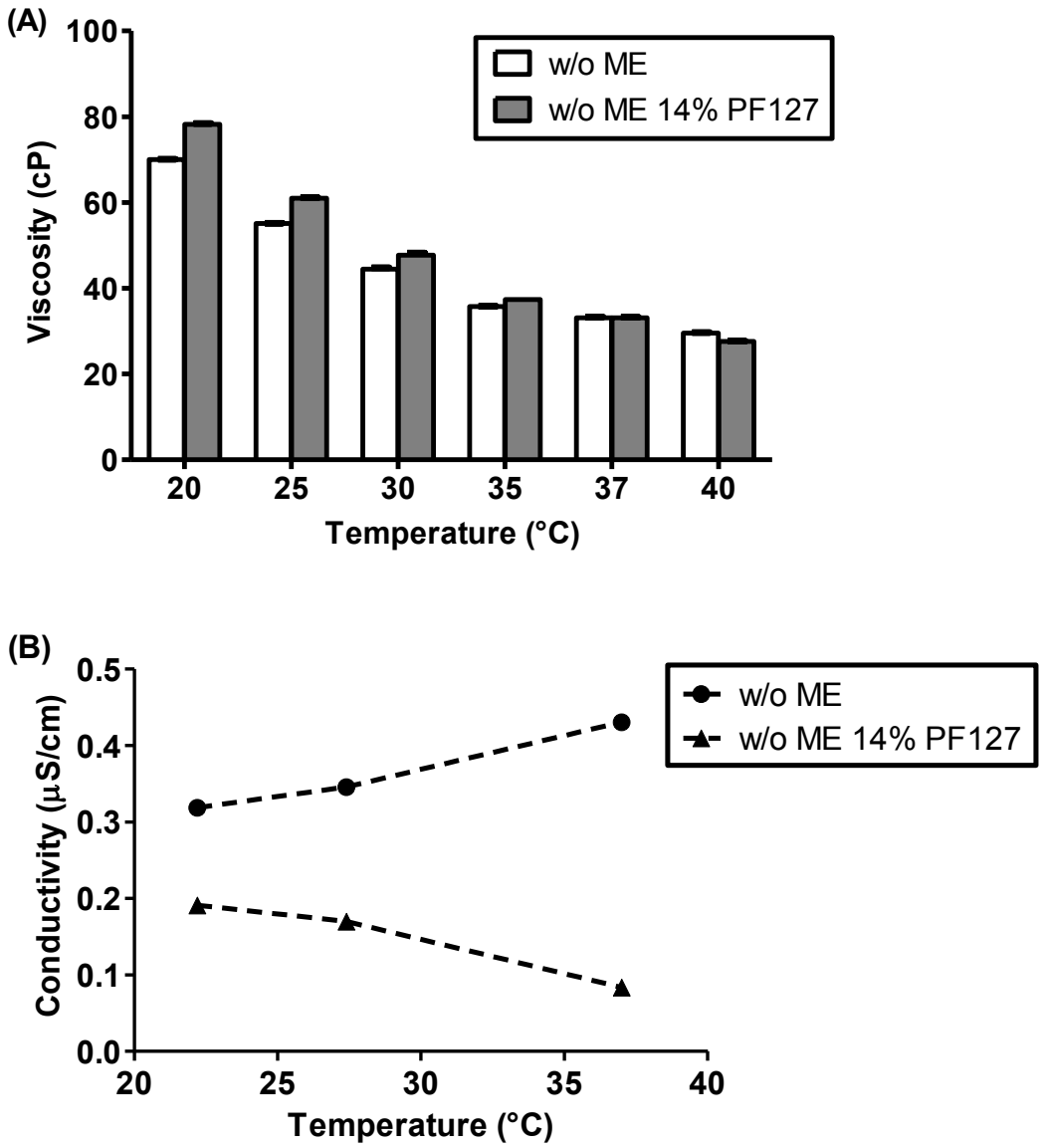

Figure 3.10 Viscosity and conductivity studies of a W/O ME and W/O ME with 14% PF127. (A) The viscosity of the W/O ME and W/O ME with 14% PF127 as a function of temperature; (B) the conductivity of the W/O ME and W/O ME with 14% PF127 at different temperatures.

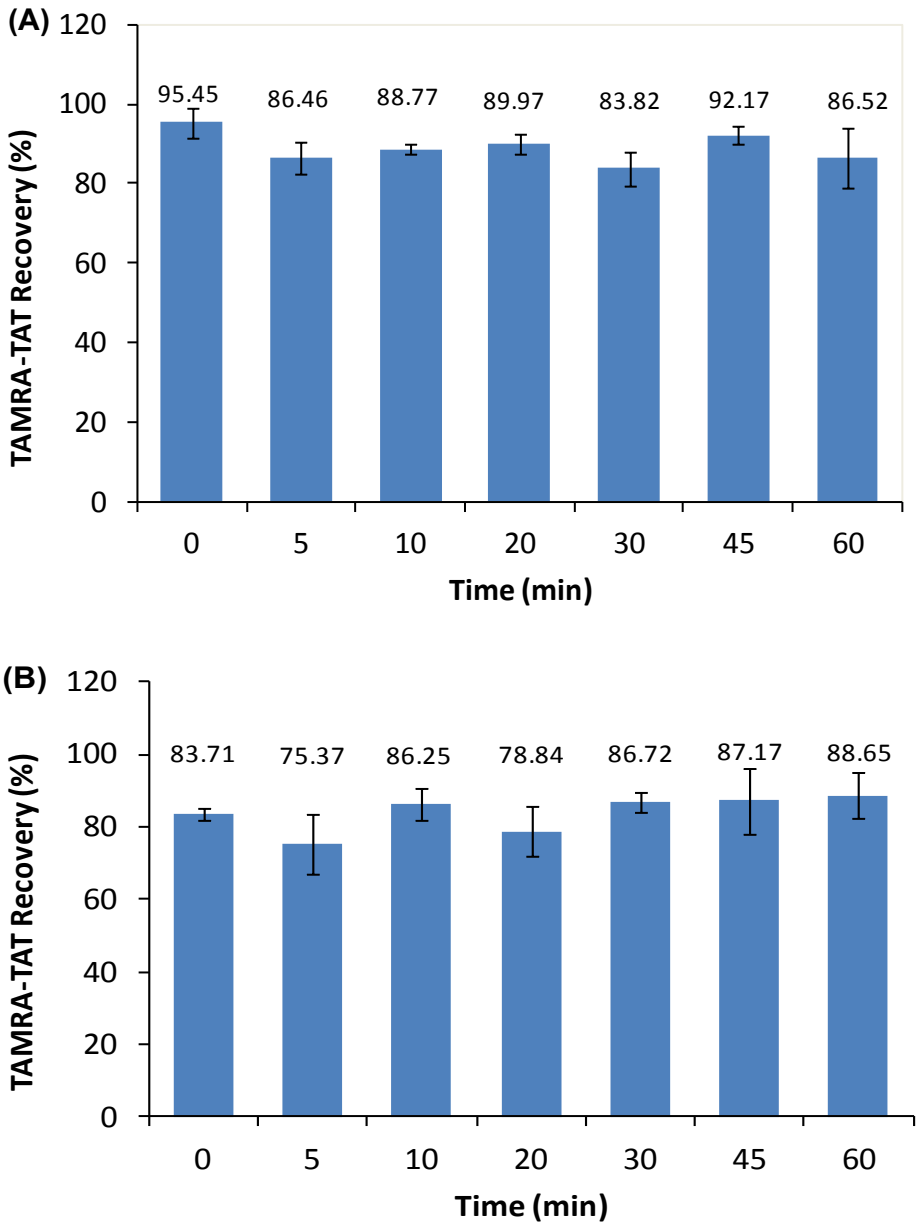

Figure 3.11 TAMRA-TAT recovery study results. (A) The TAMRA-TAT recovery from W/O microemulsion with 14% PF127 after incubation at 37˚C for different times (n = 3); (B) the TAMRA-TAT recovery from 14% PF127 after incubation at 37˚C for different time (n = 3). The difference across all 7 time points in both A and B were analyzed using one-way ANOVA and no significant difference was found for the data set in A or B. $p < 0.05$ is considered significant.

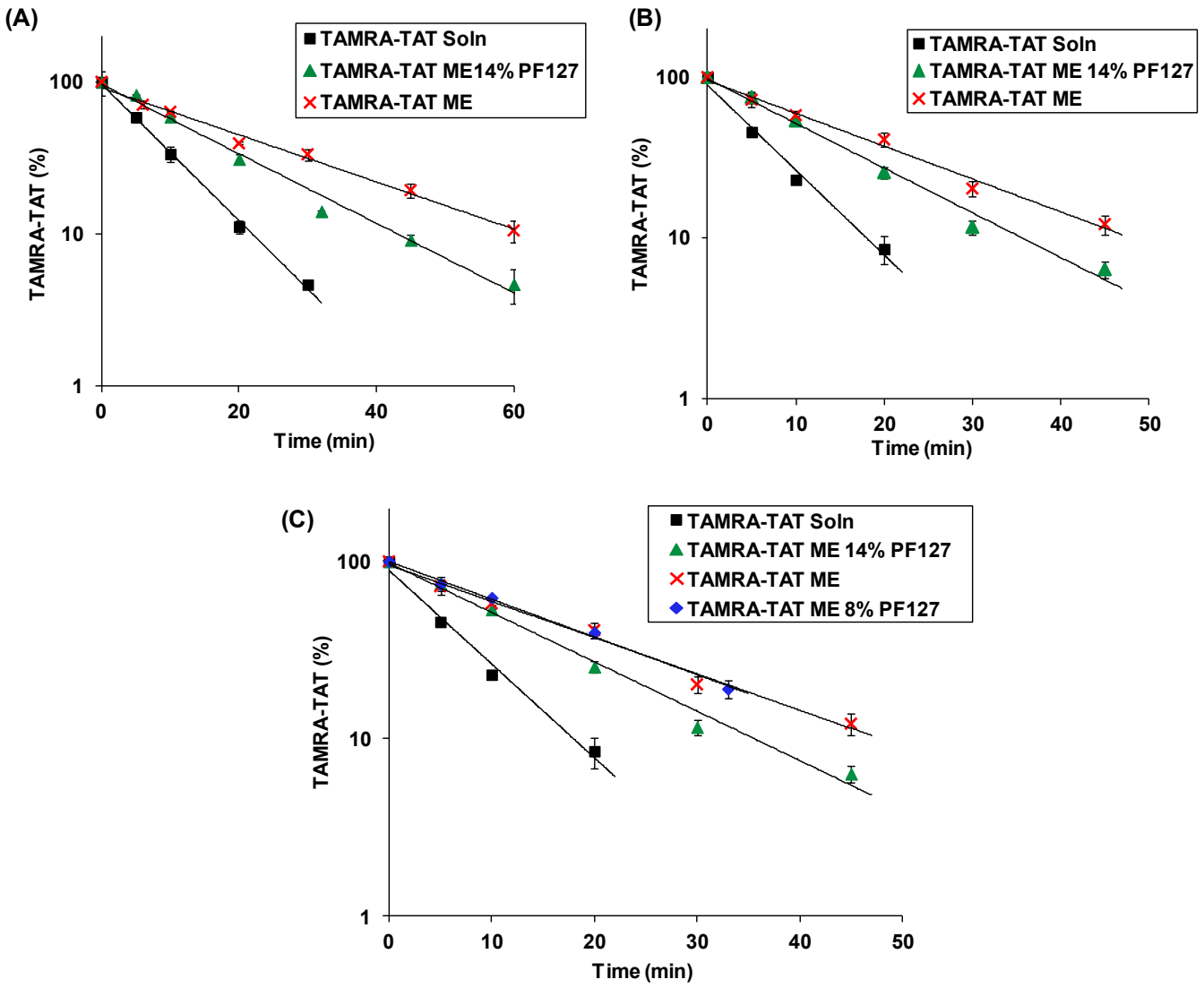

Figure 3.12 TAMRA-TAT degradation profiles in solution, W/O ME, W/O ME with 14% PF127 and W/O ME with 8% PF127 at 37°C in MSIF. The remaining TAMRA-TAT was normalized with respect to the initial concentration. Three samples were prepared for each time point for all the preparations. Data are presented as mean ± SD (*n* = 3) on a logarithmic scale. TAMRA-TAT degradation in all the preparations followed pseudo-first-order kinetics. (A) The first stability study of TAMRA-TAT ME with 14% PF127 as shown in Table 3.4; (B) the second stability study of TAMRA-TAT ME with 14% PF127 as shown in Table 3.5; (C) the degradation profile of TAMRA-TAT in ME with 8% PF127 compared to that in other preparations (Table 3.5).

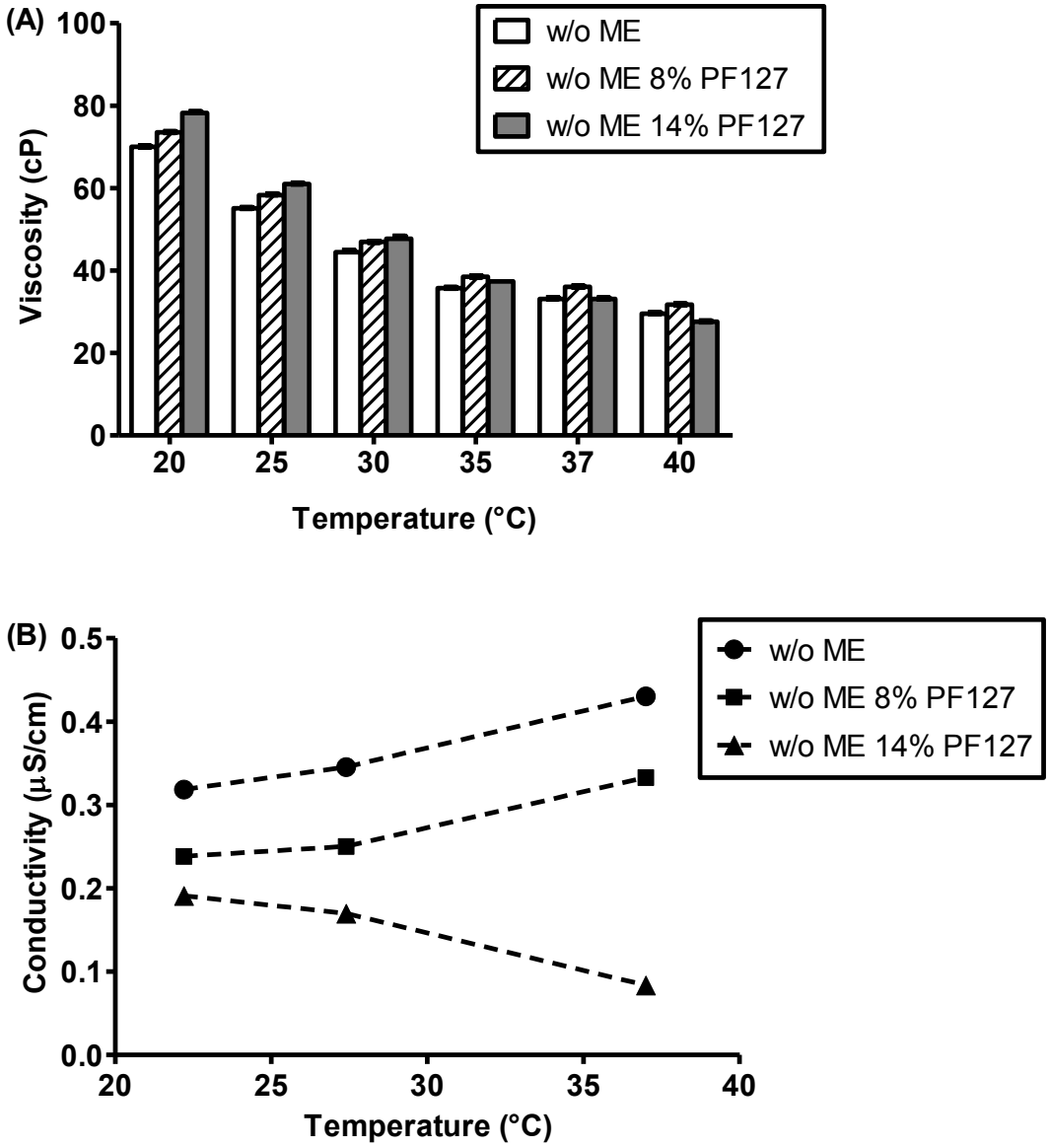

Figure 3.13 Viscosity and conductivity studies of a W/O ME, W/O ME with 8% PF127 and W/O ME with 14% PF127. (A) The viscosity of the W/O ME, W/O ME with 8% PF127 and W/O ME with 14% PF127 at different temperatures; (B) the conductivity of the W/O ME, W/O ME with 8% PF127 and W/O ME with 14% PF127 at different temperatures.

Chapter IV

Conclusions and Future Prospects

The ultimate goal of the present studies was to develop effective oral formulations for the local intestinal delivery of therapeutic peptides to treat local pathologies, like inflammatory bowel disease. A combined formulation strategy was proposed, which included: 1) the development of W/O microemulsions and hydrogel nanoparticles in W/O microemulsions as the delivery vehicle; and 2) further incorporation of the W/O microemulsions and hydrogel nanoparticles in W/O microemulsions into enteric-coated capsules to enhance site-specific delivery. The local intestinal delivery approach has well-accepted advantages as being able to maximize local drug concentration and minimize systemic side effects. The current studies focused on the first part of this combined strategy with the intention to develop an effective W/O microemulsion-based delivery vehicle first. Based on the prior research, W/O microemulsions and W/O microemulsions with Pluronic F127 were developed and explored.

The hypotheses driving these studies were:

1) the W/O microemulsion system may provide better protection to the peptide incorporated compared to peptide water solution when challenged *in vitro* and *in vivo*;

2) the W/O microemulsion with Pluronic F127 may form hydrogel nanoparticles in the W/O microemulsion when temperature increases to close to body temperature at 37˚C, which may provide better protection to the peptide incorporated compared to the W/O

microemulsion without Pluronic F127 or an aqueous solution when challenged by an enzyme-containing system at 37˚C.

4.1 W/O Microemulsions

Water-in-oil microemulsions were developed using Miglyol 812, Capmul MCM, Tween 80 and water. Miglyol 812 was the oil phase, Capmul MCM was the co-surfactant, Tween 80 was the surfactant, and water was the aqueous phase. Three phase diagrams were constructed to guide the formulation optimization. Water-in-oil microemulsions in the selected phase diagram were extensively characterized in terms of rheological properties, droplet diameter, polydispersity index, conductivity, morphology, and phase inversion studies, etc. The selected W/O microemulsion was further evaluated *in vitro* and *in vivo* using a model peptide TAMRA-TAT. The *in vitro* studies showed the half life of TAMRA-TAT in the W/O microemulsion was three-fold greater than that in water solution when challenged by MSIF at 37˚C. The *in vivo* studies in C57/BL6 mice showed that after oral gavage, TAMRA-TAT microemulsion resulted in greater fluorescence intensity in all intestine sections (duodenum, jejunum, ileum and colon) compared to the TAMRA-TAT solution or placebo microemulsion as examined by fluorescence microscopy. The *in vitro* and *in vivo* studies together suggested the W/O microemulsions developed in this study were more protective to the peptide incorporated compared to controls, and may serve as a potential delivery vehicle for local intestinal delivery of water-soluble peptides after their further incorporation into enteric-coated capsules.

The W/O microemulsions developed in this study were thermodynamically stable, and formed spontaneously at room temperature with minimal energy input. These systems may be potentially used as a platform for the oral delivery of a wide range of water-soluble and heat-labile peptides or proteins. However, there is still room for formulation improvement and additional experiments will be necessary before their applications to the

clinic. The protective effect of the W/O microemulsions to the peptide incorporated has been shown *in vitro* and *in vivo*, but the underlying mechanism was proposed without solid proof yet. The peptide incorporated in the W/O microemulsion was shown to be better protected, but the protection was not optimized. One of the formulation strategies to improve this protection is the inclusion of protease inhibitors. A comprehensive list of various pancreatic and brush-border membrane-bound proteases and their inhibitors has been reported by Sood *et al.* [2]. After both qualitative and quantitative considerations, enzyme inhibitors might work together with W/O microemulsions to provide better protection to the peptide or protein incorporated after oral delivery. Although there are concerns that protease inhibitors might interfere with digestive enzymes in the GI-tract and disrupt proper digestions of nutritive proteins, the site-specific delivery to restrict protease inhibitors to the large intestine would make this approach more feasible. A second strategy for potential formulation improvement is to engineer nanoparticles in the W/O microemulsions *in situ*, and as mentioned earlier, nanoparticles in the W/O microemulsion will provide further protection to the cargo incorporated even when phase inversion happens. The third strategy would be the combination with the enteric-coating approach. Water-in-oil microemulsions will be incorporated into enteric-coated capsules, which will enhance the local intestinal delivery to the target region of interest. Some compatibility experiments between excipients in the W/O micremulsions and hard gelation capsules were performed and showed promising results. However, more comprehensive design and experiments will be necessary before the capsule selection, like determination of the water exchange, the possible brittleness change and capsule behaviors under accelerated stability conditions. *In vivo* disintegration experiments in rats using different Eudragit polymer coated capsules containing W/O microemulsions also showed site-specific delivery as expected. The coating materials, coating technique and stability of the peptide or protein in the W/O microemulsions during the coating process, will all need to be evaluated when therapeutic cargos are included.

Another important aspect of the formulation that needs to be evaluated is their short-term and long-term potential toxicities to the local intestinal epithelium. So far, the *in vivo* animal experiments were performed in mice and further evaluation of the optimized formulation with therapeutic peptide in larger animal models is necessary and included in the future plan.

4.2 W/O Microemulsions with Pluronic F127

To overcome the limitation of the current W/O microemulsion system, i.e., phase inversion after oral administration, and to improve the protective effect to the peptide or protein incorporated, W/O microemulsions with Pluronic F127 were explored. Viscosity studies as a function of temperature and concentration were completed using 14% (wt.%) Pluronic F127 as the microemulsion aqueous phase. Phase diagram construction directed the optimization of W/O microemulsions with 14% Pluronic F127. Freeze-etch electron microscopy was proven to be a useful tool to confirm the morphology of W/O microemulsions with different amount of Pluronic F127 at low temperature, but was not able to be employed to assess their morphology at elevated temperature like 37˚C. Viscosity, conductivity, particle size, polydispersity index and turbidity (absorbance at 750 nm) together served as characterization parameters to help understand the temperature-dependent properties of W/O microemusions with different amount of Pluronic F127. The protective effects of the W/O microemulsion with 14% Pluronic F127 and W/O microemulsion with 8% Pluronic F127 were evaluated in *in vitro* enzymatic stability studies using TAMRA-TAT as the model peptide. Results showed that the $t_{1/2}$ of TAMRA-TAT in the W/O microemulsion with 14% Pluronic F127 was two-fold greater than that in water solution, but shorter than that in the W/O microemulsion without Pluronic F127, which was almost three-fold greater than that in water solution. On the contrary, the degradation profile of TAMRA-TAT in the W/O microemulsion with 8% Pluronic F127 was almost superimposed with that in the W/O microemulsion without Pluronic F127. The calculated half lives in the

W/O microemulsion and the W/O microemulsion with 8% Pluronic F127 were almost the same as well. The results from the W/O ME with 14% Pluronic F127 were not what we expected, but all were explained by the physical/chemical characterization data. The large increase in droplet diameter, polydispersity index, and absorbance at 750 nm, and the significant decrease in conductivity all indicated that there might be Pluronic F127 aggregation and droplet coalescence occurring for the W/O ME with 14% Pluronic F127 when temperature increased to around 37˚C. While for the W/O microemulsion with 8% Pluronic F127, these parameters were all similar or showing similar trends with temperature compared to the W/O ME without Pluronic F127. Therefore, it was believed that the aggregation or potential precipitation of Pluronic F127 from the W/O ME with 14% Pluronic F127 might have exposed more TAMRA-TAT associated with it to enzymes, and thus reduced the protection effect.

To develop a more protective W/O ME-based formulation, some suggestions include: (1) exploring different Pluronic polymer as the gellation agent; (2) or using combination of different Pluronics; (3) or using combination of Pluronic polymer with other polymers like carbopol. Yong *et al*. [191] utilized the combination of Pluronic F127 and F68, and obtained a solution with a gel transition temperature at 35.7 ± 0.3°C, which offered an interesting perspective to optimize formulations. Carbopol, sodium alginate and polycarbophil have been shown to lower the gelation temperature of Pluronic F127, and increase the gel strength [220]. The combination of Pluronic F127 and carbopol has been investigated for buccal mucosal delivery as well [221]. However, the large molecular weight of these polymers may be a limiting factor for how much polymer can be incorporated into our W/O ME template. Another potential strategy to improve the formulation is to modify the W/O ME template to improve the droplet size. According to our speculation, the very small droplet size in the current W/O MEs might be a limiting factor for successful gelation. If this is true, a W/O ME system with a larger droplet size might help the gel formation inside the W/O ME.

To form nanoparticles in a W/O ME, alternative nanoparticle formation methods may also be explored. Watnasirichaikul *et al.* [222, 223] investigated interfacial polymerization method to engineer nanocapsules using a W/O microemulsion template similar to Constantinides *et al*. reported [138]. They prepared poly(ethyl 2-cyanoacrylate) nanocapsules by adding Ethyl 2-cyanoacrylate monomers in chloroform to a W/O microemulsion under mechanical stirring, and resulted in nanocapsules with a central cavity surrounded by a polymer wall and a mean particle size around 150 nm. Encapsulted insulin was released in water at pH 2.5 within 3 h and no further evaluation was available.

As mentioned, there is an increasing need to deliver peptides and proteins orally to treat local diseases of the GI-tract, such as inflammatory bowel diseases. It is concluded that the type of systems proposed herein are attractive strategies to meet this need.

Appendices

This section contains the following three sections:

Appendix A *In vivo* evaluation of water-in-oil microemulsions containing recombinant firefly luciferase

Appendix B Gastrointestinal distribution and disintegration of enteric-coated capsules containing water-in-oil microemulsions in rats

Appendix C Standard operation procedure: Preparation of a water-in-oil microemulsion containing 8K-NBD

Appendix A

In Vivo Evaluation of Water-in-Oil Microemulsions Containing Recombinant Firefly Luciferase

A.1 Introduction

Firefly luciferase has been widely used in numerous biomedical, pharmaceutical and bioanalytical applications [224]. It catalyzes luciferin oxidation to oxyluciferin in the presence of ATP and magnesium, resulting in bioluminescence. The luciferin-firefly luciferase assay system has the highest quantum efficiency among the known chemiluminescence reactions [225].

To evaluate whether the W/O microemulsion system developed in this work (Chapter II) could provide protection to proteins after oral intestinal delivery, Quantilum® recombinant luciferase (Luc) expressed from a cloned gene of the North American firefly (*Photinus pyralis*) was used as a model protein. A selected W/O microemulsion containing Luc was evaluated *in vivo* in mice.

A.2 Methods

To assess the relationship of bioluminescence obtained using the IVIS® Kinetic Imaging System (Caliper Life Sciences, Hopkinton, MA, USA) versus the Quantilum® recombinant luciferase (Luc, Promega Corp., Madison, WI, USA) concentration, Luc was serially diluted in luciferase cell lysis buffer (New England BioLabs Inc., Ipswich, MA, USA) containing 1 mg/mL of BSA, and then imaged immediately after the addition of Luciferase Assay Reagent (Promega Corp., Madison, WI, USA), which contained the substrate D-luciferin, magnesium and ATP etc. The resulting luminescence was integrated and plotted against Luc concentration. As shown in Figure A.1, the luminescence was linearly

correlated to the Luc concentration over the range of 1.07 to 34.38 pg/μL using the IVIS Kinetic Imaging System.

C57/BL6 female mice were obtained from the Charles River Labs and maintained in specific pathogen-free conditions. All experiments involving mice were carried out according to the protocol approved by the UNC Institutional Animal Care and Use Committee at the University of North Carolina at Chapel Hill. Twelve-week-old C57/BL6 female mice (18-20 g) were fed with standard chow, and fasted for 2 h before the experiments. Mice had free access to water *ad libitum*. Luc W/O microemulsion (ME) was prepared, and orally gavaged to mice at the dose of 8.8 mg/kg. The composition of Luc W/O ME is shown in Table A.1. Luc diluted in PBS buffer was orally administered to mice at the same dose level (8.8 mg/kg). Placebo ME with the aqueous phase replaced by PBS buffer was orally administered as a control. At predetermined time points following oral administration, mice were given D-luciferin (Caliper Life Sciences, Hopkinton, MA, USA) by i.p. injection at a dose level of 150 mg/kg of mouse weight. Five minutes after the administration of D-luciferin, mice were sacrificed, mouse gastrointestinal tracts were harvested and imaged immediately using the IVIS Kinetic Imaging System.

A.3 Results and Discussion

The bioluminescence images of mouse GI-tract 30 min, 1 h and 4 h following oral administration were shown in Figure A.2-4, respectively. The integrated luminescence was analyzed and shown in Figure A.5. Both 30 min and 1 h following oral administration, significant luminescence was observed from the GI-tract of mice treated with Luc ME compared to Luc buffer or the placebo ME. Four hours after oral administration, there was no much luminescence observed along the GI-tract of mice treated with either Luc ME, Luc buffer or placebo ME. However, most of the luminescence observed following Luc ME administration was around the stomach area, which could be because (1) the luminescence

intensity was too low to be detected as Luc was diluted during the intestinal transit, or (2) Luc was mostly degraded as it passed down the intestinal tract. These results together indicated that Luc was better protected by the W/O microemulsion formulation compared to the PBS buffer *in vivo*.

Table A.1 Luc W/O microemulsion composition.

Ingredients	% (Wt.)
Miglyol 812/Capmul MCM (65:22, w/w)	84.0
Tween 80	10.0
Luc stock (14.37 mg/mL, Cat #: E1702)	6.0

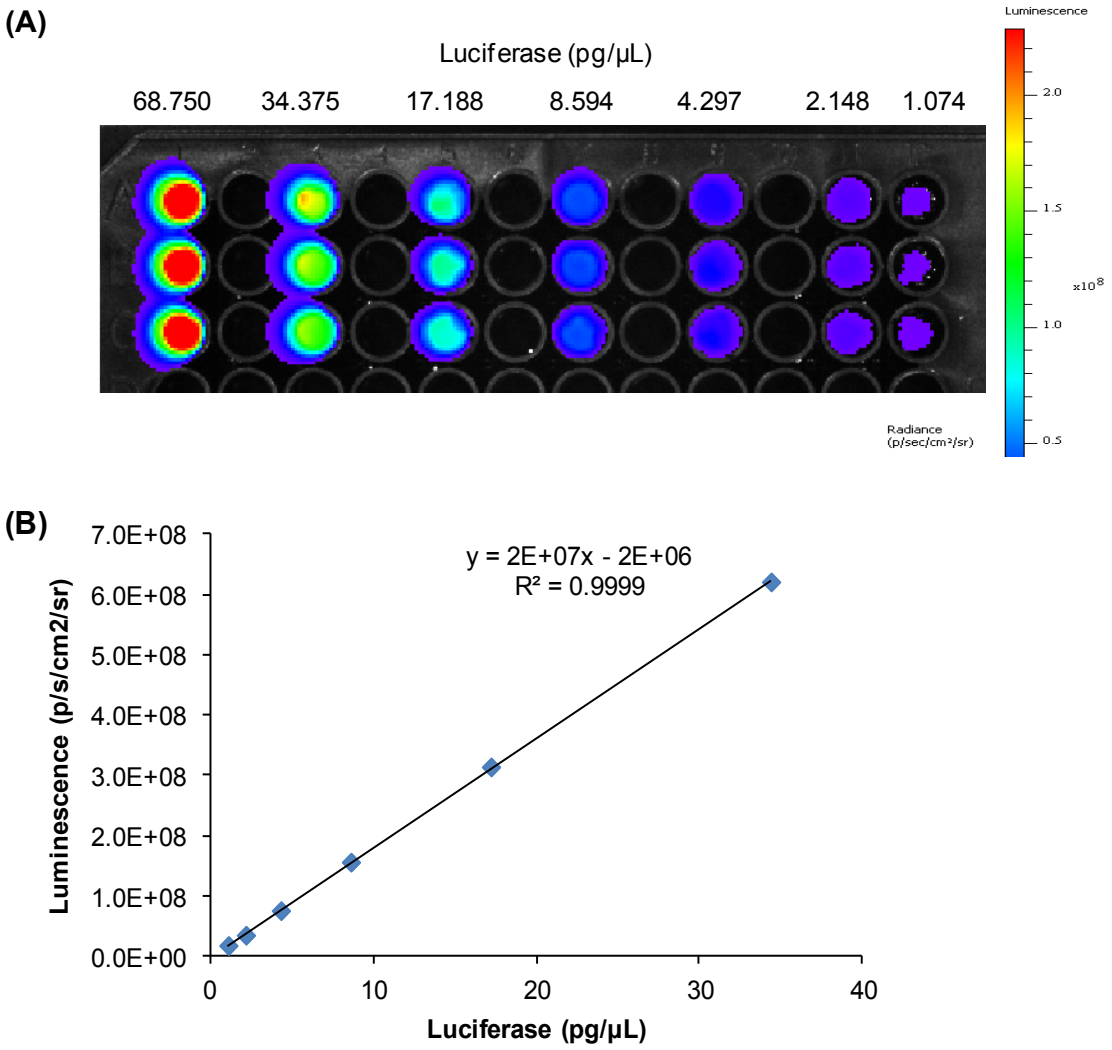

Figure A.1 *In vitro* bioluminescence imaging of recombinant firefly luciferase (Luc) in buffer as a function of concentration. (A) The bioluminescence image of Luc at different concentrations after serial dilution in luciferase cell lysis buffer. (B) The linear relationship of luminescence versus Luc concentration.

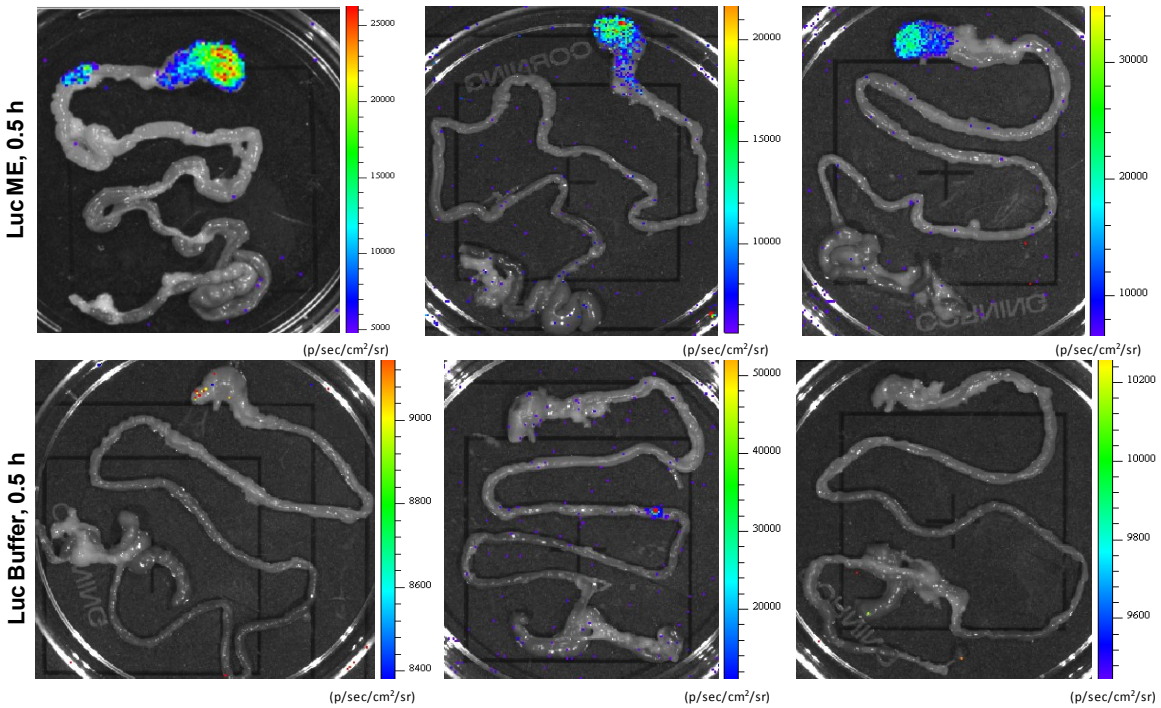

Figure A.2 The bioluminescence images of mouse GI-tract 30 min following oral administration. The top panel shows the results from mice treated with Luc ME, and the lower panel shows the results from mice treated with Luc buffer.

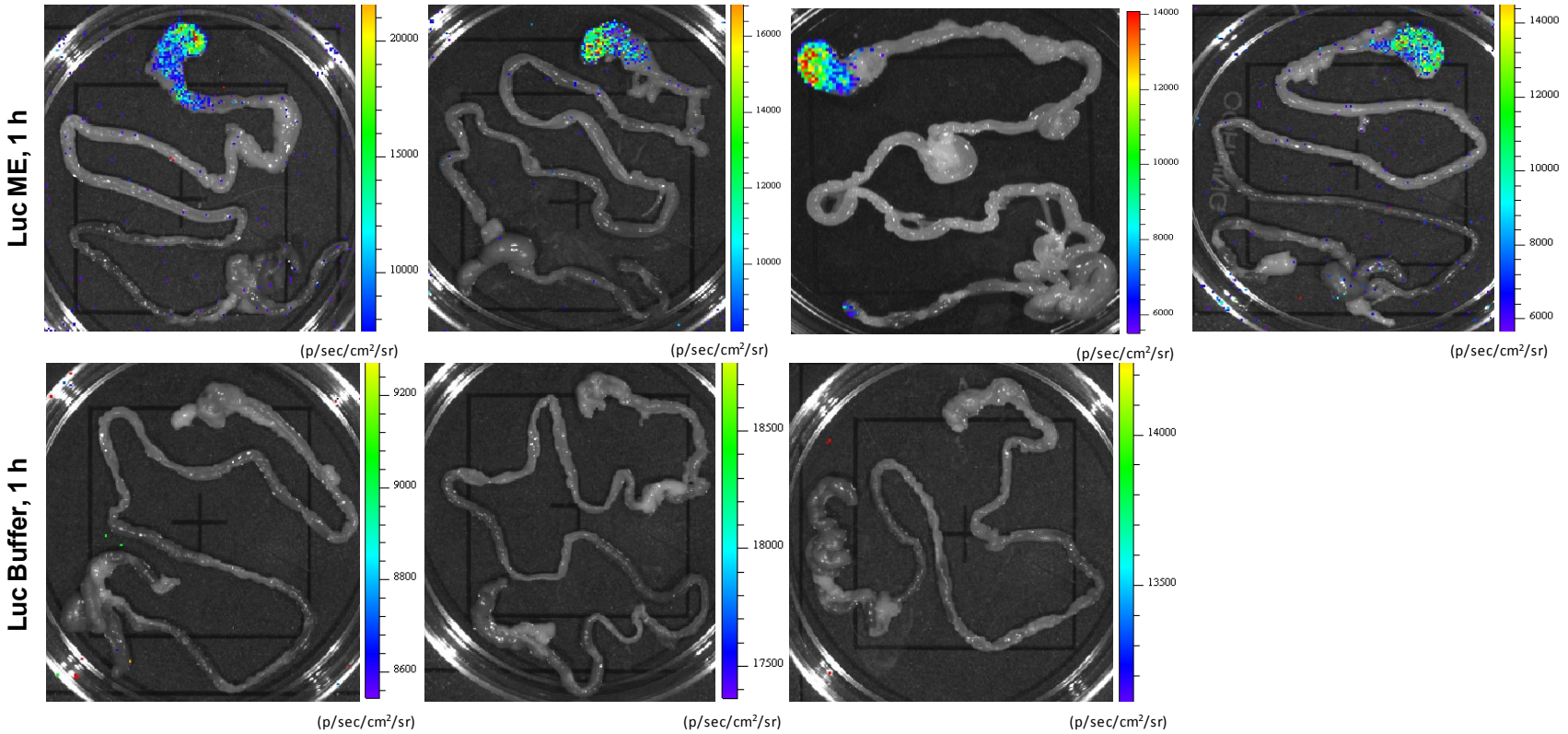

Figure A.3 The bioluminescence images of mouse GI-tract 1 h following oral administration. The top panel shows the results from mice treated with Luc ME, and the lower panel shows the results from mice treated with Luc buffer.

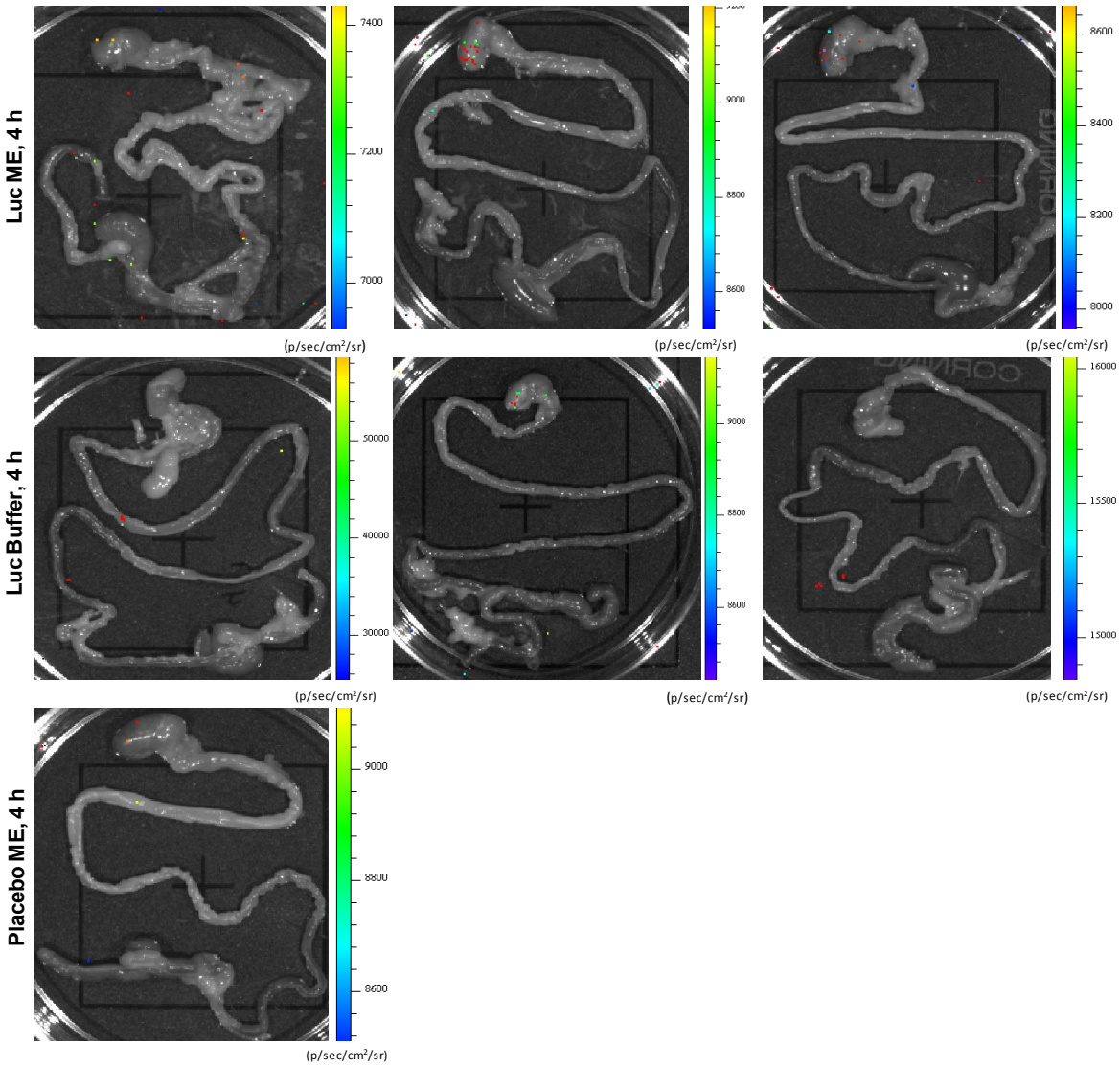

Figure A.4 The bioluminescence images of mouse GI-tract 4 h following oral administration. The top panel shows the results from mice treated with Luc ME, the middle panel shows the results from mice treated with Luc buffer, and the lower panel shows the image from the mouse treated with placebo ME.

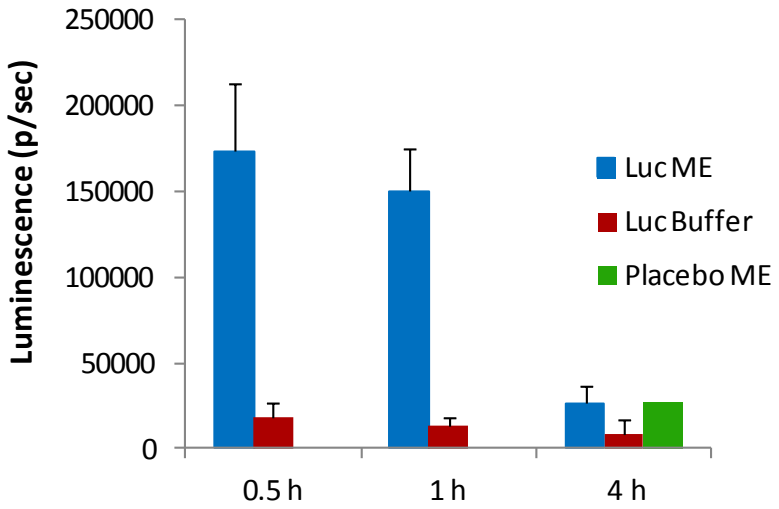

Figure A.5 Comparison of the luminescence from the GI-tract of mice following oral administration of Luc ME, Luc buffer and placebo ME, respectively.

Appendix B

Gastrointestinal Distribution and Disintegration of Enteric-Coated Capsules Containing Water-in-Oil Microemulsions in Rats

B.1 Introduction

After water-in-oil (W/O) microemulsions were developed and optimized, the microemulsion-based formulations containing therapeutic peptides or proteins would be encapsulated into enteric-coated capsules to facilitate site-specific local intestinal delivery. Based on the work reported in Chapter II, pilot studies in rats on the GI transit time and *in vivo* disintegration of the enteric-coated hard gelatin capsules containing W/O MEs were designed. The purpose of these studies was to provide proof-of-concept information for future efficacy studies in animal models.

B.2 Methods

In these studies, two fluorescent molecules TAMRA-TAT and 1,1'-dioctadecyl-3,3,3',3'-tetramethylindotricarbocyanine Iodide ('DiR', Invitrogen, Grand Island, NY, USA) were used as fluorescent markers to help visualize the *in vivo* capsule transit and disintegration process. Torpac® size 9 gelatin minicapsules (Torpac Inc., Fairfield, NJ, USA) were used as the W/O ME carriers. Four rat studies were performed and summarized as follows. All studies involving rats were carried out according to the protocol approved by the UNC Institutional Animal Care and Use Committee at the University of North Carolina at Chapel Hill.

The composition of TAMRA-TAT ME is shown in Table B.1. Eudragit L100-55 coated capsules containing TAMRA-TAT ME (20-25 µL/capsule) were prepared by a two-step coating process. After being loaded with TAMRA-TAT ME, capsules were first dip-coated with coating solution F1 (Table B.2) five times, and then painted using a brush with

coating solution F7 (Table B.2) five times. Coated capsules were dried at room temperature (RT) using a five-inch desk air fan.

Eudragit L100 coated capsules containing TAMRA-TAT ME (20-25 µL/capsule) were prepared using a similar coating process. TAMRA-TAT ME loaded capsules were first dip-coated with coating solution F9 (Table B.3, five times), then painted with coating solution F10 (Table B.3, five times), and dried at RT using a five-inch desk air fan.

The composition of 'DiR' ME is shown in Table B.4. Eudragit L100 coated capsules containing 'DiR' ME (20-25 µL/capsule) were coated in the same way as described above for the preparation of Eudragit L100 coated TAMRA-TAT ME-containing capsules .

Eudragit S100 coated capsules containing 'DiR' ME (20-25 µL/capsule) were prepared similarly. 'DiR' ME loaded capsules were first dip-coated with coating solution F11 (Table B.5, five times), then painted with coating solution F12 (Table B.5, five times), and dried at RT using a five-inch desk air fan.

Male Sprague-Dawley rats (Charles River Labs) were fasted over night before and throughout the experiments, but with free access to water *ad libitum*. Enteric-coated capsules containing TAMRA-TAT ME or 'DiR' ME were administered to rats orally using a dosing syringe (Torpac Inc., Fairfield, NJ, USA). At predetermined time points following oral administration, rats were sacrificed, the rat GI tracts were taken out and imaged using the IVIS Kinetic Imaging System via fluorescence detection. The detection wavelengths for TAMRA-TAT and 'DiR' were (Ex/Em) 535/580 nm and (Ex/Em) 745/800 nm, respectively. After the imaging, the rat GI tracts were cut open and capsules were physically searched and located.

B.3 Results and Discussion

The first study showed the GI distribution and *in vivo* disintegration of Eudragit L100-55 coated capsules containing TAMRA-TAT ME in rats (Figure B.1A). Two hours following

oral administration, all three capsules were found intact in the rat stomach. Four hours following oral administration, one capsule was found partially disintegrated in the jejunum, while the rest of the capsules stayed intact in the stomach. Eight hours following oral administration, bright fluorescence was found at the entry of the cecum and no capsules were found throughout the whole GI tract. Figure B.1B shows the images of capsules containing TAMRA-TAT ME before and after enteric coating, and their morphology after they were found in the rat GI tract following oral administration.

The second study showed the GI distribution and *in vivo* disintegration of Eudragit L100 coated capsules containing TAMRA-TAT ME in rats (Figure B.2). Similar to the first study, 2 h and 4 h following oral administration, all the capsules were found intact in the rat stomach, while 8 h after dosing, bright fluorescence was found at the distal small intestine before the cecum, which indicated one of the capsules might have disintegrated at the ileum region. After the capsules stayed in the rat stomach for 2 h and 4 h, respectively, they appeared intact without any deformation. Compared to capsules coated with Eudragit L100-55, capsules coated with Eudragit L100 seemed to be more stable in the acidic environment. An *in vitro* disintegration test using Eudragit L100 coated size 9 capsules showed that these capsules stayed intact in the 0.1 M HCl for more than 4.5 h. After being transferred to phosphate buffer of pH 6.5, the capsules disintegrated within 10 min. The slow stomach emptying of these enteric coated size 9 capsules was probably due to the relatively large size of the capsules compared to the narrow passage of the rat intestinal tract. This slow stomach emptying of size 9 minicapsules in rats was also reported by Saphier *et al*. [226].

'DiR' is a near infrared fluorescent, lipophilic molecule. The fluorescence emitted from 'DiR' is much stronger and easier to penetrate through tissues compared to TAMRA-TAT. In the third study, Eudragit L100 coated capsules containing 'DiR' ME were orally administered to rats. The GI distribution and *in vivo* disintegration of these capsules are shown in Figure B.3. To avoid the potential interference of stomach emptying between

capsules, each rat received one capsule in this study. The results showed that 4 h following oral administration, the capsule stayed intact in the stomach. In contrast, 5, 6, 7 and 8 h following oral administration, all the capsules disintegrated in the lower small intestine, respectively, and no intact capsules were found. In combination with the second study, the results indicated Eudragit L100 coated capsules could be emptied from the rat stomach 4 h following oral administration, and then disintegrate in the lower rat small intestine.

In the fourth study, the GI distribution and *in vivo* disintegration of Eudragit S100 coated capsules containing 'DiR' ME were investigated in rats. As shown in Figure B.4, 5 h following oral administration, the capsule still stayed intact in the stomach. In contrast, 6 h following oral administration, strong fluorescence was found in the lower small intestine before the cecum. Seven hours following oral administration, some fluorescence was found in the cecum and no fluorescence was found in the small intestine. Eight hours following oral administration, some fluorescence was found in the colon. Theses results indicated that the Eudragit S100 coated capsules could better facilitate colon-specific drug delivery.

In summary, with the help of fluorescent molecules and IVIS Kinetic Imaging System, the GI distribution and *in vivo* disintegration of various enteric coated minicapsules containing W/O MEs were visualized in the rat GI tract. These results confirmed that the enteric-coating strategy may facilitate site-specific delivery of W/O MEs containing theraptic peptides to the lower GI tract, such as the colon. These data provided helpful information for future efficacy studies of drug loaded W/O MEs in enteric coated capsules in animals.

Table B.1 TAMRA-TAT W/O microemulsion formulation.

Ingredients	Weight (mg)
Miglyol 812/Capmul MCM (65:22, w/w)	840
Tween 80	100
TAMRA-TAT water stock (4 mg/mL)	60

Table B.2 Eudragit L100-55 coating solutions.

Per 100 g	F1 (g)	F7 (g)
Eudragit L100-55	12.5	15
Triethyl citrate*	6.25 (50%)	3.75 (25%)
Talc	0	3.75
Acetone:IPA (60:40,v/v)	81.25	77.5

* Calculated based on the weight of Eudragit L100-55.

Table B.3 Eudragit L100 coating solutions.

Per 100 g	F9 (g)	F10 (g)
Eudragit L100	12.5	15
Triethyl citrate*	6.25 (50%)	3.75 (25%)
Talc	0	3.75
Acetone:IPA (60:40,v/v)	81.25	77.5

* Calculated based on the weight of Eudragit L100.

Table B.4 'DiR' W/O microemulsion formulation.

Ingredients	Weight (mg)
Miglyol 812/Capmul MCM (65:22, w/w)	840
Tween 80	100
Water	60
'DiR'	0.4

Table B.5 Eudragit S100 coating solutions.

Per 100 g	F9 (g)	F10 (g)
Eudragit S100	12.5	15
Triethyl citrate*	6.25 (50%)	3.75 (25%)
Talc	0	3.75
Acetone:IPA (60:40,v/v)	81.25	77.5

* Calculated based on the weight of Eudragit S100.

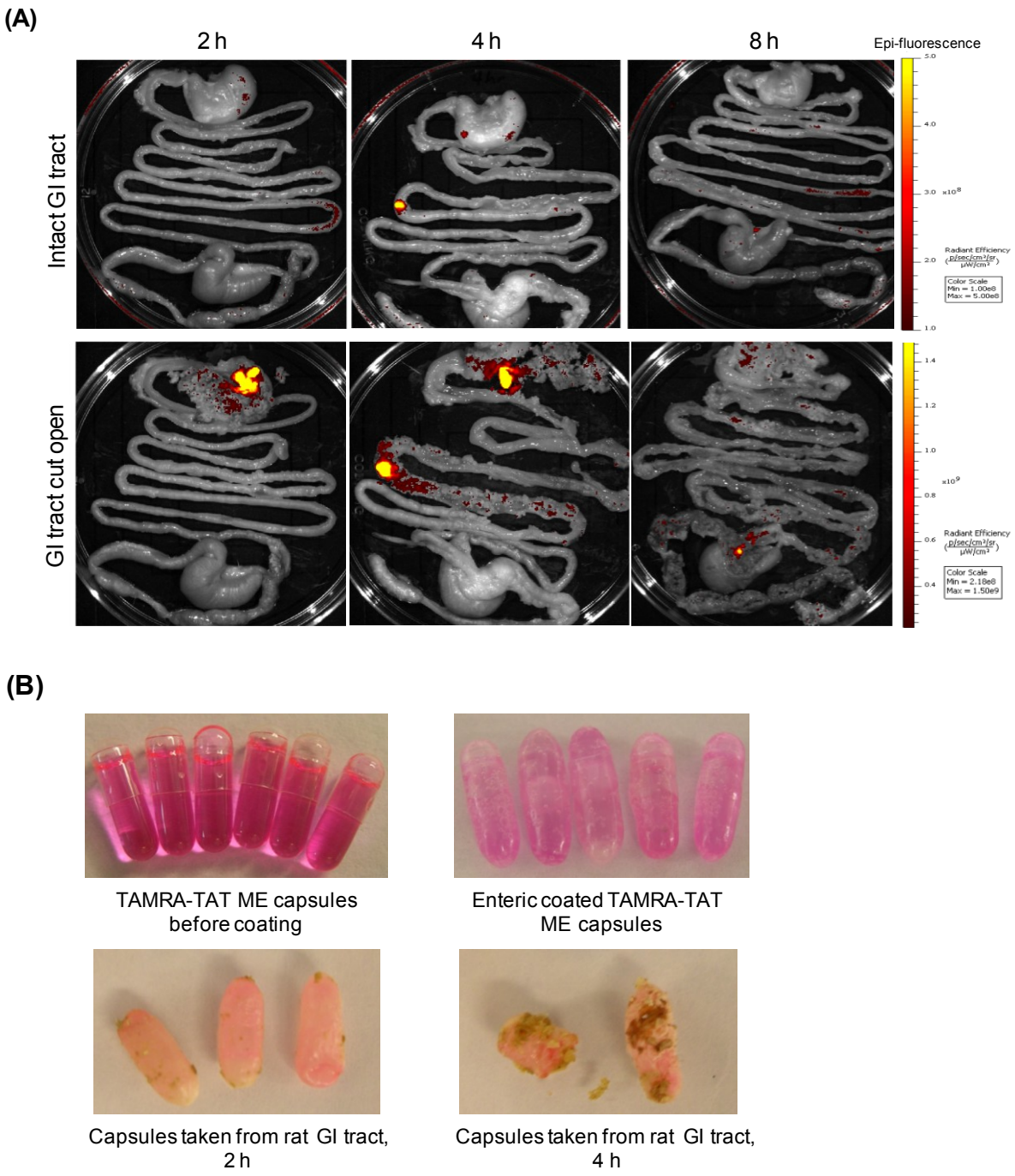

Figure B.1 (A) Rat GI distribution of Eudragit L100-55 coated capsules containing TAMRA-TAT ME 2, 4 and 8 h following oral administration. Each rat received 3 capsules in this study, and the rat weight ranged from 390-410 g. The top panel shows images of intact rat GI tracts. The lower panel shows images of the corresponding rat GI tracts after they were cut open to faciliate physical location of the capsules. (B) Pictures of TAMRA-TAT capsules before and after enteric coating (top panel), and after staying in the rat GI tract for indicated time period (lower panel).

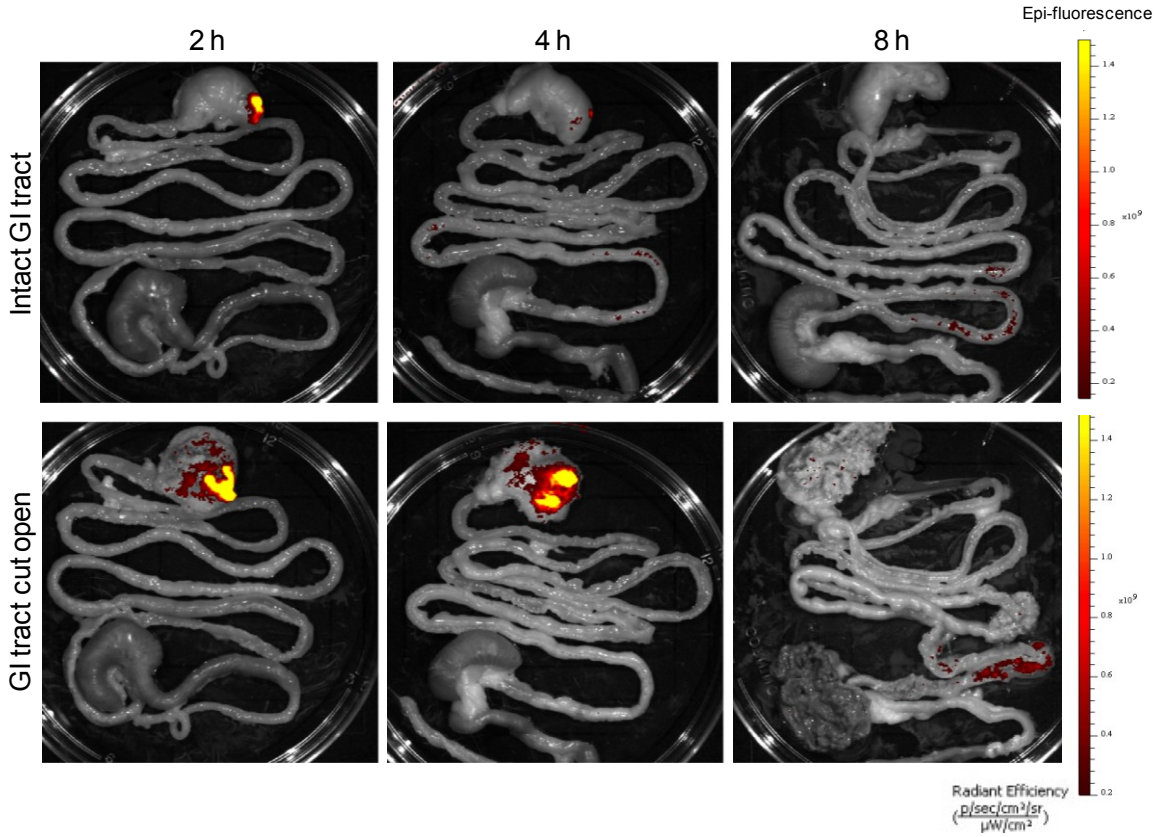

Figure B.2 Rat GI distribution of Eudragit L100 coated capsules containing TAMRA-TAT ME 2, 4 and 8 h following oral administration. Each rat received 3 capsules in this study, and the rat weight ranged from 420-470 g. The top panel shows images of intact rat GI tracts. The lower panel shows images of the corresponding rat GI tracts after they were cut open to faciliate physical location of the capsules.

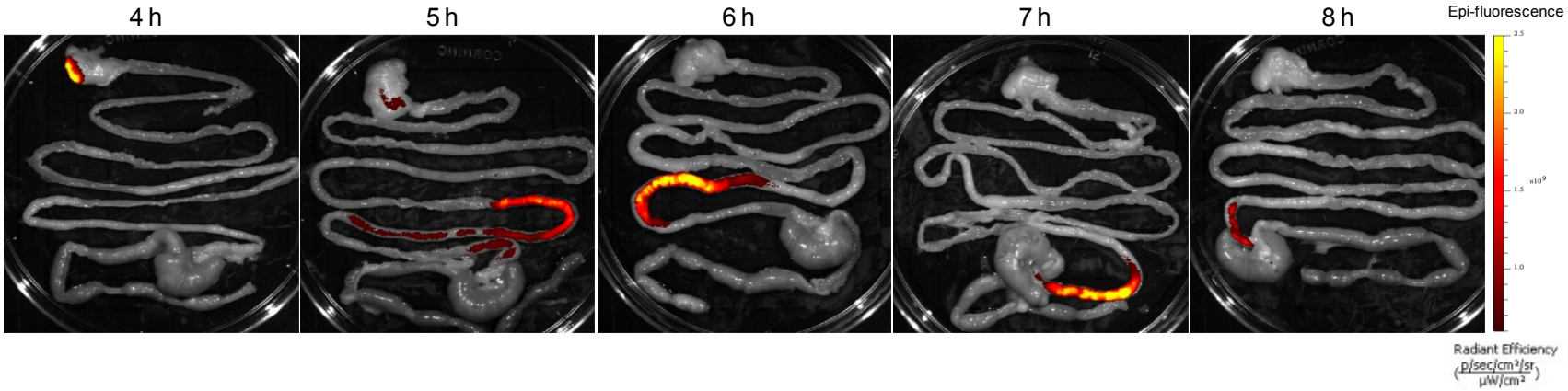

Figure B.3 Rat GI distribution of Eudragit L100 coated capsules containing 'DiR' ME after oral administration. All the GI tracts shown here were intact. Each rat received one capsule in this study, and the rat weight ranged from 250-290 g.

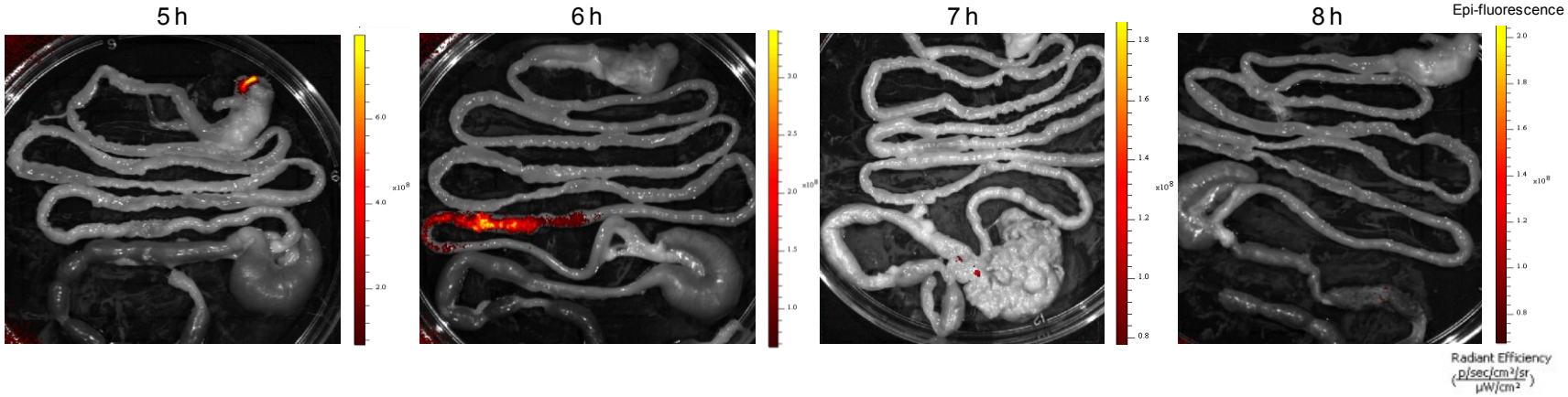

Figure B.4 Rat GI distribution of Eudragit S100 coated capsules containing 'DiR' ME after oral administration. All the GI tracts shown here were partially cut open. Each rat received 1 capsule in this study, and the rat weight ranged from 320-400 g.

Appendix C

Standard Operation Procedure: Preparation of a Water-in-Oil Microemulsion Containing 8K-NBD

C.1 Objective

This standard operation procedure describes the process to prepare 100 g of W/O microemulsion containing 8K-NBD at a final concentration of 1 mg/g in the microemulsion.

C.2 Materials

Miglyol 812, neutral oil, Sasol Germany GmbH (Eatontown, NJ, USA)

Capmul MCM NF, Abitec Corporation (Janesville, WI, USA)

Tween 80, Spectrum Chemical MFG. Corporation (Gardena, CA, USA)

8K-NBD, TheraLogics, Inc.

Deionized water, Milli-Q Advantage System

C.3 Procedure

1. To prepare an 8K-NBD stock solution at 16.67 mg/g in deionized water, weigh out 110 mg of 8K-NBD into a 20 mL scintillation vial, and then add 6.49 g of deionized water and shake well to dissolve 8K-NBD completely in deionized water.
2. Weigh out 62.76 g of Miglyol 812 and 21.24 g of Capmul MCM into a 125 mL Wheaton glass bottle.
3. Add 10 g of Tween 80 to the Wheaton glass bottle in step 2.
4. Add 6 g of 8K-NBD stock solution from step 1 to the Wheaton glass bottle in step 3.
5. Add a magnetic stir bar to the Wheaton glass bottle in step 4, and stir in an ice water bath for 20-30 minutes until the microemulsion becomes homogeneous and clear.

References

[1] Hamman JH, Enslin GM, Kotzé AF. Oral delivery of peptide drugs: Barriers and developments. BioDrugs. 2005;19(3):165-77.

[2] Sood A, Panchagnula R. Peroral route: An opportunity for protein and peptide drug delivery. Chemical Reviews. 2001;101(11):3275-304.

[3] Morishita M, Peppas NA. Is the oral route possible for peptide and protein drug delivery? Drug Discovery Today. 2006;11(19-20):905-10.

[4] Martins S, Sarmento B, Ferreira DC, Souto EB. Lipid-based colloidal carriers for peptide and protein delivery - liposomes versus lipid nanoparticles. International Journal of Nanomedicine. 2007;2(4):595-607.

[5] Lowman AM, Morishita M, Kajita M, Nagai T, Peppas NA. Oral delivery of insulin using pH-responsive complexation gels. Journal of Pharmaceutical Sciences. 1999; 88(9):933-7.

[6] Whitehead K, Shen Z, Mitragotri S. Oral delivery of macromolecules using intestinal patches: Applications for insulin delivery. Journal of Controlled Release. 2004;98(1): 37-45.

[7] Al-Hilal TA, Alam F, Byun Y. Oral drug delivery systems using chemical conjugates or physical complexes. Advanced Drug Delivery Reviews. 2012; December 7, DOI: http://dx.doi.org/10.1016/j.addr.2012.11.002. [Epub ahead of print].

[8] Graf A, Rades T, Hook SM. Oral insulin delivery using nanoparticles based on microemulsions with different structure-types: Optimisation and *in vivo* evaluation. European Journal of Pharmaceutical Sciences. 2009;37(1):53-61.

[9] Dogru ST, Çalis S, Öner F. Oral multiple w/o/w emulsion formulation of a peptide salmon calcitonin: *In vitro-in vivo* evaluation. Journal of Clinical Pharmacy and Therapeutics. 2000;25(6):435-43.

[10] Saffran M, Field JB, Pena J, Jones RH, Okuda Y. Oral insulin in diabetic dogs. Journal of Endocrinology. 1991;131(2):267-78.

[11] Musabayane C, Munjeri O, Bwititi P, Osim E. Orally administered, insulin-loaded amidated pectin hydrogel beads sustain plasma concentrations of insulin in streptozotocin-diabetic rats. Journal of Endocrinology. 2000;164(1):1-6.

[12] Edwards C. Physiology of the colorectal barrier. Advanced Drug Delivery Reviews. 1997;28(2):173-90.

[13] Siccardi D, Turner JR, Mrsny RJ. Regulation of intestinal epithelial function: a link between opportunities for macromolecular drug delivery and inflammatory bowel disease. Advanced Drug Delivery Reviews. 2005;57(2):219-35.

[14] Schiller C, Frohlich CP, Giessmann T, Siegmund W, Monnikes H, Hosten N, et al. Intestinal fluid volumes and transit of dosage forms as assessed by magnetic resonance imaging. Alimentary Pharmacology & Therapeutics. 2005;22(10): 971-9.

[15] Yamamoto A, Taniguchi T, Rikyuu K, Tsuji T, Fujita T, Murakami M, et al. Effects of various protease inhibitors on the intestinal-absorption and degradation of insulin in rats. Pharmaceutical Research. 1994;11(10):1496-500.

[16] Gibson SAW, McFarlan C, Hay S, Macfarlane GT. Significance of microflora in proteolysis in the colon. Applied and Environmental Microbiology. 1989;55(3):679-83.

[17] Bai JPF, Chang LL, Guo JH. Targeting of peptide and protein drugs to specific sites in the oral route. Critical Reviews in Therapeutic Drug Carrier Systems. 1995;12(4): 339-71.

[18] Haupt S, Rubinstein A. The colon as a possible target for orally administered peptide and protein drugs. Critical Reviews in Therapeutic Drug Carrier Systems. 2002;19(6): 499-551.

[19] Holtmann G, Kelly DG, Sternby B, DiMagno EP. Survival of human pancreatic enzymes during small bowel transit: Effect of nutrients, bile acids, and enzymes. American Journal of Physiology-Gastrointestinal and Liver Physiology. 1997;273(2): G553-G8.

[20] Langguth P, Bohner V, Heizmann J, Merkle HP, Wolffram S, Amidon GL, et al. The challenge of proteolytic enzymes in intestinal peptide delivery. Journal of Controlled Release. 1997;46:39-57.

[21] Woodley JF. Enzymatic barriers for GI peptide and protein delivery. Critical Reviews in Therapeutic Drug Carrier Systems. 1994;11(2-3):61-95.

[22] Hold GL, Pryde SE, Russell VJ, Furrie E, Flint HJ. Assessment of microbial diversity in human colonic samples by 16S rDNA sequence analysis. Fems Microbiology Ecology. 2002;39(1):33-9.

[23] Moore WEC, Holdeman LV. Human fecal flora - normal flora of 20 Japanese-Hawaiians. Applied Microbiology. 1974;27(5):961-79.

[24] McConnell EL, Short MD, Basit AW. An *in vivo* comparison of intestinal pH and bacteria as physiological trigger mechanisms for colonic targeting in man. Journal of Controlled Release. 2008;130(2):154-60.

[25] Wilson CG. The transit of dosage forms through the colon. International Journal of Pharmaceutics. 2010;395(1-2):17-25.

[26] McConnell EL, Liu F, Basit AW. Colonic treatments and targets: issues and opportunities. Journal of Drug Targeting. 2009;17(5):335-63.

[27] Nugent SG, Kumar D, Rampton DS, Evans DF. Intestinal luminal pH in inflammatory bowel disease: Possible determinants and implications for therapy with aminosalicylates and other drugs. Gut. 2001;48(4):571-7.

[28] McDougall CJ, Wong R, Scudera P, Lesser M, Decosse JJ. Colonic mucosal pH in humans. Digestive Diseases and Sciences. 1993;38(3):542-5.

[29] Friend DR. New oral delivery systems for treatment of inflammatory bowel disease. Advanced Drug Delivery Reviews. 2005;57(2):247-65.

[30] Klotz U, Schwab M. Topical delivery of therapeutic agents in the treatment of inflammatory bowel disease. Advanced Drug Delivery Reviews. 2005;57(2):267-79.

[31] Goto T, Morishita M, Nishimura K, Nakanishi M, Kato A, Ehara J, et al. Novel mucosal insulin delivery systems based on fusogenic liposomes. Pharmaceutical Research. 2006;23(2):384-91.

[32] Coco R, Plapied L, Pourcelle V, Jérôme C, Brayden DJ, Schneider Y-J, et al. Drug delivery to inflamed colon by nanoparticles: Comparison of different strategies. International Journal of Pharmaceutics. 2013;440(1):3-12.

[33] Theiss AL, Laroui H, Obertone TS, Chowdhury I, Thompson WE, Merlin D, et al. Nanoparticle-based therapeutic delivery of prohibitin to the colonic epithelial cells ameliorates acute murine colitis. Inflammatory Bowel Diseases. 2011;17(5):1163-76.

[34] Van den Mooter G, Vervoort L, Kinget R. Characterization of methacrylated inulin hydrogels designed for colon targeting: *in vitro* release of BSA. Pharmaceutical Research. 2003;20(2):303-7.

[35] Tozaki H, Komoike J, Tada C, Maruyama T, Terabe A, Suzuki T, et al. Chitosan capsules for colon-specific drug delivery: Improvement of insulin absorption from the rat colon. Journal of Pharmaceutical Sciences. 1997;86(9):1016-21.

[36] Tozaki H, Nishioka J, Komoike J, Okada N, Fujita T, Muranishi S, et al. Enhanced absorption of insulin and (Asu1,7)eel-calcitonin using novel azopolymer-coated pellets for colon-specific drug delivery. Journal of Pharmaceutical Sciences. 2001; 90(1):89-97.

[37] Cheng CL, Gehrke SH, Ritschel WA. Development of an azopolymer based colonic release capsule for delivering proteins/macromolecules. Methods and Findings in Experimental and Clinical Pharmacology. 1994;16(4):271-8.

[38] Cheng K, Lim LY. Insulin-loaded calcium pectinate nanoparticles: Effects of pectin molecular weight and formulation pH. 2004;30(4):359-67.

[39] Saffran M, Kumar GS, Savariar C, Burnham JC, Williams F, Neckers DC. A new approach to the oral administration of insulin and other peptide drugs. Science. 1986; 233(4768):1081-4.

[40] Katsuma M, Watanabe S, Kawai H, Takemura S, Masuda Y, Fukui M. Studies on lactulose formulations for colon-specific drug delivery. International Journal of Pharmaceutics. 2002;249:33-43.

[41] Simon GL, Gorbach SL. The human intestinal microflora. Digestive Diseases and Sciences. 1986;31(9):S147-S62.

[42] Hill MJ, Drasar BS. The normal colonic bacterial flora. Gut. 1975;16(4):318-23.

[43] Sinha VR, Kumria R. Microbially triggered drug delivery to the colon. European Journal of Pharmaceutical Sciences. 2003;18(1):3-18.

[44] Rubinstein A. Microbially controlled drug delivery to the colon. Biopharmaceutics & Drug Disposition. 1990;11(6):465-75.

[45] Scheline RR. Metabolism of foreign compounds by gastrointestinal microorganisms. Pharmacological Reviews. 1973;25(4):451-523.

[46] Kinget R, Kalala W, Vervoort L, van den Mooter G. Colonic drug targeting. Journal of Drug Targeting. 1998;6(2):129-49.

[47] Peppercorn MA, Goldman P. The role of intestinal bacteria in the metablism of salicylazosulfapyridine. The Journal of Pharmacology and Experimental Therapeutics. 1972;181(3):555-62.

[48] Azadkhan AK, Piris J, Truelove SC. Experiment to determine active therapeutic moiety of sulfasalazine. Lancet. 1977;2(8044):892-5.

[49] Chan R, Pope D, Gilbert A, Sacra P, Baron JH, Lennard-Jones J. Studies of two novel sulfasalazine analogs, ipsalazide and balsalazide. Digestive Diseases and Sciences. 1983;28(7):609-15.

[50] Travis SPL, Tysk C, Desilva HJ, Sandberggertzen H, Jewell DP, Jarnerot G. Optimum dose of olsalazine for maintaining remission in ulcerative-colitis. Gut. 1994;35(9):1282-6.

[51] Thomas M. Parkinson, Joseph P. Brown, Robert E. Wingard J, inventors; Dynapol, Palo Alto, Calif., assignee. Polymeric agent for releasing 5-aminosalicylic acid or its salts into the gastrointestinal tract. Patent 4,190,716. Feb 26, 1980.

[52] Kennedy DA, Vembu N, Fronczek FR, Devocelle M. Synthesis of mutual azo prodrugs of anti-inflammatory agents and peptides facilitated by α-aminoisobutyric acid. The Journal of Organic Chemistry. 2011;76(23):9641-7.

[53] Yang L, Chu JS, Fix JA. Colon-specific drug delivery: New approaches and *in vitro/in vivo* evaluation. International Journal of Pharmaceutics. 2002;235(1-2):1-15.

[54] Bigucci F, Luppi B, Monaco L, Cerchiara T, Zecchi V. Pectin-based microspheres for colon-specific delivery of vancomycin. Journal of Pharmacy and Pharmacology. 2009; 61(1):41-6.

[55] Sande SA. Pectin-based oral drug delivery to the colon. Expert Opinion on Drug Delivery. 2005;2(3):441-50.

[56] Sinha VR, Kumria R. Polysaccharide matrices for microbially triggered drug delivery to the colon. Drug Development and Industrial Pharmacy. 2004;30(2):143-50.

[57] Chourasia MK, Jain SK. Polysaccharides for colon targeted drug delivery. Drug Delivery. 2004;11(2):129-48.

[58] Brondsted H, Kopecek J. Hydrogels for site-specific drug delivery to the colon: *In vitro* and *in vivo* degradation. Pharmaceutical Research. 1992;9(12):1540-5.

[59] Thakur BR, Singh RK, Handa AK. Chemistry and uses of pectin - A review. Critical Reviews in Food Science and Nutrition. 1997;37(1):47-73.

[60] Rubinstein A, Radai R, Ezra M, Pathak S, Rokem JS. *In vitro* evaluation of calcium pectinate - a potential colon-specific drug delivery carrier. Pharmaceutical Research. 1993;10(2):258-63.

[61] Rubinstein A, Radai R. In-vitro and in-vivo analysis of colon specificity of calcium pectinate formulations. European Journal of Pharmaceutics and Biopharmaceutics. 1995;41(5):291-5.

[62] Rubinstein A, Radai R, Friedman M, Fischer P, Rokem JS. The effect of intestinal bacteria adherence on drug diffusion through solid films under stationary conditions. Pharmaceutical Research. 1997;14(4):503-7.

[63] Atyabi F, Inanloo K, Dinarvand R. Bovine serum albumin-loaded pectinate beads as colonic peptide delivery system: Preparation and *in vitro* characterization. Drug Delivery. 2005;12(6):367-75.

[64] Kristl J, Smidkorbar J, Struc E, Schara M, Rupprecht H. Hydrocolloids and gels of chitosan as drug carriers. International Journal of Pharmaceutics. 1993;99(1):13-9.

[65] Yamamoto A, Tozaki H, Okada N, Fujita T. Colon-specific delivery of peptide drugs and anti-inflammatory drugs using chitosan capsules. Stp Pharma Sciences. 2000; 10(1):23-34.

[66] Fetih G, Fausia H, Okada N, Fujita T, Attia M, Yamamoto A. Colon-specific delivery and enhanced colonic absorption of [Asu1,7]-eel calcitonin using chitosan capsules containing various additives in rats. Journal of Drug Targeting. 2006;14(3):165-72.

[67] Bayat A, Dorkoosh FA, Dehpour AR, Moezi L, Larijani B, Junginger HE, et al. Nanoparticles of quaternized chitosan derivatives as a carrier for colon delivery of insulin: *Ex vivo* and *in vivo* studies. International Journal of Pharmaceutics. 2008; 356(1-2):259-66.

[68] Zhang H, Alsarra IA, Neau SH. An *in vitro* evaluation of a chitosan-containing multiparticulate system for macromolecule delivery to the colon. International Journal of Pharmaceutics. 2002;239(1-2):197-205.

[69] Smoum R, Rubinstein A, Srebnik M. Chitosan-pentaglycine-phenylboronic acid conjugate: A potential colon-specific platform for calcitonin. Bioconjugate Chemistry. 2006;17(4):1000-7.

[70] Roberfroid M. Dietary fiber, inulin, and oligofructose - a review comparing their physiological-effects. Critical Reviews in Food Science and Nutrition. 1993;33(2): 103-48.

[71] Dysseler P, Hoffem D. Inulin, an alternative dietary fiber - properties and quantitative-analysis. European Journal of Clinical Nutrition. 1995;49:S145-S52.

[72] Gibson GR, Roberfroid MB. Dietary modulation of the human colonic microbiota - introducing the concept of prebiotics. Journal of Nutrition. 1995;125(6):1401-12.

[73] Wang X, Gibson GR. Effects of the in-vitro fermentation of oligofructose and inulin by bacteria growing in the human large-intestine. Journal of Applied Bacteriology. 1993; 75(4):373-80.

[74] Vervoort L, Kinget R. *In vitro* degradation by colonic bacteria of inulinHP incorporated in Eudragit RS films. International Journal of Pharmaceutics. 1996;129(1):185-90.

[75] Vervoort L, Rombaut P, Van den Mooter G, Augustijns P, Kinget R. Inulin hydrogels. II. *In vitro* degradation study. International Journal of Pharmaceutics. 1998;172:137-45.

[76] Tripodo G, Pitarresi G, Cavallaro G, Palumbo FS, Giammona G. Controlled release of IgG by novel UV induced polysaccharide/poly(amino acid) hydrogels. Macromolecular Bioscience. 2009;9(4):393-401.

[77] Hehre EJ, Sery TW. Dextran-splitting anaerobic bacteria from the human intestine. Journal of Bacteriology. 1952;63(3):424-6.

[78] Basan H, Gümüşderelioğlu M, Tevfik Orbey M. Release characteristics of salmon calcitonin from dextran hydrogels for colon-specific delivery. European Journal of Pharmaceutics and Biopharmaceutics. 2007;65(1):39-46.

[79] Chen L, Li X, Pang Y, Li L, Zhang X, Yu L. Resistant starch as a carrier for oral colon-targeting drug matrix system. Journal of Materials Science: Materials in Medicine. 2007;18(11):2199-203.

[80] Chen L, Li X, Li L, Guo S. Acetylated starch-based biodegradable materials with potential biomedical applications as drug delivery systems. Current Applied Physics. 2007;7(Supplement 1):e90-e3.

[81] Chen L, Pu H, Li X, Yu L. A novel oral colon-targeting drug delivery system based on resistant starch acetate. Journal of Controlled Release. 2011;152(Supplement 1):e51-e2.

[82] Katsuma M, Watanabe S, Kawai H, Takemura S, Sako K. Effects of absorption promoters on insulin absorption through colon-targeted delivery. International Journal of Pharmaceutics. 2006;307(2):156-62.

[83] Yang LB, Watanabe S, Li JH, Chu JS, Katsuma M, Yokohama S, et al. Effect of colonic lactulose availability on the timing of drug release onset *in vivo* from a unique

colon-specific drug delivery system (CODES^{TM}). Pharmaceutical Research. 2003; 20(3):429-34.

[84] Mortensen PB, Holtug K, Bonnen H, Clausen MR. The degradation of amino-acids, proteins, and blood to short-chain fatty-acids in colon is prevented by lactulose. Gastroenterology. 1990;98(2):353-60.

[85] Van den Mooter G. Colon drug delivery. Expert Opinion on Drug Delivery. 2006;3(1): 111-25.

[86] Kimura Y, Makita Y, Kumagai T, Yamane H, Kitao T, Sasatani H, et al. Degradation of azo-containing polyurethane by the action of intestinal flora: Its mechanism and application as a drug delivery system. Polymer. 1992;33(24):5294-9.

[87] Yamaoka T, Makita Y, Sasatani H, Kim S-I, Kimura Y. Linear type azo-containing polyurethane as drug-coating material for colon-specific delivery: Its properties, degradation behavior, and utilization for drug formulation. Journal of Controlled Release. 2000;66:187-97.

[88] Schacht E, Gevaert A, Kenawy ER, Molly K, Verstraete W, Adriaensens P, et al. Polymers for colon specific drug delivery. Journal of Controlled Release. 1996;39: 327-38.

[89] Leopold CS. Coated dosage forms for colon-specific drug delivery. Pharmaceutical Science & Technology Today. 1999;2(5):197-204.

[90] Touitou E, Rubinstein A. Targeted enteral delivery of insulin to rats. International Journal of Pharmaceutics. 1986;30(2-3):95-9.

[91] Rao S, Ritschel WA. Colonic drug-delivery of small peptides. Stp Pharma Sciences. 1995;5(1):19-29.

[92] Ritschel WA. Microemulsions for improved peptide absorption from the gastrointestinal-tract. Methods and Findings in Experimental and Clinical Pharmacology. 1991;13(3):205-20.

[93] Kraeling MEK, Ritschel WA. Development of a colonic release capsule dosage form and the absorption of insulin. Methods and Findings in Experimental and Clinical Pharmacology. 1992;14(3):199-209.

[94] Gwinup G, Elias AN, Domurat ES. Insulin and C-peptide levels following oral administration of insulin in intestinal-enzyme protected capsules. General Pharmacology: The Vascular System. 1991;22(2):243-6.

[95] Elias AN, Gordon I, Vaziri ND, Chune G, Pandian MR, Gwinup G, et al. Effective portal insulin delivery with enzyme-protected capsules in pancreatectomized pigs. General Pharmacology: The Vascular System. 1992;23(1):55-9.

[96] Elias AN, Gordon IL, Porzio R, Willis ML, Pandian MR, Gwinup G. Intracecally administered insulin in chronically diabetic pigs. Current Therapeutic Research-Clinical and Experimental. 1997;58(1):16-25.

[97] Geary RS, Wade Schlameus H. Vancomycin and insulin used as models for oral delivery of peptides. Journal of Controlled Release. 1993;23(1):65-74.

[98] Hong S, Yum S, Yoo H-J, Kang S, Yoon J-H, Min D, et al. Colon-targeted cell-permeable NFκB inhibitory peptide is orally active against experimental colitis. Molecular Pharmaceutics. 2012;9(5):1310-9.

[99] Paul W, Sharma CP. Tricalcium phosphate delayed release formulation for oral delivery of insulin: A proof-of-concept study. Journal of Pharmaceutical Sciences. 2008;97(2):875-82.

[100] Jain D, Panda AK, Majumdar DK. Eudragit S100 entrapped insulin microspheres for oral delivery. AAPS PharmSciTech. 2005;6(1):E100-7.

[101] Jelvehgari M, Milani PZ, Siahi-Shadbad MR, Monajjemzadeh F, Nokhodchi A, Azari Z, et al. *In vitro* and *in vivo* evaluation of insulin microspheres containing protease inhibitor. Arzneimittel-Forschung-Drug Research. 2011;61(1):14-22.

[102] Torres D, Rodriguez M, Cuna M. Microencapsulated lipid cores for site-specific delivery of corticosteroid and peptide drugs to the colonic region. Stp Pharma Sciences. 2003;13(1):49-56.

[103] Mahkam M. Using pH-sensitive hydrogels containing cubane as a crosslinking agent for oral delivery of insulin. Journal of Biomedical Materials Research Part B: Applied Biomaterials. 2005;75B(1):108-12.

[104] Ramkissoon-Ganorkar C, Liu F, Baudyš M, Kim SW. Modulating insulin-release profile from pH/thermosensitive polymeric beads through polymer molecular weight. Journal of Controlled Release. 1999;59(3):287-98.

[105] Chiu H-C, Hsiue G-H, Lee Y-P, Huang L-W. Synthesis and characterization of pH-sensitive dextran hydrogels as a potential colon-specific drug delivery system. Journal of Biomaterials Science, Polymer Edition. 1999;10(5):591-608.

[106] Davis SS. The design and evaluation of controlled release systems for the gastrointestinal tract. Journal of Controlled Release. 1985;2:27-38.

[107] Davis SS, Hardy JG, Fara JW. Transit of pharmaceutical dosage forms through the small-intestine. Gut. 1986;27(8):886-92.

[108] Gazzaniga A, Maroni A, Sangalli ME, Zema L. Time-controlled oral delivery systems for colon targeting. Expert Opinion on Drug Delivery. 2006;3(5):583-97.

[109] Wilding IR, Davis SS, Pozzi F, Furlani P, Gazzaniga A. Enteric coated timed release systems for colonic targeting. International Journal of Pharmaceutics. 1994;111(1): 99-102.

[110] Gonzalez-Rodriguez ML, Maestrelli F, Mura P, Rabasco AM. *In vitro* release of sodium diclofenac from a central core matrix tablet aimed for colonic drug delivery. European Journal of Pharmaceutical Sciences. 2003;20(1):125-31.

[111] Wilding IR, Davis SS, Bakhshaee M, Stevens HNE, Sparrow RA, Brennan J. Gastrointestinal transit and systemic absorption of captopril from a pulsed-release formulation. Pharmaceutical Research. 1992;9(5):654-7.

[112] Zhang Y, Zhang ZR, Wu F. A novel pulsed-release system based on swelling and osmotic pumping mechanism. Journal of Controlled Release. 2003;89(1):47-55.

[113] Maroni A, Curto MDD, Serratoni M, Zema L, Foppoli A, Gazzaniga A, et al. Feasibility, stability and release performance of a time-dependent insulin delivery system intended for oral colon release. European Journal of Pharmaceutics and Biopharmaceutics. 2009;72(1):246-51.

[114] Del Curto MD, Maroni A, Foppoli A, Zema L, Gazzaniga A, Sangalli ME. Preparation and evaluation of an oral delivery system for time-dependent colon release of insulin and selected protease inhibitor and absorption enhancer compounds. Journal of Pharmaceutical Sciences. 2009;98(12):4661-9.

[115] Klein S, Stein J, Dressman J. Site-specific delivery of anti-inflammatory drugs in the gastrointestinal tract: An in-vitro release model. Journal of Pharmacy and Pharmacology. 2005;57(6):709-19.

[116] Hodges LA, Connolly SM, Band J, O'Mahony B, Ugurlu T, Turkoglu M, et al. Scintigraphic evaluation of colon targeting pectin-HPMC tablets in healthy volunteers. International Journal of Pharmaceutics. 2009;370(1-2):144-50.

[117] Kimura T, Sato K, Sugimoto K, Tao R, Murakami T, Kurosaki Y, et al. Oral administration of insulin as poly(vinyl alcohol)-gel spheres in diabetic rats. Biological & Pharmaceutical Bulletin. 1996;19(6):897-900.

[118] Jiang HL, Zhu KJ. Bioadhesive fluorescent microspheres as visible carriers for local delivery of drugs. I: Preparation and characterization of insulin-loaded PCEFB/PLGA microspheres. Journal of Microencapsulation. 2002;19(4):451-61.

[119] Li Y, Jiang HL, Jin JF, Zhu KJ. Bioadhesive fluorescent microspheres as visible carriers for local delivery of drugs. II: Uptake of insulin-loaded PCEFB/PLGA microspheres by the gastrointestinal tract. Drug Delivery. 2004;11(6):335-40.

[120] Lamprecht A, Yamamoto H, Takeuchi H, Kawashima Y. Microsphere design for the colonic delivery of 5-fluorouracil. Journal of Controlled Release. 2003;90(3):313-22.

[121] Lamprecht A, Ubrich N, Yamamoto H, Schäfer U, Takeuchi H, Maincent P, et al. Biodegradable nanoparticles for targeted drug delivery in treatment of inflammatory bowel disease. Journal of Pharmacology and Experimental Therapeutics. 2001;299 (2):775-81.

[122] Lamprecht A, Schafer U, Lehr CM. Size-dependent bioadhesion of micro- and nanoparticulate carriers to the inflamed colonic mucosa. Pharmaceutical Research. 2001;18(6):788-93.

[123] Laroui H, Dalmasso G, Nguyen HTT, Yan Y, Sitaraman SV, Merlin D. Drug-loaded nanoparticles targeted to the colon with polysaccharide hydrogel reduce colitis in a mouse model. Gastroenterology. 2010;138(3):843-53.

[124] Matsuzawa A, Morishita M, Takayama K, Nagai T. Absorption of insulin using water-in-oil-in-water emulsion from an enteral loop in rats. Biological & Pharmaceutical Bulletin. 1995;18(12):1718-23.

[125] Morishita M, Kajita M, Suzuki A, Takayama K, Chiba Y, Tokiwa S, et al. The dose-related hypoglycemic effects of insulin emulsions incorporating highly purified EPA and DHA. International Journal of Pharmaceutics. 2000;201(2):175-85.

[126] Manosroi A, Bauer KH. Effects of gastrointestinal administration of human insulin and a human insulin-DEAE-dextran complex entrapped in different compound liposomes on blood-glucose in rats. Drug Development and Industrial Pharmacy. 1990;16(9):1521-38.

[127] Sharma A, Sharma US. Liposomes in drug delivery: Progress and limitations. International Journal of Pharmaceutics. 1997;154(2):123-40.

[128] Basit AW, Short MD, McConnell EL. Microbiota-triggered colonic delivery: Robustness of the polysaccharide approach in the fed state in man. Journal of Drug Targeting. 2009;17(1):64-71.

[129] Antosova Z, Mackova M, Kral V, Macek T. Therapeutic application of peptides and proteins: Parenteral forever? Trends in Biotechnology. 2009;27(11):628-35.

[130] Sarciaux JM, Acar L, Sado PA. Using microemulsion formulations for oral drug delivery of therapeutic peptides. International Journal of Pharmaceutics. 1995;120(2): 127-36.

[131] Wang J, Chow D, Heiati H, Shen W-C. Reversible lipidization for the oral delivery of salmon calcitonin. Journal of Controlled Release. 2003;88(3):369-80.

[132] Kipnes M, Dandona P, Tripathy D, Still JG, Kosutic G. Control of postprandial plasma glucose by an oral insulin product (HIM2) in patients with type 2 diabetes. Diabetes Care. 2003;26(2):421-6.

[133] Russell-Jones GJ. Use of targeting agents to increase uptake and localization of drugs to the intestinal epithelium. Journal of Drug Targeting. 2004;12(2):113-23.

[134] Goldberg M, Gomez-Orellana I. Challenges for the oral delivery of macromolecules. Nat Rev Drug Discov. 2003;2(4):289-95.

[135] Ma Z, Lim TM, Lim L-Y. Pharmacological activity of peroral chitosan-insulin nanoparticles in diabetic rats. International Journal of Pharmaceutics. 2005;293(1-2): 271-80.

[136] Lawrence MJ, Rees GD. Microemulsion-based media as novel drug delivery systems. Advanced Drug Delivery Reviews. 2000;45(1):89-121.

[137] Cheng M-B, Wang J-C, Li Y-H, Liu X-Y, Zhang X, Chen D-W, et al. Characterization of water-in-oil microemulsion for oral delivery of earthworm fibrinolytic enzyme. Journal of Controlled Release. 2008;129(1):41-8.

[138] Constantinides PP, Scalart JP, Lancaster C, Marcello J, Marks G, Ellens H, et al. Formulation and intestinal absorption enhancement evaluation of water-in-oil microemulsions incorporating medium-chain glycerides. Pharmaceutical Research. 1994;11(10):1385-90.

[139] Ritschel WA. Microemulsion technology in the reformulation of cyclosporine: The reason behind the pharmacokinetic properties of Neoral. Clinical transplantation. 1996;10(4):364-73.

[140] Lyons KC, Charman WN, Miller R, Porter CJH. Factors limiting the oral bioavailability of N-acetylglucosaminyl-N-acetylmuramyl dipeptide (GMDP) and enhancement of absorption in rats by delivery in a water-in-oil microemulsion. International Journal of Pharmaceutics. 2000;199(1):17-28.

[141] Kim SK, Lee EH, Vaishali B, Lee S, Lee Y-k, Kim C-Y, et al. Tricaprylin microemulsion for oral delivery of low molecular weight heparin conjugates. Journal of Controlled Release. 2005;105(1-2):32-42.

[142] Constantinides PP. Lipid microemulsions for improving drug dissolution and oral absorption: Physical and biopharmaceutical aspects. Pharmaceutical Research. 1995;12(11):1561-72.

[143] Kompella UB, Lee VHL. Delivery systems for penetration enhancement of peptide and protein drugs: Design considerations. Advanced Drug Delivery Reviews. 2001; 46(1-3):211-45.

[144] Dave SH, Tilstra JS, Matsuoka K, Li F, Karrasch T, Uno JK, et al. Amelioration of chronic murine colitis by peptide-mediated transduction of the IκB kinase inhibitor NEMO binding domain peptide. The Journal of Immunology. 2007;179(11):7852-9.

[145] Product Information: MIGLYOL® 810, 812, 818, 829, 840 neutral oils for pharmaceuticals and cosmetics. Febuary 10, 2011 [cited; Available from: http://abstracts.aapspharmaceutica.com/expoaaps07/Data/EC/Event/Exhibitors/263/cb63fb76-28f4-4948-a6d0-ae249dae9c30.pdf

[146] Technical data: Capmul MCM, NF. Febuary 10, 2011 [cited; Available from: http://www.abiteccorp.com/i_templates/administration/tinymce/uploaded/File/Capmul%20Tech%20Data/Capmul%20MCM%20NF%20TDS%20I-4.pdf

[147] FDA Inactive Ingredient Database for Approved Drug Products. http://www.accessdata.fda.gov/scripts/cder/iig/getiigWEB.cfm. Last accessed on August 15, 2012.

[148] J. Tilstra, K.K. Rehman, T. Hennon, S.E. Plevy, P. Clemens, Robbins PD. Protein transduction: Identification, characterization and optimization. Biochemical Society Transactions. 2007;35(Part 4):811-5.

[149] Scott Swenson E, Curatolo WJ. (C) Means to enhance penetration: (2) Intestinal permeability enhancement for proteins, peptides and other polar drugs: Mechanisms and potential toxicity. Advanced Drug Delivery Reviews. 1992;8(1):39-92.

[150] Constantinides PP, Lancaster CM, Marcello J, Chiossone DC, Orner D, Hidalgo I, et al. Enhanced intestinal absorption of an RGD peptide from water-in-oil microemulsions of different composition and particle size. Journal of Controlled Release. 1995;34(2):109-16.

[151] Constantinides PP, Welzel G, Ellens H, Smith PL, Sturgis S, Yiv SH, et al. Water-in-oil microemulsions containing medium-chain fatty acids/salts: Formulation and intestinal absorption enhancement evaluation. Pharmaceutical Research. 1996;13(9 SUPPL.):S219.

[152] Mehta SK, Bala K. Tween-based microemulsions: A percolation view. Fluid Phase Equilibria. 2000;172(2):197-209.

[153] Lang J, Lalem N, Zana R. Quaternary water in oil microemulsions. 1. Effect of alcohol chain length and concentration on droplet size and exchange of material between droplets. The Journal of Physical Chemistry. 1991;95(23):9533-41.

[154] Constantinides PP, Scalart JP. Formulation and physical characterization of water-in-oil microemulsions containing long- versus medium-chain glycerides. International Journal of Pharmaceutics. 1997;158(1):57-68.

[155] Constantinides PP, Yiv SH. Particle size determination of phase-inverted water-in-oil microemulsions under different dilution and storage conditions. International Journal of Pharmaceutics. 1995;115(2):225-34.

[156] Spernath A, Aserin A. Microemulsions as carriers for drugs and nutraceuticals. Advances in Colloid and Interface Science. 2006;128-130:47-64.

[157] Patel A, Vavia P. Preparation and *in vivo* evaluation of SMEDDS (self-microemulsifying drug delivery system) containing fenofibrate. The AAPS Journal. 2007;9(3):E344-E52.

[158] Grunwald J, Rejtar T, Sawant R, Wang Z, Torchilin VP. TAT peptide and its conjugates: proteolytic stability. Bioconjugate Chemistry. 2009;20(8):1531-7.

[159] Chauhan A, Tikoo A, Kapur AK, Singh M. The taming of the cell penetrating domain of the HIV Tat: myths and realities. Journal of Controlled Release. 2007;117(2):148-62.

[160] Guo L, Ma E, Zhao H, Long Y, Zheng C, Duan M. Preliminary evaluation of a novel oral delivery system for rhPTH1-34: *in vitro* and *in vivo*. International Journal of Pharmaceutics. 2011;420(1):172-9.

[161] Cole ET, Cadé D, Benameur H. Challenges and opportunities in the encapsulation of liquid and semi-solid formulations into capsules for oral administration. Advanced Drug Delivery Reviews. 2008;60(6):747-56.

[162] Fan Y, Li X, Zhou Y, Fan C, Wang X, Huang Y, et al. Improved intestinal delivery of salmon calcitonin by water-in-oil microemulsions. International Journal of Pharmaceutics. 2011;416(1):323-30.

[163] Yoshitomi H NT, Frederick G, Dillsaver M, Higuchi T. Effect of triglyceride on small intestinal absorption of cefoxitin in rats. The Journal of Pharmacy and Pharmacology. 1987;39(11):887-91.

[164] Oliyai R, Stella VJ. Prodrugs of peptides and proteins for improved formulation and delivery. Annual Review of Pharmacology and Toxicology. 1993;33:521-44.

[165] Sharma G, Wilson K, van der Walle CF, Sattar N, Petrie JR, Kumar MNVR. Microemulsions for oral delivery of insulin: design, development and evaluation in streptozotocin induced diabetic rats. European Journal of Pharmaceutics and Biopharmaceutics. 2010;76(2):159-69.

[166] Danielsson I, Lindman B. The definition of a microemulsion. Colloids and Surfaces. 1981;3:391-2.

[167] Bhargava HN, Narurkar A, Lieb LM. Using microemulsions for drug delivery. Pharmaceutical Technology. 1987;11(3):46, 48, 50, 52, 54.

[168] Hoar TP, Schulman JH. Transparent water-in-oil dispersions: the oleopathic hydro-micelle. Nature. 1943;152:102-3.

[169] Schulman JH, Stoeckenius W, Prince LM. Mechanism of formation and structure of micro emulsions by electron microscopy. Journal of Physical Chemistry. 1959;63(10): 1677-80.

[170] Shinoda K, Friberg S. Microemulsions - colloidal aspects. Advances in Colloid and Interface Science. 1975;4(4):281-300.

[171] Friberg S, Burasczenska I. Microemulsions in the water-potassium oleate-benzene system. Progress in Colloid and Polymer Science. 1978;63:1-9.

[172] Ruckenstein E, Chi JC. Stability of microemulsions. Journal of the Chemical Society, Faraday Transactions 2: Molecular and Chemical Physics. 1975;71:1690-707.

[173] Ruckenstein E. Thermodynamic stability of microemulsions. Journal of Colloid and Interface Science. 1978;66(2):369-71.

[174] Lawrence MJ. Microemulsions as drug delivery vehicles. Current Opinion in Colloid & Interface Science. 1996;1(6):826-32.

[175] Kawakami K, Yoshikawa T, Moroto Y, Kanaoka E, Takahashi K, Nishihara Y, et al. Microemulsion formulation for enhanced absorption of poorly soluble drugs: I. Prescription design. Journal of Controlled Release. 2002;81(1-2):65-74.

[176] Ma P, Rahima Benhabbour S, Feng L, Mumper RJ. 2′-Behenoyl-paclitaxel conjugate containing lipid nanoparticles for the treatment of metastatic breast cancer. Cancer

Letters. 2012 August 16, DOI: http://dx.doi.org/10.1016/j.canlet.2012.08.009. [Epub ahead of print].

[177] Dong X, Mattingly CA, Tseng M, Cho M, Adams VR, Mumper RJ. Development of new lipid-based paclitaxel nanoparticles using sequential simplex optimization. European Journal of Pharmaceutics and Biopharmaceutics. 2009;72(1):9-17.

[178] Liu D, Kobayashi T, Russo S, Li F, Plevy S, Gambling T, et al. *In vitro* and *in vivo* evaluation of a water-in-oil microemulsion system for enhanced peptide intestinal delivery. The AAPS Journal. 2013;15(1):288-98.

[179] Dumortier G, Grossiord JL, Agnely F, Chaumeil JC. A review of poloxamer 407 pharmaceutical and pharmacological characteristics. Pharmaceutical Research. 2006;23(12):2709-28.

[180] Alexandridis P, Alan Hatton T. Poly(ethylene oxide)-poly(propylene oxide)-poly(ethylene oxide) block copolymer surfactants in aqueous solutions and at interfaces: thermodynamics, structure, dynamics, and modeling. Colloids and Surfaces A: Physicochemical and Engineering Aspects. 1995;96(1-2):1-46.

[181] Vadnere M, Amidon G, Lindenbaum S, Haslam JL. Thermodynamic studies on the gel-sol transition of some pluronic polyols. International Journal of Pharmaceutics. 1984;22(2-3):207-18.

[182] Lau BK, Wang Q, Sun W, Li L. Micellization to gelation of a triblock copolymer in water: thermoreversibility and scaling. Journal of Polymer Science Part B: Polymer Physics. 2004;42(10):2014-25.

[183] Malmsten M, Lindman B. Self-assembly in aqueous block copolymer solutions. Macromolecules. 1992;25(20):5440-5.

[184] Malmsten M, Lindman B. Effects of homopolymers on the gel formation in aqueous block copolymer solutions. Macromolecules. 1993;26(6):1282-6.

[185] Mortensen K, Brown W, Nordén B. Inverse melting transition and evidence of three-dimensional cubatic structure in a block-copolymer micellar system. Physical Review Letters. 1992;68(15):2340-3.

[186] Matthew JE, Nazario YL, Roberts SC, Bhatia SR. Effect of mammalian cell culture medium on the gelation properties of Pluronic® F127. Biomaterials. 2002;23(23): 4615-9.

[187] Kurumada K-i, Robinson BH. Viscosity studies of pluronic F127 in aqueous solution. In: Miguel M, Burrows HD, eds. Progress in Colloid and Polymer Science: Springer Berlin / Heidelberg 2004;123:12-5.

[188] Malmsten M, Lindman B. Water self-diffusion in aqueous block copolymer solutions. Macromolecules. 1992;25(20):5446-50.

[189] Gilbert JC, Richardson JL, Davies MC, Palin KJ, Hadgraft J. The effect of solutes and polymers on the gelation properties of Pluronic F127 solutions for controlled drug delivery. Journal of Controlled Release. 1987;5(2):113-8.

[190] Yang Y, Wang J, Zhang X, Lu W, Zhang Q. A novel mixed micelle gel with thermo-sensitive property for the local delivery of docetaxel. Journal of Controlled Release. 2009;135(2):175-82.

[191] Yong CS, Choi JS, Quan QZ, Rhee JD, Kim CK, Lim SJ, et al. Effect of sodium chloride on the gelation temperature, gel strength and bioadhesive force of poloxamer gels containing diclofenac sodium. International Journal of Pharmaceutics. 2001;226(1-2):195-205.

[192] Choi HG, Lee MK, Kim MH, Kim CK. Effect of additives on the physicochemical properties of liquid suppository bases. International Journal of Pharmaceutics. 1999; 190(1):13-9.

[193] Pisal SS, Paradkar AR, Mahadik KR, Kadam SS. Pluronic gels for nasal delivery of vitamin B-12. Part I: preformulation study. International Journal of Pharmaceutics. 2004;270(1-2):37-45.

[194] Ryu JM, Chung SJ, Lee MH, Kim CK, Shim CK. Increased bioavailability of propranolol in rats by retaining thermally gelling liquid suppositories in the rectum. Journal of Controlled Release. 1999;59(2):163-72.

[195] Kim EY, Gao ZG, Park JS, Li H, Han K. RhEGF/HP-beta-CD complex in poloxamer gel for ophthalmic delivery. International Journal of Pharmaceutics. 2002;233(1-2):159-67.

[196] R.C. Rowe, Sheskey PJ, Quinn ME, eds. Handbook of pharmaceutical excipients. 6th ed. London, UK: The Pharmaceutical Press 2009.

[197] Park YJ, Yong CS, Kim HM, Rhee JD, Oh YK, Kim CK, et al. Effect of sodium chloride on the release, absorption and safety of diclofenac sodium delivered by poloxamer gel. International Journal of Pharmaceutics. 2003;263(1-2):105-11.

[198] Anderson BC, Pandit NK, Mallapragada SK. Understanding drug release from poly(ethylene oxide)-b-poly(propylene oxide)-b-poly(ethylene oxide) gels. Journal of Controlled Release. 2001;70(1-2):157-67.

[199] Pec EA, Wout ZG, Johnston TP. Biological activity of urease formulated in poloxamer 407 after intraperitoneal injection in the rat. Journal of Pharmaceutical Sciences. 1992;81(7):626-30.

[200] Wang PL, Johnston TP. Enhanced stability of two model proteins in an agitated solution environment using poloxamer 407. Journal of Parenteral Science and Technology. 1993;47(4):183-9.

[201] Bromberg LE. Interactions among proteins and hydrophobically modified polyelectrolytes. Journal of Pharmacy and Pharmacology. 2001;53(4):541-7.

[202] Katakam M, Banga AK. Use of poloxamer polymers to stabilize recombinant human growth hormone against various processing stresses. Pharmaceutical Development and Technology. 1997;2(2):143-9.

[203] Stratton LP, Dong AC, Manning MC, Carpenter JF. Drug delivery matrix containing native protein precipitates suspended in a poloxamer gel. Journal of Pharmaceutical Sciences. 1997;86(9):1006-10.

[204] Goodner KL. Estimating turbidity (NTU) from absorption data. May 1, 2009 [cited 2013 February 6]; Available from: http://www.sensusflavors.com/t-r-pdf/SEN-TN-0010-Turbidity,_Tea,_And_UV-VIS.pdf

[205] Balch RT. Measurement of turbidity with a spectrophotometer Industrial and Engineering Chemistry (Analytical Edition). 1931;3(2):124-7.

[206] Attwood D, Collett JH, Tait CJ. The micellar properties of the poly(oxyethylene)-poly(oxypropylene) copolymer Pluronic F127 in water and electrolyte solution. International Journal of Pharmaceutics. 1985;26(1-2):25-33.

[207] Klucel Hydroxypropylcellulose physical and chemical properties. 2001 [cited 2013 February 22]; Available from: http://www.brenntagspecialties.com/en/downloads/Products/Multi_Market_Principals/Aqualon/Klucel_HPC_Booklet.pdf

[208] Antunes FE, Gentile L, Tavano L, Rossi CO. Rheological characterization of the thermal gelation of poly(n-isopropylacrylamide) and poly(n-isopropylacrylamide) co-acrylic acid. Applied Rheology. 2009;19(4):42064(9 pages).

[209] Schild HG. Poly(n-isopropylacrylamide): experiment, theory and application. Progress in Polymer Science. 1992;17(2):163-249.

[210] Haque A, Morris ER. Thermogelation of methylcellulose.1. Molecular-structures and processes. Carbohydrate Polymers. 1993;22(3):161-73.

[211] Silva SMC, Pinto FV, Antunes FE, Miguel MG, Sousa JJS, Pais AACC. Aggregation and gelation in hydroxypropylmethyl cellulose aqueous solutions. Journal of Colloid and Interface Science. 2008;327(2):333-40.

[212] Carotenuto C, Grizzuti N. Thermoreversible gelation of hydroxypropylcellulose aqueous solutions. Rheologica Acta. 2006;45(4):468-73.

[213] Han CK, Bae YH. Inverse thermally-reversible gelation of aqueous n-isopropylacrylamide copolymer solutions. Polymer. 1998;39(13):2809-14.

[214] Lebon F, Caggioni M, Bignotti F, Abbate S, Gangemi F, Longhi G, et al. Coil-to-globule transition of poly(n-isopropylacrylamide) doped with chiral amino acidic comonomers. Journal of Physical Chemistry B. 2007;111(9):2372-6.

[215] Wanka G, Hoffmann H, Ulbricht W. Phase diagrams and aggregation behavior of poly(oxyethylene)-poly(oxypropylene)-poly(oxyethylene) triblock copolymers in aqueous solutions. Macromolecules. 1994;27(15):4145-59.

[216] Jeong B, Kim SW, Bae YH. Thermosensitive sol-gel reversible hydrogels. Advanced Drug Delivery Reviews. 2002;54(1):37-51.

[217] Alexandridis P. Amphiphilic copolymers and their applications. Current Opinion in Colloid & Interface Science. 1996;1(4):490-501.

[218] Ruel-Gariepy E, Leroux JC. In situ-forming hydrogels - review of temperature-sensitive systems. European Journal of Pharmaceutics and Biopharmaceutics. 2004; 58(2):409-26.

[219] Alexandridis P, Holzwarth JF, Hatton TA. Micellization of poly(ethylene oxide)-poly(propylene oxide)-poly(ethylene oxide) triblock copolymers in aqueous solutions: thermodynamics of copolymer association. Macromolecules. 1994;27(9):2414-25.

[220] Ryu J-M, Chung S-J, Lee M-H, Kim C-K, Chang-Koo S. Increased bioavailability of propranolol in rats by retaining thermally gelling liquid suppositories in the rectum. Journal of Controlled Release. 1999;59(2):163-72.

[221] Shin S-C, Kim J-Y. Enhanced permeation of triamcinolone acetonide through the buccal mucosa. European Journal of Pharmaceutics and Biopharmaceutics. 2000; 50(2):217-20.

[222] Watnasirichaikul S, Davies N, Rades T, Tucker I. Preparation of biodegradable insulin nanocapsules from biocompatible microemulsions. Pharmaceutical Research. 2000;17(6):684-9.

[223] Watnasirichaikul S, Rades T, Tucker IG, Davies NM. Effects of formulation variables on characteristics of poly (ethylcyanoacrylate) nanocapsules prepared from w/o microemulsions. International Journal of Pharmaceutics. 2002;235(1-2):237-46.

[224] Vieira J, Pinto da Silva L, Esteves da Silva JCG. Advances in the knowledge of light emission by firefly luciferin and oxyluciferin. Journal of Photochemistry and Photobiology B: Biology. 2012;117:33-9.

[225] Seliger HH, McElroy WD. Spectral emission and quantum yield of firefly bioluminescence. Archives of Biochemistry and Biophysics. 1960;88(1):136-41.

[226] Saphier S, Rosner A, Brandeis R, Karton Y. Gastro intestinal tracking and gastric emptying of solid dosage forms in rats using X-ray imagining. International Journal of Pharmaceutics. 2010;388(1-2):190-5.